Stearylated Peptides for Therapeutic siRNA Delivery and Their Cellular Uptake Mechanisms

by

Ran Pan

A thesis
presented to the University of Waterloo
in fulfillment of the
thesis requirement for the degree of
Doctor of Philosophy
in
Chemical Engineering - Nanotechnology

Waterloo, Ontario, Canada, 2015

AUTHOR'S DECLARATION

I hereby declare that I am the sole author of this thesis. This is a true copy of the thesis, including any required final revisions, as accepted by my examiners. I understand that my thesis may be made electronically available to the public.

Abstract

Small interfering RNA (siRNA) shows great potential as a powerful tool in gene therapy, due to its ability to regulate gene expression in a highly selective manner. siRNA is a double-stranded RNA consisting of 21–23 nucleotides and has the ability to trigger RNA interference (RNAi). RNA interference is the post-transcriptional gene silencing process where siRNA molecules bind to the complementary sequence in the target messenger RNA (mRNA), thereby inhibiting the expression of the target protein in cells. However, the clinical applications of siRNA are limited by the nature of naked siRNA molecules: Relatively large molecular weight, anionic nature and poor stability in physiological fluids of siRNA decrease its ability to permeate plasma membranes and result in inefficient cellular uptake. Thus, the development of efficient and safe delivery systems for siRNA has been an important research focus. Several strategies have been developed to aid in siRNA delivery, and peptide-based siRNA delivery reagents have been recognized as a promising approach for both *in vitro* and *in vivo* applications for more than a decade.

The present study focuses on the design, modification and evaluation of novel co-assembling, cell-penetrating peptides for siRNA delivery, including the following aspects: (1) design of new peptide sequences with incorporation of stearic acid, and modification of existing peptide sequences; (2) studying and improving serum stability without compromising gene-silencing efficacy; (3) investigation of the knockdown efficiency and toxicity of the resulting peptide/siRNA complexes in cultured cells and an animal model; (4) evaluation of

biocompatibility of the peptide/siRNA complexes *in vitro*; (5) studying of the internalization pathway, intracellular trafficking, and uptake mechanisms of the peptide/siRNA complexes.

We previously reported a library of cell-penetrating, amino acid-pairing peptides that facilitate effective siRNA delivery to mammalian cells without causing cytotoxicity, but they are unstable in serum-containing media. Here, we investigated the possibility of conjugating the peptide with diethylene glycol to improve its serum stability without compromising its gene-regulation capability. One of the most promising peptides in our library, C6M1 (with sequence: RLWRLLWRLWRRLWRLLR), was conjugated with diethylene glycol. The incorporated/co-assembled siRNA complexes increased in stability in serum from less than 24 hours to up to 72 hours, with highly efficient cellular uptake and more than 90% cell viability profile. The gene-silencing ability of diethylene glycol conjugated-peptide/siRNA complexes was comparable to that of non-conjugated peptide/siRNA at both mRNA and protein levels. Despite the improved serum stability, the silencing efficiency of siRNA delivered by C6M1 and the modified DM1 (degylated C6M1) ranged from 40% to 60%, and the less efficient knockdown ability might be due to the entrapment of siRNA in endosome/lysosome vesicles.

Therefore, designing new sequences to enhance the endosomal escape of the complexes was required. A series of co-assembling, cell-penetrating peptides was designed, which comprised a variant of a nuclear localization sequence, i.e. PKPKRKV, 0-6 histidine residues and an optional stearic acid group. Among these candidates, the peptide STR-HK, with sequence of STR-HHHPKPKRKV, exhibited good characteristics as a safe and efficient siRNA delivery vector, facilitating efficient siRNA delivery to mammalian cells with only a 15%-20% decrease in its cell viability. Moreover, the intratumoral injection of the STR-

HK/siRNA complexes achieved high anti-tumor activity in mice, with an inhibition rate of 62.8%. Our data revealed that introducing stearic acid into the peptide sequence improved its transfection ability, and the addition of histidine residues enhanced its endosome escape efficiency.

However, the previously designed peptide STR-HK and the STR-HK/siRNA complexes induced strong cytotoxicity *in vitro* with increasing amounts of peptide, i.e., the cell viability of STR-HK/siRNA complexes dropped to 50% when the peptide concentration increased to 4 μM. To decrease the toxicity of the delivery cargos, and further improve the gene-silencing efficiency, we designed a new series of cell-penetrating, co-assembling peptides, with the incorporation of stearic acid and a selected number of lysine, histidine and valine residues. The number of lysine, histidine and valine amino acids was carefully examined with respect to its binding affinity with siRNA molecules, and its gene-silencing efficacy induced by the corresponding peptide/siRNA complexes on a range of cell lines. Within the newly designed peptide family, the most pronounced gene silencing could be achieved with the peptide STR-H3K3V6, sequence STR-HHHKKKVVVVVV. The cell viability was further improved compared to the peptide STR-HK. In addition, to address possible immune responses, the biocompatibility of the peptide STR-H3K3V6 was evaluated in terms of complement activation and cytokine activation, and no obvious responses were observed *in vitro*.

Understanding the uptake mechanisms of our peptide-based siRNA delivery systems will facilitate the development of safe and efficient gene delivery vectors. Thus, the internalization process and intracellular trafficking of the STR-KV/siRNA complexes was explored. Heparin treatments revealed that the electrostatic interaction of our complexes with heparan sulphate

proteoglycans (HSPGs) at the cell surface was required to trigger the uptake process. Using physical and chemical endocytic inhibitors, it was found that the STR-KV/siRNA complexes mainly enter cells through an energy-independent mechanism, most likely involving direct translocation. The intracellular trafficking and internalization kinetics experiments further confirmed our complexes were uptaken through a non-endocytic pathway.

Acknowledgements

I would like to take this opportunity to express my gratitude to the people who gave me the possibility to complete this thesis. Firstly, I would like to thank my supervisor, Prof. Pu Chen, who gave me unlimited help and support, and provided me valuable advisory and critical comments on my work during the four years of study. He has always been an amazing teacher and guided me through difficulties, not only in the research, but also in my life. His industrious on work has always been a great example to me, and his enthusiasm for science has inspired me enormously in research.

I would also like to express my sincere gratitude to my PhD examination committee members who monitored my work and provided constructive comments on my proposal and thesis: Prof. Marc Aucoin and Prof. Micheal Tam from Chemical Engineering department, Prof. Shawn Wettig from the Pharmacy department, Prof. Elizabeth Gillies from the University of Western Ontario.

I also appreciated people who contributed to experiments and provided suggestions on my PhD research study. Professor Yongfang Yuan from School of Medicine of Shanghai Jiao Tong University, and her students who have collaborated with us on the *in vivo* studies. I would like to thank Dr. Feng Xu from AMOF of the UHN research center in Toronto who performed the confocal microscopy in this thesis, and his advices on the fluorescence studies and techniques. I would like to give my special thanks to the siRNA delivery subgroup members, Wen Xu, Dafeng, Chu, Tanya Sheinin, Mousa Jafari, Yong Ding and Sheng Lu, who provided various help and suggestions during my four years study and research.

I would also like to thank our current and previous group members, your comments and suggestions improved my research and presentation skills. In addition, I want to thank the Chemical Engineering department of the University of Waterloo, and the Waterloo Institute for Nanotechnology, for accepting me as a PhD student and allowing me to conduct my research here. I am deeply grateful to the financial support from the Natural Sciences and Engineering Research Council of Canada (NSERC), and the Canada Research Chairs (CRC) Program.

In the end, I would like to thank my family and my friends for providing me unlimited support and enormous encouragement on staying on the path. Without their love, I would not be able to walk this far, and none of my achievements would come true.

Table of Contents

List of Figures

List of Tables

List of Abbreviations

Acronym	Full name
AAV	Adenovirus-associated vectors
ABC	ATP-binding cassette
AD	Alzheimer's disease
AFM	Atomic Force Microscopy
AIDS	Acquired immunodeficiency syndrome
AMD	Age-related macular degeneration
ATCC	American Type Culture Collection
ATP	Adenosine triphosphate
BBB	Blood-brain barrier
BCSFB	Blood-cerebrospinal fluid barrier
Bcl-2	B-cell lymphoma 2
BSA	Bovine serum albumin
CHO-K1	Chinese hamster ovary
CLSM	Confocal laser scanning microscopy
Clu	Clusterin
CME	Clathrin-mediated endocytosis
CvME	Caveolae-mediated endocytosis
CPP	Cell-penetrating peptide
Cpz	Chlorpromazine
CSPGs	Chondroitin sulfate proteoglycans
DEG	Diethylene glycol
DDAB	Dimethyldioctadecyl-ammonium bromide
DLS	Dynamic light scattering
DM1	DEGylated C6M1
DMEM	Dulbecco's Modified Eagle Medium
DMRIE	Dimyristyloxypropyl-3-dimethylhydroxyethyl ammonium bromide
DOGS	Dioctadecylamido glycylspermine
DOPC	1,2-oleoyl-sn-glycero-3-phosphocholine
DOPE	1,2-dioleoyl-sn-glycero-3-phosphoethanolamine
DOTAP	1-oleoyl-2-[6-[(7-nitro-2-1, 3-benzoxadiazol-4-yl) amino]hexanoyl]-3-trimethylammonium propane
DOTMA	N-[1-(2,3-dioleoyloxy) propyl]-N,N,Ntrimethylammonium chloride
dsRNA	Double-stranded RNA
ED50	Effective dose for 50 percent of the group
EDTA	Ethylenediaminetetraacetic acid

EIPA	5-(N-ethyl-N-isopropyl) amiloride
EMEM	Eagle's Minimum Essential Medium
ELISA	Enzyme-linked immunosorbent assay
EtBr	Ethidium bromide
EPR	Enhanced permeability and retention
FACS	Fluorescence-activated cell sorting
FBS	Fetal bovine serum
FDA	Food and Drug Administration
FTIR	Fourier Transform Infrared
GAGs	Glycosaminoglycans
GAPDH	Glyceraldehyde 3-phosphate dehydrogenase
GFP	Green fluorescence protein
GnT-V	N-acetyglucosaminyltransferase V
HAART	Highly active anti-retroviral therapy
HBV	Hepatitis B virus
HCV	Hepatitis C virus
HD	Huntington's disease
HIV	Human immunodeficiency virus
HPV	Human papillomavirus
HSPGs	Heparan sulphate proteoglycans
IC50	Half maximal inhibitory concentration
IFN	Interferon
IL	Interleukin
LacCer	Lactosylceramide
LDH	Lactate dehydrogenase
LNPs	Lipid nanoparticles
LV	Lentivirus vectors
MBCD	Methyl-β-cyclo- dextrin
MDR	Multidrug resistance
MEM	Minimum Essential Medium
MR	Molar ratio
NC	Negative control
NLS	Nuclear localization sequence
nt	nucleotides
P-gp	P-glycoprotein
PAMAM	Poly amidoamine
PBS	Phosphate-bufferred saline
PCR	Polymerase chain reaction
PCL	Poly caprolactone

PD	Parkinson's diseases
PDI	Poly dispersity index
PEG	Poly ethylene glycol
PEI	Poly ethyleneimine
PFA	Paraformaldehyde
PLA	Poly-d,l-lactide
PLL	Poly-L-lysine
PPI	Poly propylenimine
PrP	Prion protein
PTGS	Post-transcriptional gene silencing
RISC	RNA-induced silencing complex
RNAi	RNA interference
RSV	Respiratory syncytial virus
RT-PCR	Reverse transcriptase PCR
SCA-1	Spinocerebellar ataxia type 1
SC5b-9	S-protein-bound C terminal complex
shRNA	Short hairpin RNA
siRNA	Small interfering RNA
SNALP	Stable nucleic-acid-lipid particle
STR	Stearic acid
TCC	Terminal Complement Complex
TEM	Transmission electron microscopy
TLRs	Toll-like receptors
TNF	Tumor necrosis factor
VEGF	Vascular endothelial growth factor

Chapter 1

Introduction

1.1 Overview

The discovery of RNA interference (RNAi) by Fire et al. in 1998 has been widely regarded as the most promising breakthrough in gene therapy [1]. RNA interference is a highly efficient regulatory process present in most eukaryotic cells by which double-stranded RNA (dsRNA) cleaves complementary mRNA, resulting in post-transcriptional gene silencing. RNAi has been used in various areas, ranging from basic research to clinical applications, e.g. it can be used to determine the biological functions of proteins or pathways [2, 3]. Also, since short interfering RNA (siRNA) can turn off problematic genes, it shows tremendous promise in curing human diseases, e.g. cancer, HIV, viral infections, neurodegenerative disorders, and others [4-8]. The first clinical application with siRNA started in 2004 for age-related macular degeneration (AMD) [9], following with multiple clinical trials in different diseases conducted in past 10-15 years. Among these therapeutic applications, ALN-TTR02 (Alnylam Pharmaceuticals) was reported a success in Phase II clinical trial, and a Phase III study was initiated in mid 2014, which was the first siRNA-based drug evaluated in Phase III clinical trials [10-13].

In basic experiments and therapeutic treatments, the long dsRNAs are commonly used to trigger the RNAi process as precursors of short interfering RNA[14]. After introduced into cytoplasm, the long dsRNA is firstly processed by the enzyme Dicer into siRNAs, and the siRNAs are then loaded onto RNA-induced silencing complexes (RISC) to initiate the RNAi processes [15, 16]. These post-processed siRNA are short duplexed RNA molecules, with a typical constitution of 19–23 nucleotides (nt) followed by two nucleotides at the 3' end overhang on both the sense and anti-sense strands, approximately 7.5 nm long and 2 nm in diameter [4]. In addition to dsRNAs, synthesized siRNAs was also demonstrated to suppress silence targeting genes effectively [20]. After combining with siRNA, RISC then unwinds the RNA duplexes and releases the sense strand of siRNA, resulting in a functional siRNA-RISC complex with guide strand of siRNA that directs a specific recognition of complementary mRNA [17-19]. The targeting mRNA is then cleaved near the middle of the region bound by the siRNA strand. After cleavage, the m7G cap or the poly-A tail that are essential to RNA stability is missing, induced a further degradation of mRNA fragments and prevention of protein expression. A schematic representation of RNA interference process is shown in Figure 1.1 [21].

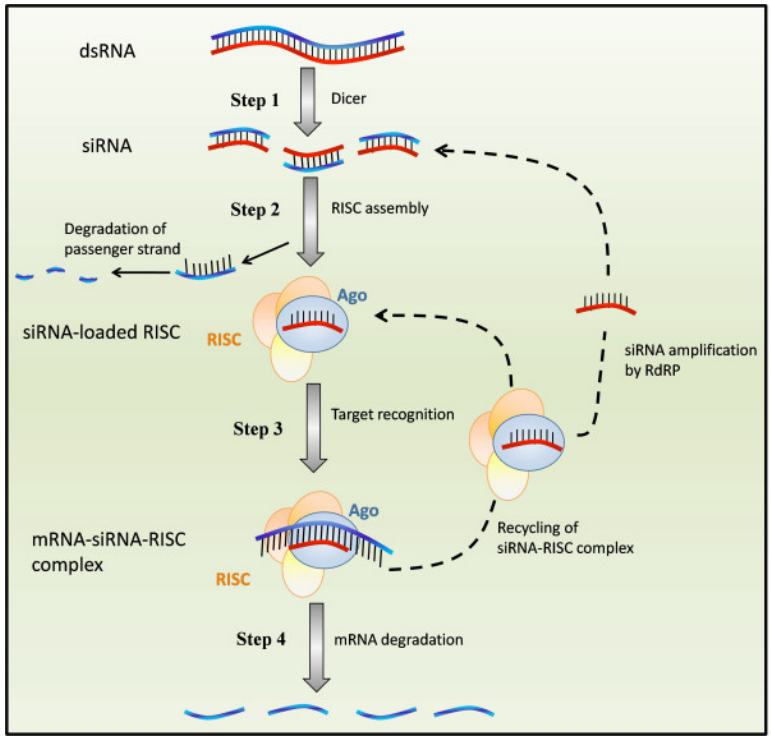

Figure 1.1 Schematic representations of RNA interference processes (Adapted from [10]). Step 1: dsRNA cleaves into fragments of 21-23 base pairs siRNA by the enzyme Dicer. Step 2: siRNAs are loaded into RISC and the sense strand is discarded and degraded, and the anti-sense strand remains within RISC as template. Step 3: the anti-sense strand assembles into an active RISC complex, which contains the siRNA bound to targeting mRNAs. Step 4: mRNA degradation is induced.

Despite abundant promises, the development of RNAi therapies is limited by the unfavorable physicochemical properties of siRNAs, e.g., relatively large molecule weight, negatively charged surface, hydrophilicity, sensitivity to nuclease degradation, instability with short plasma half-lives (15 min to 1 hour) [16, 22]. It has been reported that chemical modifications in the sugars and the phosphate ester backbone of siRNA can improve its

nuclease resistance [9-11], and conjugation with hydrophobic groups with siRNAs can enhance its cell uptake with minor decrease of silencing efficiency. The development of efficient and safe delivery systems for siRNA has been applied as the main solution to overcome the obstacles [23]. The delivery systems can either self-assembled or covalently conjugated with siRNAs, designed to protect siRNAs from degradation while reducing the clearance rate of siRNAs and increasing the retention time. In addition, the delivery system should ensure effective biodistribution of siRNAs in the human body, facilitating cellular uptake and endosome release of siRNAs, while not inducing immune responses and have minimal toxicity. Different delivery strategies have been developed [24], including viral-based strategy, as well as cationic polymers [25-28] and lipid- [29-31] or peptide-based [32-35] vectors. Viral-based delivery strategies are considered the most efficient delivery systems [36], which have been applied in various *in vivo* studies [36, 37], e.g., Huntington's disease, Alzheimer disease, Amyotrophic lateral sclerosis, and others. Although they exhibited high efficiency *in vivo*, the application of viral vectors is limited because of strong inflammatory responses caused by viruses [38]. Cationic lipids have been used to deliver siRNAs, and satisfactory results are achieved both *in vitro* and *in vivo*. However, studies demonstrate that cationic lipids may stimulate specific immune and anti-inflammatory responses [31], and may cause rapid elimination by reticuloendothelial system [39]. Although modifications have been made to address the toxicity issues, long term *in vivo* safety still remain in question and requires further investigation. Synthetic and natural polymers have been developed as siRNA carriers, which also suffer from toxicity and immunogenicity issues [33]. Thus, the clinical applications of polymer-based strategies have been hindered. Peptide-based carriers have

been developed as an alternative for safer *in vitro* and *in vivo* delivery. Consisted of 5–30 amino acids, the peptides can cross cell membranes and facilitate cellular uptake of various molecules pharmaceuticals [40], such as siRNAs, DNAs, proteins, and others.

Our group is focused on developing peptide-based siRNA delivery systems. A few peptide libraries have been designed and developed by our group members in past several years, in the aim of deliver siRNAs into cell with minimal toxicity. After high throughput screening, several peptides with high transfection efficiency were selected for further investigation. Physicochemical characterizations were studied first, including the interaction between peptides and siRNAs; the size and zeta potential; the morphology of the complexes, and others. The cellular uptake efficiency, as well as the cytotoxicity, knockdown efficiency on various cell lines, biocompatibility were then investigated with optimized concentrations and combinations of peptide/siRNA complexes. The uptake pathway and endosome release mechanism of complexes was also explored with selected candidates. To investigate the potential gene therapy *in vivo*, a human tumor xenograft in a nude mice model was applied to evaluate the *in vivo* efficacy and toxicity.

Based on the results reported in this work, strategies could be developed to design efficient peptides to construct functional nanocarriers for *in vitro* siRNA delivery and cancer gene therapy.

1.2 Objective

The main objective of this study is to develop a safe and efficient peptide-based siRNA delivery system. To achieve this goal, modification and design of peptides are applied and

studied in each chapter, including the interactions of peptide with siRNA, silencing efficiency and toxicity *in vitro* and *in vivo*, biocompatibility and serum stability of complexes, and also the cellular uptake pathways.

The specific objectives are listed in the following:

(1) Design of peptides to achieve high siRNA transfection efficiency and low cytotoxicity, including newly designed peptides and structurally modified peptides.
(2) Characterize of peptide/siRNA complexes, including peptide and siRNA binding capacity and morphologies studies.
(3) Investigate of silencing efficacy, toxicity, serum stability and biocompatibility of the complexes *in vitro* on selected cell lines.
(4) Evaluate of the antitumor activity of complexes *in vivo* on a mouse xenograft tumor model.
(5) Study the cellular internalization mechanism of the complexes.

1.3 Thesis outline

This thesis consists of seven chapters. The scope of each chapter is listed as follows:

Chapter 1 gives a brief introduction of the thesis, including siRNA structure, RNA interference mechanisms, and the promising future of peptide-based siRNA delivery system. The research objectives and thesis organization are also given here.

Chapter 2 presents a review of current and potential therapeutic applications of siRNAs, current gene delivery approaches including physical methods and viral and non-viral carrier-

based delivery system. Cellular internalization pathways of siRNA delivery vectors are also reviewed in this chapter.

In order to improve the serum stability of a previously reported peptide C6M1, a diethylene glycol moiety was added to C6M1. Physicochemical characterizations, serum stability, transfection efficiency of C6M1/siRNA and DM1/siRNA were conducted in Chapter 3. The diethylene glycol modification could improve the complexes stability without compromising the transfection efficiency.

However, the knockdown efficiency of both complexes is very low. To enhance the transfection efficiency, a new peptide library was developed and evaluated in Chapter 4. The possibility of the introducing stearic acid into the peptide design was studied, with respect to complexes formulation, transfection efficiency, cytotoxicity, and *in vivo* xenograft model investigation. Peptide STR-HK showed great gene-silencing efficiency both in vitro and in vivo, yet the cell viability of complexes decreased with increasing amounts of peptide.

To further improve the performance of peptide and complexes, a peptide library with a combination of stearic acid, lysine, and valine was developed and the structure-activity relationship of peptides is explored in Chapter 5. The optimal peptide with lowest cytotoxicity and highest transfection efficiency was determined on various cell lines.

In Chapter 6, the cellular uptake mechanism of the most promising candidates in chapter 5 is investigated. The specificity of several chemical endocytosis inhibitors and internalization kinetics of the complexes were also studied. Chapter 7 summarizes the original contributions of this research and recommendations for future work.

The peptides used in each chapter are listed below:

Table 1.1 Summary of peptides used in this thesis

Chapter	**Peptide**	**Sequences**
Chapter 3	C6M1	Acetyl-RLWRLLWRLWRRLWRLLR-NH_2
	DM1	Degylation-RLWRLLWRLWRRLWRLLR-NH_2
Chapter 4	H0K	Acetyl-PKPKRKV-NH_2
	HK	Acetyl-HHHPKPKRKV-NH_2
	STR-H0K	Stearyl-PKPKRKV-NH_2
	STR-HK (main)	Stearyl-HHHPKPKRKV-NH_2
	STR-H6K	Stearyl-HHHHHHPKPKRKV-NH_2
Chapter 5	STR-H0K3V6	Stearyl-KKKVVVVVV-NH_2
	STR-H3K3V6 (main)	Stearyl-HHHKKKVVVVVV-NH_2
	STR-H6K3V6	Stearyl-HHHHHHKKKVVVVVV-NH_2
	STR-H3K6V6	Stearyl-HHHKKKKKKVVVVVV-NH_2
	STR-H3K9V6	Stearyl-HHHKKKKKKKKKVVVVVV-NH_2
	STR-H3K3V9	Stearyl-HHHKKKVVVVVVVVV-NH_2
Chapter 6	STR-KV	Stearyl-HHHKKKVVVVVV-NH_2

Chapter 2

Literature Review

2.1 RNAi Technology

2.1.1 Applications of RNAi technology

The applications of RNAi involve basic scientific research in gene therapy, e.g., functional genomics study [41, 42], the development of gene-specific drugs [7], and others. In basic biology research, short interfering RNA is a powerful tool to determine the biological functions of proteins or pathways [2, 3]. In pharmaceutical research, short interfering RNAs have been used as potential therapeutic agent to turn off problematic genes. Additionally, short interfering RNA therapies have been widely and effectively applied in the treatment of a variety of human diseases. Various studies have reported the success of silencing the disease genes by administration of siRNAs. SiRNAs show promising results as therapeutic agents for viral infections, cancer, HIV, and the applications of siRNAs have been extended into central nervous system therapeutics, as well as cardiovascular therapeutics, brain injuries, neurodegenerative disorders, and other fields [4-8]. Several types of diseases that are very common and are well studied in siRNAs field will be discussed in this chapter.

Cancer

Cancer is one of the leading causes of death around world, especially in low- and mid-income countries. The number of deaths caused by cancer keeps growing, and is estimated to rise to 13.1 million in 2030 [15]. Current cancer treatment involves chemotherapy, radiation and surgery, and through significant progress has been made, there are still limitations. Studies demonstrate that various genes are involved in cancer development, and the mutations of these genes might cause uncontrollable cell proliferations and/or differentiations [43]. RNAi has advantages over regular cancer therapies, e.g., the specificity to inhibit target genes, and the relatively low toxicity to human beings. The application of RNAi technology provides a safe and efficient approach to reduce the expression of various oncogenes to a controllable level [4].

Oncogenesis. A number of genetic mutations are found in human cancer and can drive oncogenesis actively. The oncogene Bcl-2 for instance, is overexpressed in various human tumors [44]. Studies demonstrate siRNAs targeting the Bcl-2 gene can induce cell apoptosis both *in vitro* and *in vivo* [45]. Around 80 oncogenes are identified in breast cancer [4], including clusterin (Clu) [46], myelocytomatosis viral oncogene homolog (c-Myc), murine double minute clone-2 (MDM2) [47], FOXM1 [48], and others. Overexpression of Clu is reported to be associated with elevated tumor size. The silencing of Clu by siRNAs induced a decrease of cell proliferation and an increase of apoptosis rate *in vitro*, and a reduction of tumor increasing rate [46].

Cell proliferation. Silencing the genes related to cell cycle might result in hindering cell division. Akt2 is related to the mitochondria subcellular localization and activation of p70S6K

pathway, and siRNA-targeting Akt2 can induce arrest of cell cycle in G0/G1 state [49]. Malignant transformation leads to tumor cell growth, adhesion, and migration. Studies show that N-acetyglucosaminyltransferase V (GnT-V) is overexpressed in various malignant tumors, and siRNA-targeting GnT-V has shown the potential of reducing cell proliferation rate and thus reducing metastasis and invasion possibilities [50].

Angiogenesis. Angiogenesis is essential for neoplasia, and tumor metastasis, and is controlled by pro- and anti-angiogenic molecules in tumor [51]. Inhibition of angiogenesis results in limited tumor growth at a diameter of 2 mm [51, 52]. Vascular endothelial growth factor (VEGF) is up-regulated in various tumors, and RNAi technique applied to silence VEGF can successfully inhibit angiogenesis. Silencing VEGF intravenously and intratumorally in a pancreatic tumor xenograft model significantly down-regulated the expression of VEGF and thus reduced cancer cell proliferation and tumor growth [53]. An up to 97% decrease of tumor volumes was achieved by local delivery of chitosan/siRNA nanoplexes into rats with breast tumors [54].

Chemotherapy resistance. Drug resistance limits the effectiveness of chemotherapy. The explanation of multidrug resistance (MDR) mechanisms involves the overexpression of P-glycoprotein (P-gp) [55], ATP-binding cassette (ABC) transporters [56], multidrug resistance-associated protein-1 (MRP1), and others. P-gp siRNA treatment induced almost complete restoration of intracellular accumulation of doxorubicin [57]. Silencing of the MRP1 gene leads to 85% to 90% reduction in MRP1 expression in doxorubicin-resistant MCR-7 cell line

[58]. Treatment with siRNA targeting on MRP1 resulted in the decrease of MRP protein in various human cancer cell lines, and improved epirubicin efficiency *in vivo* [59].

Neurodegenerative diseases

Neurodegenerative disorders are progressive diseases, accompanied by age-related loss of specific subsets of neural cells, and include Huntington's disease (HD), Parkinson's diseases (PD), Alzheimer's disease (AD), and others. Currently, an effective therapy for most neurodegenerative diseases is unavailable [60], and the expensive treatments available may improve the symptoms or provide symptomatic relief, but may not change the progress of the diseases [61]. The estimated cost for the treatment of Alzheimer's disease in the U.S. is 100 billion annually in 1990s [62], and the number still keeps rising. A series of challenges for neurodegenerative disease therapies involve the effective crossing of blood-brain barrier (BBB) and blood-cerebrospinal fluid barrier (BCSFB) [63]. RNAi-based therapies have emerged as a promising treatment in neurodegenerative disease, which provides an approach to inhibit disease related genes.

The first siRNA-based therapy for Huntington's disease was reported in 2005, which demonstrated a success of inhibition of the target gene in striatum and cerebellum *in vivo*, and showed a significant improvement in pathology and behavior [64]. APP, BACE-1 and Tau are related to the treatment of Alzheimer's diseases. Inhibition of BACE or APP expression resulted in the reduction of Aβ production in cultured neurons [65] or transgenic mouse overexpressing mutant APP [66]. Several successful investigations of RNAi-based therapy of neurodegenerative diseases on different animal models are summarized in Table 2.1 [67].

Table 2.1 Summary of RNAi-based therapies of neurodegenerative diseases *in vivo* [67]

Disease	Animal model	Agent	Age	Stage	Outcome
HD	HD-N171-82Q	rAAV1-shRNA	4 weeks	Presympt	Partial prevention of inclusion formation, gait and rotarod abnormal phenotypes
	R6/1	rAAV5-shRNA	6-8 weeks	Presympt	Reduction in striatal inclusions, limited rescue of motor function and transcriptional dysregulation
	R6/2	Liposome-siRNA	Postnatal day 2	Presympt	Partial rescue of inclusion formation, weight loss, rotarod and open field. Mild effect on longevity
	HD190QG	rAAV5-shRNA	8-12 weeks	Sympt	Reduced aggregates and increased DARPP-32 expression; no behavioral/lifespan improvement
SCA1	Ataxin1(Q82)	rAAV1-shRNA	7 weeks	Presympt	Prevention of inclusion formation and cell loss with partial improvement in rotarod performance

FALS	SOD1(G93A)	Lentivirus-shRNA	7 days	Presympt	Delayed rotarod and gait abnormalities, weight loss, motor neuron death and animal demise
	SOD1(G93A)	Lentivirus-shRNA	40 days	Presympt	Delayed disease onset, slowed motor dysfunction, reduced cell death and muscle atrophy
	SOD1(G93A)	Transgenic-shRNA	Breeding	Presympt	Delayed disease onset, death and partial prevention of motor neuron demise
	SOD1(G93A)	Transgenic-shRNA	Breeding	Presympt	Reversion to wild type behavioral and histopathological phenotype
AD	APP double transgenic	Lentivirus-shRNA	10 months	Sympt	Reduced Aβ production, amyloid plaques and neuronal death; improved learning/memory
	lv-APP	HSV-shRNA	4 weeks	Wild type	Reduced APP expression and Aβ production by immunostaining
PD	lv-αsyn	Lentivirus-shRNA	Adult	Wild type	Silenced human synuclein transgene; no additional assessment

1) Transgenic mice expressing shRNA were crossed with the mouse model of the disease. 2) Only in low copy number SOD1(G93A) transgenics. 3) The hippocampi of 4-week-old mice were co-injected with lentivirus expressing APP containing a disease mutation and herpes

simplex virus encoding a shRNA targeting the APP transgene. 4) Wild-type rats were coinjected with lentivirus expressing a human α-synuclein transgene and the therapeutic vector.

Virus infection diseases

Diseases caused by viral infection are another major causes of death worldwide. RNAi-based therapies have been demonstrated effective to treat and prevent viral infections [68], including hepatitis B virus (HBV), hepatitis C virus (HCV), human papillomavirus (HPV), human immunodeficiency virus (HIV), and others.

HIV is a retrovirus that causes acquired immunodeficiency syndrome (AIDS). Despite decades of research, 33.4 million people are affected by AIDS and the number keeps increasing [8]. Current HIV treatment utilizes highly active anti-retroviral therapy (HAART) to improve the lives of patients, by decreasing the appearance of anti-HIV resistant strains [69]. However, HAART is limited by possible drug resistant variants, as well as the toxicities [70]. Studies show that siRNA targeting on various viral genes inhibits HIV replications effectively, including reverse transcriptase [71], Tat [72], Rev [73], Gag [74], CD4 [75], CCR5 [76], and others. The inhibition of CD4 through RNAi process [75] can successfully suppress viral entry, viral load, and others. Treatment with siRNA targeting CCR5 resulted in down-regulation target of the gene and an inhibition of HIV replications in various human cell lines and primary cell lines [77]. The first clinical trial of RNAi-based therapy for AIDS treatment was initiated in 2007 with a short hairpin siRNA (shRNA) vector rHIV7-shI-TAR-

CCR5RZ (clinical government code NCT00569985), and the study is still ongoing but not recruiting participants.

HSV-2 is essential for HIV-1 transmission [78], and more than 20% of U.S. population is affected by HSV-2 [79]. Treatment with siRNA targeting on UL-39 genes in HSV-1 can reduce the expression of target gene and thus inhibit HSV-1 replication *in vitro* [80]. In addition, siRNA-based microbicindes provides effective protection on mice against HSV-1 infection [81].

HPV Infection results in patients who develop malignant tumors. Cervical cancer remains the most common cancer type in developing countries, and 0.5 million cases occur each year around the world [82]. More than 90% of cervical cancers are driven by viral protein E6 and E7 [83]. Studies show that treatment with siRNA targeting HPV 16/18 E6/E7 genes inhibits cervical cancer proliferation both *in vitro* and *in vivo* [84, 85]. Additionally, silencing E7 by siRNAs induced cancer cell apoptosis, and the expression of E7 can be reduced by 4-fold through RNAi processes [86].

2.1.2 RNAi in clinical trials

Successes of *in vivo* experiments cultivated sufficient interest and confidence to initiate clinical applications. The first clinical trial with siRNA started in 2004 for treating age-related macular degeneration (AMD) [9]. Currently, multiple clinical trials are being conducted in areas including cancer treatments, diabetic retinopathy, hepatitis C, and others. Several of these clinical trials are listed in Table 2.2 [10, 87, 88].

Most siRNAs are administered by local delivery in clinical trials, especially the one with delivery strategy based on naked siRNAs. However, systemic administration is also required when intravitreal and/or intranasal routes are not appropriate for the diseases. Hypercholesterolemia, for instance, is treated through intravenous injection, in a Phase I trial was initiated by Tekmira with developed drug PRO-040201 targeting ApoB [89]. However, Tekmira terminated this clinical trial in early 2010, due to immune system activations. In contrast, ALN-PCS02 (developed by Alnylam Pharmaceuticlas) has been reported success on reduction of cholesterol in Phase I trial treating the same disease. In addition, Alnylam also successfully developed various siRNA-based candidates, including ALN-TTRsc, ALN-PCS02, ALN-VSP02, and others. To treat TTR-mediated amyloidosis, ALN-TTR02 was reported to significantly knockdown target protein by up to 93% in Phase II clinical trials, while this siRNA formulation was generally safe and well tolerated. Alnylam initiated Phase III trials of ALN-TTR02 with their partner Sanofi in mid 2014, and this is the first siRNA-based drug evaluated in a Phase III clinical trial [10-13].

Table 2.2 RNAi therapeutics clinical pipeline [10, 87, 88]

Candidate	**Target gene**	**Disease**	**Phase**	**Status**	**Clinical Trial Gov. Identifier**
ALN-RSV01	Nucleocapsid	RSV infections	II	Completed	NCT00658086
TKM-100201	VP24, VP35, Zaire Ebola l-polymerase	Ebola virus infection	I	Terminated	NCT01518881
TKM-080301	PLK1	Cancer	I/II	Recruiting	NCT01262235

ALN-VSP02	KIF11 and VEGF	Solid tumours	I	Completed	NCT01158079
siRNA–EphA2–DOPC	EPHA2	Advanced cancers	I	Active	NCT01591356
Atu027	PKN3	Advanced solid cancers	I/II	Recruiting	NCT01808638
CALAA-01	RRM2	Solid tumours	I	Terminated	NCT00689065
siG12D LODER	KRAS	Pancreatic cancers	II	Active	NCT01676259
PRO-040201	APOB	Hypercholeste-rolemia	I	Terminated	NCT00927459
ALN-PCS02	PCSK9	Hypercholeste-rolemia	I	Completed	NCT01437059
ALN-TTR02	TTR	TTR-mediated amyloidosis	III	Recruiting	NCT01960348
ALN-TTRsc	TTR	TTR-mediated amyloidosis	I	Recruiting	NCT01814839
			II	Recruiting	NCT01981837
ARC-520	Two conserved regions of HBV transcripts	Hepatitis B	I	Recruiting	NCT01872065

			II	Recruiting	NCT02065336
ND-L02-s0201	SERPINH1	Liver fibrosis	I	Completed	NCT01858935
AGN211745	FLT1	Age-related macular degeneration	II	Terminated	NCT00363714
PF-655	DDIT4	Age-related macular degeneration	II	Completed	NCT00713518
(PF-04523655)		Choroidal neovascularizatio n, diabetic retinopathy and diabetic macular edema	II	Completed	NCT01445899
Bevasiranib	VEGFA	Macular degeneration	II	Completed	NCT00259753
		Diabetic macular edema	II	Completed	NCT00306904
QPI-1007	CASP2	Optic atrophy and non-arteritic anterior ischemic optic neuropathy	I	Completed	NCT01064505
		Acute primary angle-closure	II	Active	NCT01965106

		glaucoma			
SYL1001	TRPV1	Ocular pain and dry eye syndrome	I/II	Recruiting	NCT01776658
SYL040012	ADRB2	Ocular hypertension and open angle glaucoma	II	Completed	NCT01739244
I5NP	TP53	Kidney injury and acute renal failure	I	Completed	NCT00554359
		Delayed graft function and complications of kidney transplant	I/II	Active	NCT00802347
RXI-109	CTGF	Cicatrix and scar prevention	I	Active	NCT01780077
		Hypertrophic scar		Recruiting	NCT02030275
		Keloid		Recruiting	NCT02079168
TD101	KRT6A (N171K mutation)	Pachyonychia congenita		Completed	NCT00716014

Despite the exciting potential, various challenges limit the application of RNAi in therapeutics, including the instability of unmodified siRNA molecules in bloodstream, the off-

target effects, the possibility of activating immune responses, and others. The development of a safe and efficient delivery strategy is now in urgent need.

2.2 Current delivery systems

2.2.1 Challenges and barriers

siRNA therapies have several advantages over traditional small molecule drugs. First, siRNAs can be rationally designed, while the traditional small molecule drug requires heavy screening processes prior to *in vivo* test, which is time-consuming and may be unsuccessful sometimes. In addition, siRNA therapies have relatively high specificity on their targeting sites, while traditional drugs are usually nonspecific accompanied by extensive side effects [90]. On the other hand, the applications of siRNA are limited by their poor stability, pharmacokinetics and off-target effects. Figure 2.1 lists the biological *in vivo* barriers of siRNAs [91].

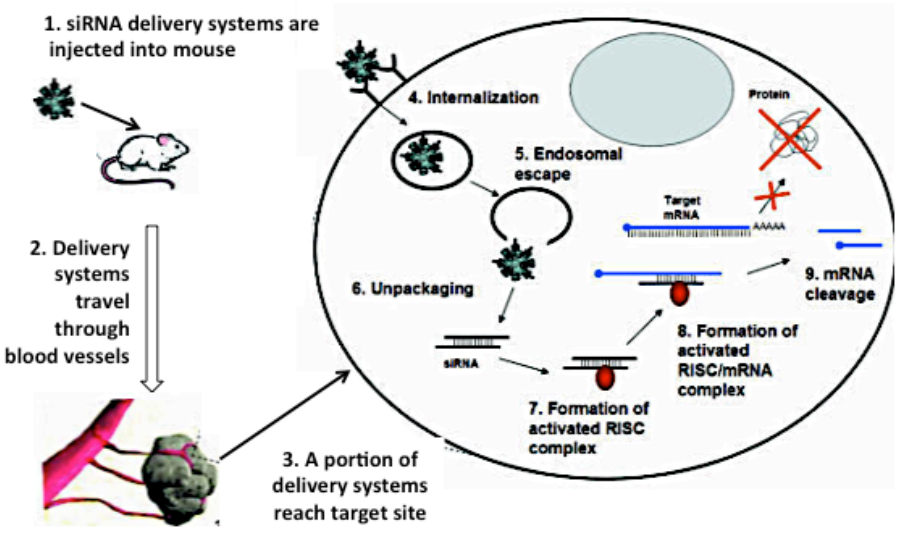

Figure 2.1 Schematic representations of *in vivo* siRNA systemic delivery key steps [91]**.** Steps 1-3 represent the *in vivo* delivery steps of siRNA systems. Steps 4-9 represent the processes of *in vitro* delivery steps of siRNA systems.

1) Biological instability

SiRNAs are relatively stable in various conditions; for instance, their biological activity will not be changed with either short exposure to high temperature (less than 95ºC) or long incubation at low temperature (less than 1 year at 4ºC) [92], as long as no nuclease is present in the environment. However, during systemic delivery, siRNAs are exposed to nuclease degradation, and the reported half-life of unmodified siRNAs under physiological conditions ranges from 15 min to 1 hour [16, 22]. In addition, several studies demonstrate that siRNAs are preferentially taken up by the kidney, and will be eliminated within 1 hour due to their relatively low molecular weight (~13 kDa) [14, 15].

2) Off-target effects

Although it is believed to be highly specific and only affects the gene with a complementary sequence, RNAi also has the ability to induce non-specific off-target gene silencing [93]. Various mechanisms have been proposed, and it has been noticed that siRNAs can induce gene regulation of unintended transcripts through partial sequence complementarity in the seed region of siRNAs (positions 2-7) to the of the off target gene [94].

3) Immune response

Long dsRNA or high levels of siRNAs may stimulate the immune system and the production of cytokines both *in vitro* and *in vivo*, which involves the activation of interferon (IFN) and pro-inflammatory cytokines, e.g., IL-6, TNF-α, and COX-2 [95, 96]. Studies show

that the induction of the innate immune response is mediated by the binding of pattern recognition receptors known as Toll-like receptors (TLRs) with siRNA molecules, including TLR-3, TLR-7 and TLR-8 [97, 98]. SiRNAs induced immune response do so in a sequence-dependent manner, for instance, TLR-7 and TLR-8 are more likely to be activated if siRNAs contain a 5'-GUCCUUCAA-3' motif [99, 100].

4) Cellular uptake

Due to the anionic nature and relatively large molecular weight, siRNAs cannot cross the cell membrane by themselves, and thus a delivery strategy is required to promote cellular internalization. Delivered by various delivery systems, siRNAs are mainly internalized through an endocytic pathway. After taking up the external nanoparticles, the early endosomes subsequently turn into late endosomes and then are relocated to lysosomes, which contain various nucleases to digest siRNAs with an acidic pH around 4.5. The siRNAs not escaping from endosome will be degraded eventually [101].

Some chemical modifications on siRNA molecules have been proposed to overcome these barriers without compromising the efficacy. Nuclease resistance, for instance, can be improved by introduction of a $-O-CH_2-$ linker at the 2'-fluoro, 2'-O-methyl, 2'-halogen, 2'-amine, 2'-deoxy, and the bridging of 2'- and 4'-position of sugar of the ribose [15]. Moreover, 2'-O-methyl on the sense strand can decrease the immune activation [102], and on the antisense strand can minimize the off-target effects [103, 104]. Besides, modifications on the backbone [105] and nucleobase [106] to protect siRNAs in serum and cytoplasm have also been investigated with success.

In spite of these efforts, a safe and efficient delivery strategy is still required to facilitate the uptake of siRNAs to target cells to activate the RNAi processes. The efficient siRNA delivery strategies developed in the last 15 years involve different physical approaches, viral and non-viral delivery systems, and the direct uptake of naked siRNAs on certain cell lines [107]. Physical methods of mediating siRNA delivery, e.g., microinjection, electro-permeabilization, have been investigated in siRNA application for more than 10 years [108, 109]. Physical methods are highly efficient to deliver into small amounts of cells, and may avoid the stimulation of possible immune responses [109], but it will induce cell damage and lack the potential to be used for *in vivo* and therapeutic applications [110]. Viral delivery strategies, as well as the lipid-, polymer-, and peptide-based strategies, and targeting strategy will be discussed here.

2.2.2 Viral based delivery systems

Viral vector systems are considered as the most efficient strategy to deliver siRNAs into cells [36]. Various virus-based delivery strategies have been developed and optimized *in vitro* and *in vivo*, evaluating RNAi in the treatment of neurodegenerative diseases, retinal diseases, cardiac disease, viral infections, and cancer. Adeno-associated virus vectors (AAV) and lentivirus vectors (LV) are the most frequently used siRNA delivery vectors in a number of *in vivo* studies [36, 37], including mouse models of Huntington's disease, Alzheimer disease, Amyotrophic lateral sclerosis, and others.

AAV serotype 1 vectors that mediate siRNA targeting of the human ataxin-1 gene driven by the pol III H1 promoter have been used to treat a mouse model of spinocerebellar ataxia type 1 (SCA-1) [107, 111]. Following injection into the cerebellum, the vector can resolve the disease-related inclusions found in SCA-1 mice and improve motor coordination. The first therapeutic application of viral vector-mediated siRNA was reported using LV vectors to target the prion protein (PrP) [112]. The LV/siRNA vector was injected into the hippocampus of mice with previously established prion disease. Reduction of up to 80% of hippocampal PrP mRNA expression was achieved with a single focal injection. Early behavioral deficits of prion disease were prevented, and the lifespan of the mice was increased by 23.5%. Unfortunately, non-specific cytotoxic effects were observed following treatment with LV/siRNA vectors. The comparisons of AAV and LV based delivery strategies are summarized in Table 2.3 [15].

Table 2.3 Comparison of AAV and LV based delivery systems [15]

	Adenovirus-associated vectors (AAV)	**Lentivirus vectors (LV)**
Gene expression	Transient or stable	Transient or stable
Integration into cell genome	No	Yes
Immune stimulation	Very low	Low
Advantages	Non-inflammatory, non-pathogenic	Persistent gene transfer in most tissues
Disadvantages	Small packaging size (4.5 kb)	Integration might induce oncogenesis in some applications

Although exhibiting high efficiency *in vivo*, the application of viral vectors is limited as a result of the strong inflammatory responses and caused by viruses [38]. Moreover, viruses can be rapidly eliminated by antibodies and immune systems of the host. Additionally, viruses may cause fatal diseases including allergy and virus infections. The clinical trials have been put on hold before the success development of a safe and suitable viral system [90, 113].

2.2.3 Lipid based delivery systems

Liposomes are the most commonly used methods for siRNA delivery, with an aqueous core enclosing hydrophilic drug in a phospholipid bilayer [114]. Lipoplexes are the complexes formed by liposomes and siRNAs, via hydrophobic and electrostatic interactions. The hydrophobic tails of lipids align with each other inside the lipoplexes, while the hydrophilic heads align outside to form a stable complex in aqueous solutions. Electrostatic interactions occur between the positive charges of the cationic lipids and the negatively charged phosphate backbone of siRNAs. The formulation of lipoplexes is highly effective, by general mixing of two components and incubating for different time periods.

Cationic liposomes are the most commonly used non-viral delivery systems for nucleic acids, including plasmid DNAs, siRNAs, and oligonucleotides. Consisting of a positively charged cap, cationic lipids form complexes with siRNAs through electrostatic interactions, and can facilitate cellular uptake by interacting with negatively charged cell membranes [115].

Although satisfactory results have been obtained both *in vitro* and *in vivo*, the severe toxicity and inflammatory effects limits the applications of siRNA delivery [116]. In addition, studies show that cationic lipids may activate the complement immune system causing rapid elimination by macrophages in reticuloendothelial system, and the high cytotoxicity to macrophage and other immune cells is a major concern (ED50 less than 50 nmol/l) [39]. Well-developed cationic lipids based siRNA delivery strategy involves N-[1-(2,3-dioleoyloxy) propyl]-N,N,Ntrimethylammonium chloride (DOTMA), dioctadecylamido glycylspermine (DOGS), 3b[N-(N′,N′-dimethylaminoethane)-carbamoyl) cholesterol (DC-Chol), dimethyldioctadecyl-ammonium bromide (DDAB), dimyristyloxypropyl-3-dimethylhydroxyethyl ammonium bromide (DMRIE), and 1-oleoyl-2-[6-[(7-nitro-2-1, 3-benzoxadiazol-4-yl) amino]hexanoyl]-3-trimethylammonium propane (DOTAP) [117].

Neutral liposomes have been developed in the past decade, characterized of non-toxic and no immune activation. 1, 2-distearoyl-sn-glycero-3-phosphocholine (DSPC), 1,2-oleoyl-sn-glycero-3-phosphocholine (DOPC) and 1,2-dioleoyl-sn-glycero-3-phosphoethanolamine (DOPE) have been proven to be successful for *in vitro* and *in vivo* siRNA delivery [118]. It has been reported that systemic intravenous injection of DOPC/siRNA nanoparticles can inhibit target protein expression 10-fold more efficient than cationic lipids/siRNA nanoparticles [119-121]. The third type of liposome based siRNA delivery systems is solid lipid-based strategy, e.g., stable nucleic acid lipid particles (SNALPs). The lipid bilayer of SNALPs consists by cationic and fusogenic lipids, which are coated with polyethylene glycol to avoid detection by macrophages and increase the circulation half-life of nanoparticles. Studies show the intravenous injection of SNALP/siRNA nanoparticles can inhibit

apolipoprotein B for 11 days [122], and the Phase I clinical trial of SNALP/siRNA targeting Plk1 was initiated in 2010 by Tekmira Pharmaceuticals (Burnaby, BC, Canada) (TKM080301) [123]. Alnlam Pharmaceuticals also developed SNALP based siRNA therapy, and initiated Phase I trial in 2009 (ALN-VSP02) [89].

Several modifications have been made to lipid-based carriers to increase their efficiency. Polyethylene glycol is added to carriers to prolong their circulation time in the blood and avoid being taken up by reticuloendothelial system, which is also known as "Stealth Liposome" [124]. Conjugating with a suitable antibody with high specificity and affinity for the target antigen, the efficiency of liposome uptake by the target tissue is increased [125]. Selected examples of the lipid-based siRNA therapeutic applications reported *in vivo* are shown in Table 2.4 [126]. Commercially available lipid-based transfection reagents include Lipofectamine (Invitrogen, life technology), RNAifect (Qiangen), Oligofectamine (Invitrogen, life technology), and others.

Table 2.4 Examples of liposome/siRNA delivery systems applied *in vivo* [125]

Liposomes	**siRNA target**	**Animal model**	**Results (gene silencing)**
DOPC liposomes	EphA2	Orthotopic model of advanced ovarian cancer in female athymic nude mice	86-91% reduction of tumor growth with combination therapy (siRNA-liposomes and paclitaxel), 35-50% reduction of tumor growth with siRNA-liposomes alone
SNALP	HBV	Female CD-1	Specific dose-dependent reduction

	(modified)	mice	in HBV-mRNA
SNALP	ApoB	Cynomolgus monkeys	Dose dependent silencing of ApoB mRNA (about 90% for the 2.5 mg/kg dose)
SNALP	ApoB (modified)	Balb/C mice	Potent silencing of ApoB mRNA (82%). Significant reduction in serum ApoB (74%), and cholesterol (52%)
DOTAP liposomes	TLR-4	Fenake C57BL/6 mice	Potent induction of both type I and II interferon response and activation of STAT1
scL-HoKc	HER-2 (modified)	Tumor xenograft in female athymic nude mice	Silencing of target gene (virtually elimination of HER-2), downstream components and significan tumor growth inhibition
CCLA-based cationic liposomes	c-raf	Human breast tumor xenograft model in SCID mice	73% tumor growth inhibition
DDAB/chlesterol liposomes	Caveolin-1	Male CD1 mice	Selective reduction of caveolin-1 expression by about 90% within 96h
LIC-101	Bcl-2 (human)	Model of liver metastasis in male BALB/c	75% tumor growth reduction

		mice	
LNP01	Factor VII	C57BL/6 mice	Accumulation in liver (over 90%). Reversible, long-duration gene silencing without loss of activity following repeated administration

2.2.4 Polymer and dendrimer based delivery systems

Linear or branched cationic polymers with repeated units of monomers are another class of siRNA delivery system. Mono-dispersed dendrimers are highly branched cationic, the structures of which are usually three-dimensional spherical. The advantages of polymeric carriers in siRNA delivery are the precise nanoscopic size, controllable molecular weight, and the abundance of readily accessible terminal functional groups [127].

Several polymers have been designed and used in siRNA delivery: Poly(amidoamine) (PAMAM) dendrimers, poly(propylenimine) (PPI), poly(ethyleneimine) (PEI), poly-(L-lysine) (PLL), poly(caprolactone) (PCL), poly(d,l-lactide) (PLA), and others. The modifications of these polymers and dendrimers have been investigated both *in vitro* and *in vivo* for siRNA therapy [16].

PEI, a synthetic polymer, has been successfully used in siRNA delivery both *in vitro* [128] and *in vivo* [129]. In addition, studies show that PEIs can facilitate the endosome release of siRNAs to cytoplasm, due to it consisting of large number of protonable amino moieties [114].

However, studies also show that PEIs may induce toxicity *in vivo* [130]. To overcome this, researchers investigated the relationship between molecular weight of PEIs and the biological activity, and demonstrate that PEIs with low molecular weight exhibit good biocompatibility with relatively low transfection efficiency [128]. Conjugated low molecular weight PEIs (1.8 kDa) with PEG-stabilized liposomes, a micelle-like nanoparticles (MNP) have been developed with improved siRNA delivery efficiency and biocompatibilities [131].

PCL has been used in siRNA delivery for the past decade. A self-assembled MNP, consisting of monomethoxy poly(ethylene glycol) – block – poly(ε-caprolactone) – block – poly(2-aminoethyl ethylene phosphate) (PPEEA) (mPEG-b-PCL-b-PPEEA), has been developed and well characterized for siRNA delivery [132]. The biocompatible and biodegradable PPEEA can bind with siRNAs, while the PEG provides steric protection from nuclease degradation (Figure 2.2). It has been reported that siRNA delivered by these polymers induced 40% - 70% green fluorescence protein (GFP) suppression in cells, and successfully delivered to tumor in various animal models [133-135].

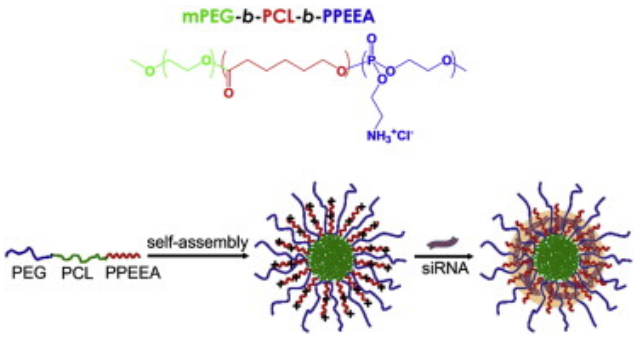

Figure 2.2 Structure mPEG-b-PCL-b-PPEEA MNP siRNA drug delivery systems [132].

To protect the complexes from degradation in serum, the complexes are coated or conjugated with PEG molecules. The triblock dendrimers PAMAM-PEG-PLL have been shown to be efficient nano-vectors for the delivery of siRNAs [136]. In this siRNA delivery system, the tertiary amine groups in the PAMAM dendrimer acts as a proton sponge and plays a vital role in endosomal escape and cytoplasmic delivery of siRNA. PLL is used to interact with siRNA and form stable structures, while PEG is used as a linker and also protects the system from nuclease attack.

2.2.5 Cell-penetrating peptide based delivery systems

Cell penetrating peptides (CPPs) are a class of peptides 5–30 amino acids long defined by the ability to cross cell membranes and the capacity to facilitate the cellular uptake of various molecular cargos [40]. A summary of current CPPs is listed in Table 2.5 [137]. CPPs based siRNA delivery system is relatively convenient compared with viruses or RNA chemical modification strategy.

Table 2.5 Summary of cell penetrating peptides [136]

CPPs	**Sequence**	**Origin**
Cationic		
R6H4	RRRRRRHHHH	Designed
Penetratin	RQIKIWFQNRRMKWKK	Antennapedia

		homeodomain
(RXR)4	$(R\text{-}Ahx_8\text{-}R)_4$	Designed
R9	RRRRRRRRR	Designed
NLS	CGYGPKKKRKVGG	SV40 NLS peptide
	PKKKRKV	Simian SV40 large tumor antigen
KAFAK	KAFAKLAARLYRKALARQLGVAA	Designed
hCT(9–32)	LGTYTQDFNKFHTFPQTAIGVGAP	A hormone secreted by the C cells of the thyroid
TAT	YGRKKRRQRRR	HIV-TAT domain
DPV3	RKKRRRESRKKRRRES	Human heparin binding proteins and/or anti-DNA antibodies
Amphipathic		
RGD	GRGDSY	Various circulating proteins
Sweet arrow peptide (SAP)	$(VRLPPP)_3$	N-terminal domain of γ-zein
hLF	KCFQWQRNMRKVRGPPVSCIKR	Antimicrobial peptides
MPG	GALFLGWLGAAGSTMGAPKKKRKV	HIV glycoprotein 41 protein

pVEC	LLIILRRRIRKQAHAHSK	Murine vascular endothelialcadherin protein
ARF(1–22)	MVRRFLVTLR IRRACGPPRVRV	p14ARF protein
BPrPp (1–28)	MVKSKIGSWILVLFVAMWSDVG LCKKRP	The N-terminus of the unprocessed bovine prion protein
Bac7	RRIRPRPPRLPRPRPRPLPFPRPG	Bactenecin family of antimicrobial peptides
MAP	KLALKLALKALKAALKLA	Chimeric
DPRSFL	DPRSFL	Proteinase activated receptor 1 (PAR-1)
VP22	NAATATRGRSAASRPTQRPRAP ARSASRPRRPVQ	Herpes simplex virus (HSV)
vT5	DPKGDPKGVTVTVTVTVTGKGD PKPD	Viral proteins
C105Y	CSIPPEVKFNKPFVYLI	The residues 359–374 of 1-antitrypsin
CADY	GLWRALWRLLRSLWRLLWRA	Designed
Pep-1	KETWWETWWTEWSQPKKRKV	A tryptophan-rich cluster
p28	LSTAADMQGVVTDGMASGLDK DYLKPDD	Azurin
Hydrophobic		

PFV	PFVYLI	C105Y
SG3	RLSGMNEVLSFRWL	A randomized peptide library
Pep-7	SDLWEMMMVSLACQY	CHL8
FGF	PIEVCMYREP	Cellular and viral proteins

CPPs can be classified into several groups: cationic CPPs, hydrophobic CPPs, and amphipathic CPPs. Charged residues play an important role in the cellular uptake of cationic CPPs [138]. Studies on arginine-based peptides (from R3 to R12) have shown that the minimal sequence for cellular uptake is R8 and that increasing the number of arginine residues increases the level of uptake [139]. Studies also suggest that at least eight positive charges are needed for efficient uptake of several other cationic CPPs [140]. CPPs with positively charged residues can interact with cell surface glycosaminoglycans (GAGs) and enter the cell through endocytic pathways [138]. Although charged residues are very important in the uptake of cationic CPPs, other residues are also crucial. The uptake of Penetratin (RQIKIWFQNRRMKWKK), for instance, is abolished by the mutation of W14 to F [90, 141]. Nuclear localization sequences (NLSs) is another group of CPPs with lower than eight positively charged residues. Nuclear localization sequences are amino acid sequences, with the ability to translocate into the cell nucleus. Examples of NLSs [142] involve the mutation of simian virus 40 (SV40) with sequences of PKKKRKV, Oct-6 (GRKRKKRT), SDC3 (FKKFRKF), and others. Since the number of positively charged residues in a NLS is usually

below eight, most of NLSs are not efficient siRNA delivery vectors [143]. They must be conjugated to hydrophobic segments to become amphipathic CPPs to be efficiently taken up by the cell.

The first discovered CPP was the transactivating transcriptional activator (Tat) from human immunodeficiency virus 1 (HIV-1) by two independent groups in 1988 [144]. Sequence RKKRRQRRR, residues 49 to 57 from the Tat protein, is responsible for the cell penetrating properties of the Tat protein. Tat has been studied on multiple cell lines to deliver oligonucleotides [145], proteins and fluorophores.

The first study of CPP mediated siRNA delivery was published in 2003 with peptide MPG [146]. MPG (GALFLGFLGAAGSTMGAWSQPKKKRKV), derived from NLS SV40, can induce an 80% reduction of luciferase activity *in vitro* after combined with siRNAs. Some modifications have been made to peptide MPG, and the derivatives as MPG-NLS and MPGα show enhanced transfection efficiency and increased binding affinity to siRNA molecules [147]. Several cell lines, such as HeLa [146], HEK-293 [148], and SW-620 [149], mediated by MPG/siRNA delivery systems shows good gene silencing results.

Penetratin (RQIKIWFQNRRMKWKK) is another CPP that has been extensively examined for siRNA delivery [150]. Unlike most CPPs, penetratin enters cells in an energy-independent matter, as penetratin can be internalized at both 4 and 37 °C. Studies on the penetratin sequence by Drin and co-workers demonstrate that the basic amino acids and the tryptophan at position 6 are crucial for efficient cellular uptake [151].

hCT (9-32) peptide, listed in Table 2.5, mediated siRNA delivery demonstrated knockdown results of a G protein-coupled receptor, i.e., the human Neuropeptide Y Y1 receptor [152]. siRNAs can be effectively delivered into HEK-293 cells with a comparable knockdown results induced by lipofection/siRNA complexes, while minimal cytotoxicity has been observed. The details of recent developed CPPs based siRNA delivery strategies can be found in a variety of reviews [40, 138, 153-156].

2.2.6 Targeting strategy for siRNA delivery systems

In order to reduce systemic toxicity while improving therapeutic efficiency, a conjugation with targeting ligands is the most commonly adopted methods. Passive targeting is developed based on enhanced permeability and retention (EPR) effect since 1986 [157, 158]. Passive accumulation has been applied in siRNA delivery system design, e.g., 80% tumor protein suppression has been observed after intravenous injection of liposome/siRNA into mice, followed by the accumulation of nanoparticles in tumor cells [120]. The EPR effect does not lead to exclusive tumor targeting, thus the efficacy of passive targeting is relatively low [158].

To enhance the accumulation of siRNAs in desired tumor sites, the active targeting strategy is incorporated in the design of siRNA delivery systems. The commonly adopted targeting ligands [159] involve antibodies, aptamers, small molecules, chemical modified polymers, short peptides, fatty acids, and others.

Antibody has been widely used to target cells of interests. Transferrin conjugated liposome can induce the nanoparticle accumulated in targeting sites 20 min after intravenous injection [160]. Human epidermal growth factor receptor-2 (Her2) antibody conjugated with siRNA delivery systems results an inhibited breast tumor cell proliferation [161]. However, the drawbacks of antibody targeting strategy include the relatively large size, and possibility of immunogenicity when long-term administered [162].

Another active targeting strategy is incorporating aptamers into siRNA delivery systems. Aptamers are characterized with high stability, unlimited shelf-life, no observed stimulation of immune responses [114], but the number of well-established aptamers for specific disease targeting is limited to a great degree.

Tumor homing peptides remain a useful targeting strategy in developing siRNA delivery system. Arg-Gly-Asp (RGD) peptide for instance, listed in Table 2.5, has been effectively employed as targeting ligands. Chitosan conjugated with RGD exhibited an 80% *in vivo* mRNA suppression, and a 51% *in vivo* protein inhibition [164].

2.3 Cellular uptake pathway and endosome escape

Typically, there are two main kinds of uptake pathways for nano-complexes: the endocytic pathway and the non-endocytic pathway. CPPs can be internalized through different pathways (Figure 2.3 [165]), including direct penetrating and enydocytic pathways. The internalization process can be influenced by various factors, including changes in membrane properties, particle shapes or charges, particle sizes [166]. After internalized through endocytic pathway, the carrier/siRNA nanoparticles tend to be trapped in endosome/lysosome vesicles, and degraded by multiple enzymes eventually. Thus, an efficient strategy needs to be applied to facilitate endosome escape, e.g. proton sponge effect, or the addition of fusogenic reagents.

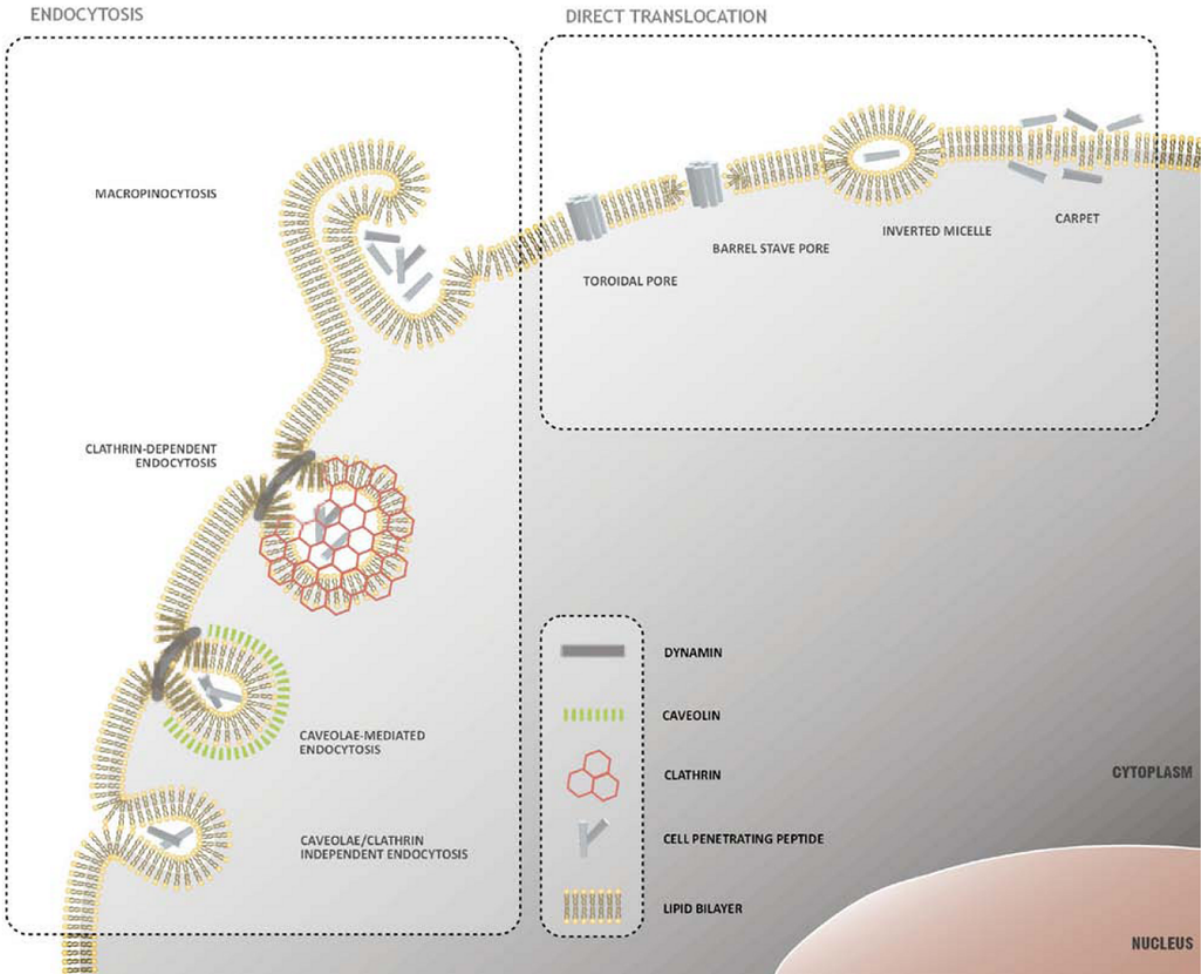

Figure 2.3 Intracellular uptake pathways of CPP/siRNA nanoparticles [164].

2.3.1 Uptake pathways and internalization mechanisms of CPP/siRNA complexes

Endocytic membrane trafficking is a complicated process by which cells internalize solutes and fluids from the extracellular matrix. The endocytic pathways are divided into four groups: macropinocytosis, phagocytosis, clathrin-mediated endocytosis (CME), and caveolae-mediated endocytosis (CvME).

Macropinocytosis is a signal dependent endocytosis [167]. This process presents in antigen-presenting cells, e.g., it may take place on macrophages cells when they actively responsed to colony stimulating factor-1 or epidermal growth factors. A number of CPPs are taken up by cells through macropinocytosis. TAT-PTD peptides, as well as TAT fusion proteins, are internalized through macropinocytosis [168]. Several inhibitors are reported to suppress macropinocytosis [166], e.g., rottlerin, amiloride, cytochalasin D, latrunculins, LY290042, sodium azide, and others.

Phagocytosis mainly occurs in phagocytic cells, i.e., monocytes, neutrophils, macrophages and dendritic cells [169], while the other three types of endocytosis presents in almost all types of cell lines. Phagocytosis is mediated by membrane extensions, which are used to uptake large particles such as bacteria [170]. Phagocytosis is also mediated by various receptors, e.g., mannose receptor [171], scavenger receptor [172], fragment crystallizable receptor [173], and complement receptor [173]. The inhibitors used to identify phagocytosis pathway [166] involve amiloride, cytochalasin D, latrunculins, wortmannin, LY290042, sodium azide, and others.

Clathrin-mediated endocytosis is a type of pathway that requires GTPase dynamine and receptors, while clathrin helps to form a coated cavity in the cell membrane with size ranges from 100 nm to 150 nm [174]. Lipoproteins with relatively low density are usually internalized through CME pathway [174]. Different from the other three types of endocytosis, nano-particles internalized via CME are directly integrated into late endosomes, and

eventually transported into lysosomes [175]. The inhibitors related to CME pathway [166] include chlorpromazine, monodansylcadaverine, phenylarsine oxide, sodium azide, and others.

Caveolae-mediated endocytosis is a receptor-specific pathway with size ranges from 50 nm to 100 nm, which requires the presenting of cholesterol and dynamin [176]. CvME is mediated by various receptors, e.g., insulin receptors [177] and epidermal growth factors [178], and others. Studies show TAT-rhodamine [179], as well as TAT-GFP [180], are internalized through CvME pathway. In addition, amphipathic CPPs with proline riched sequences [181], as well as certain viruses (e.g., SV40), bacteria, and bacteria toxins [182], are also internalized via CvME. Inhibitors such as filipin, nystatin, cholesterol oxidase, statins, genestein, MBCD, sodium azide, and others are normally used to characterize CvME pathway [166].

Direct penetration is a receptor- and energy-independent uptake pathway that is driven by plasma membrane potentials, which allows nanoparticles to cross the cell membrane directly and avoid entrapment in endosome/lysosome vesicles. Thus, siRNAs internalized through direct penetration may achieve a better biological activity. Various CPPs-based siRNA delivery systems are reported to enter the cells through direct penetration, including CADY [183], HR-9 [184], and TAT in some cases [185].

The uptake pathway of CPP-based siRNA delivery system are subject by various factors, including particle sizes, surface charges, particle shapes, cell types, and others. Studies demonstrated that the internalization of certain nanoparticles might involve several pathways at the same time, which may be due to heterogeneity of the complexes [186]. Another factor that may influence cellular uptake pathways is the concentrations of nano-vectors. It has been

noted that CPPs at low concentrations are commonly internalized through endocytic pathways, while CPPs at high concentrations tend to be taken up via direct penetrations [187, 188].

As discussed previously, various biological tools are explored to determine the specific cellular uptake pathway for certain nano-vectors. Endocytosis pathway inhibitors that specifically block one or several pathways can be used to determine the pathways involved in the internalization processes. Inhibitors for each pathway are discussed previously. It is worth noticing that sodium azide, an inhibitor of mitochondrial oxidative phosphorylation, is involved in all kinds of endocytosis pathways [189-191]. Also, the impact of temperature is another method commonly adopted to determine whether the internalization of certain nano-vectors is through energy-independent pathways.

Other useful tools to investigate uptake pathways include the molecular probes, markers, and dyes. Transferrin is a classic molecular probe specifically internalized through the CME pathway. Caveolin-1 is the popular marker for CvME. Dextran is an essential probe for macropinocytosis. LysoTrackers is a widely used dye for endosome/lysosome vesicles, and it is commonly used in combination with confocal microscopy to study the intracellular trafficking of nanoparticles.

2.3.2 Endosome escape mechanisms and strategies

After endocytosis, nanoparticles might be trapped in endosome/lysosome vesicles. Figure 2.4 illustrates the overall endosome escape processes for siRNA delivery systems [192].

A number of mechanisms have been proposed. One of these mechanisms is the formation of pores on cellular/endosomal membranes. Complexes with high binding affinity to the lipid bilayers can insert into membranes and then create a pore on the membranes. Cationic amphiphilic peptide is one of the best-known examples of a complex capable of pore formation on cellular/endosomal membranes.

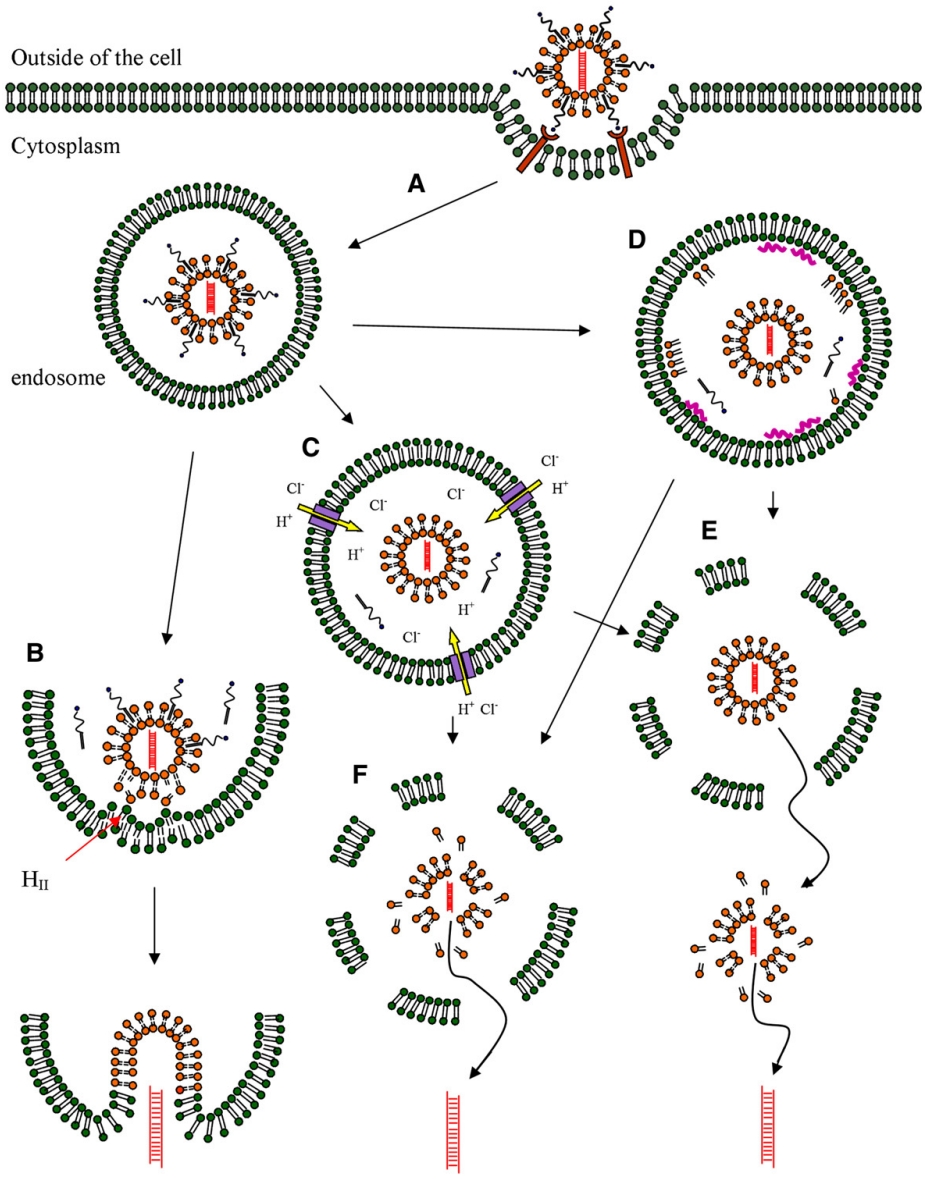

Figure 2.4 Endosome escape in lipoplex mediated siRNA delivery [192]. A. Lipoplex containing siRNA (shown as orange lipid bilayer and red siRNA) with PEG and targeting ligand on the tip (shown as blue circle) are taken up by target cell via receptor mediated endocytosis. B. The cationic lipid of the lipoplex forms ion pairs with the anionic endosomal lipid (PEG molecules may leave the lipoplex spontaneously or under appropriate design) and can further form the inverted hexagonal phase (HII). This leads to the fusion of the lipoplex with endosomal membrane and release the siRNA into cytoplasm. C. Lipoplex containing

molecules having buffer capacity in endosomal pH range can trigger proton sponge effect that causes the influx of Cl− and swelling of the endosome. D. Free highly positive charged molecules (shown with orange colored cationic lipid and purple colored PEI or oligo-arginine) can interact with anionic endosomal membrane and destabilize it by excludingwater. E. Intact lipoplex mayescape from the ruptured endosome and de-assemble in the cytoplasm and release siRNA if the particle is not too large for the “holes” of the ruptured endosome. F. Lipoplex may also de-assemble inside the endosome and directly release siRNA out of the ruptured endosome.

Another proposed mechanism for endosomal escape is through proton sponge effect. The proton sponge effect is induced by the influx of ions into endosome, leading to an increase of osmolality and the following rupture of endosomal membrane, with entrapped complexes released eventually [192]. Nanoparticles containing histidine residues may apply to this mechanism [40, 193]. The imidazole group of histidine with a pKa of 6 is able to absorb protons in the acidic environment of endosomes. The incorporation of polyethyleneimine is another way to introduce protonable groups into siRNA delivery systems [194].

Photochemical internalization is also proposed as an endosome escape strategy. When photosensitive complexes exposed to light, they will trigger the generation of highly reactive singlet oxygen. Singlet oxygen disrupts the endosomal membrane causing the release of the particles into the cytoplasm [195]. A number of photosensitizers can be used to formulate delivery systems with lipids [196], polymers [197], and CPPs [198].

Endosomolytic reagents that are able to disrupt endosomal membranes can be used in combination with CPPs to enhance endosome release of complexes. Chloroquine for instance,

can disrupt endosomal membranes by inhibiting endosome acidification processes [137]. However, chloroquine is not suitable for *in vivo* applications. Several other reagents with similar membrane disruption capabilities are also used for siRNA delivery purposes [138], including ammonium chloride, methylamine, and others. As alternatives, a number of endosomolytic peptides, also known as fusogenic peptides, can be used to improve endosome escape. These peptides undergo conformational changes in response to acidification of the endosome. HA2 peptide, derived from influenza virus, is the most commonly used fusogenic peptide. Studies demonstrate that fusion of HA2 with penetratin can improve transfection efficiency compared to penetration alone [139]. Similarly, the biological activity of TAT can be enhanced by fusion with HA2 [140].

Chapter 3

DEGylation enhanced the stability of peptides-siRNA complexes in serum

3.1 Introduction

Since the discovery of RNA interference in mammals [1], short interfering RNA (siRNA), also known as small interfering RNA, has shown great potential as a powerful tool in gene therapy [23]. siRNA is a double-stranded RNA consisting of 21 – 23 nucleotides and has the ability to bind to the complementary sequence in a target mRNA, thereby inhibiting the expression of the target protein in cells [1]. However, the application of siRNA is limited by the nature of naked siRNA molecules, such as the relatively large molecular weight, anionic nature, poor stability in physiological fluids, which decreases their ability to permeate plasma membranes and results in an inefficient cellular uptake [199]. Thus, the development of efficient and safe delivery systems for siRNA has been an important research pursuit [23].

Several strategies have been developed to aid in siRNA delivery [200], including the use of cationic polymers [201-203], and lipid- [204-206] and peptide-based [90, 144, 207, 208] non-viral vectors. These vectors form complexes with negatively charged siRNA molecules,

thus facilitating their cellular uptake and protecting them from nuclease interactions [209, 210].

Recently, we reported the development of a library of peptide-based siRNA carriers that cause gene knockdown without inducing cellular toxicity [211]. However, a major limitation of these carriers is that the transfection efficacy is reduced by the presence of serum, resulting in reduced gene knockdown efficiency. There are several ways that siRNA delivery systems might be affected by the presence of serum. For example, the positively charged complexes formed by siRNA and carriers might interact with negatively charged serum proteins, e.g., albumin, which would change the surface charge on complexes and cause the complexes to aggregate [212, 213]. Moreover, interactions with serum components could cause the disassembly of the siRNA delivery system and expose siRNA molecules to nucleases [214].

Currently, conjugating delivery complexes with polyethylene glycol (PEG) is a commonly used technique for improving the serum stability of gene delivery systems [215-218]. Conjugating with PEG molecules sterically shields the complexes [219] and reduces the interactions between the complexes and serum components [220]. PEGylation is also thought to decrease the uptake of the carrier/siRNA complexes by the reticuloendothelial system, which would prolong their circulation time in the blood [216]. However, after being conjugated with PEG, the gene delivery systems frequently exhibit reduced target specificity *in vivo* due to steric hindrance between the PEGylated systems and the target area [221]. It has also been suggested that transfection efficiency might by reduced by PEGylation because adding PEG molecules has the potential to reduce electrostatic interaction between positively charged delivery systems and negatively charged cell membranes [222].

Herein, we report the results of conjugating one of the most promising library peptides [211], C6M1 (results has been published in [223-225]), with a short ethylene glycol, diethylene glycol (DEG), instead of PEG, considering the small size of the peptide and that anything to conjugate it should be comparable in size. The aim of this study is to determine whether DEGylation can improve the complex's serum stability without compromising its transfection efficiency. For this purpose, we compared peptide/siRNA complexes that were either modified with DEGylation or without. Serum stability was examined by gel electrophoresis assay. Cellular uptake efficiency and cytotoxicity of complexes were investigated in Chinese hamster ovary (CHO-K1) cells. The efficiency of gene silencing in CHO-K1 cells was evaluated using RT-PCR and GAPDH assays, and it was evaluated in mouse endothelial cells that encoded the enhanced green fluorescence protein (GFP cells) using the eGFP silencing assay.

This Chapter is based on the work published in Journal of Nanoscience and Nanotechnology, with authorship as: Ran Pan, Wen Xu, Mousa Jafari, Baoling Chen, Tatiana Sheinin, Pu Chen.

3.2 Materials and Methods

3.2.1 Preparation of complexes

Synthesized by CanPeptide Inc (Quebec, Canada), C6M1 and DEGylated C6M1 (termed DM1) peptides were dissolved in RNase free water (Thermo scientific, Ottawa, Canada) at a concentration of 1 mM, followed by sonication for 10 min, and were stored at -20°C. The peptide/siRNA (both C6M1/siRNA and DM1/siRNA) complexes were prepared in RNase free water for characterization experiments, and were prepared in Opti-MEM (Invitrogen, Carlsbad, CA, USA) for transfection experiments. The peptide/siRNA complexes were prepared at different molar ratio ranged from 1/1 to 80/1 depending on the designed experiment, by slowly mixing the peptide solution into siRNA solution. The complexes were incubated at room temperature for 30 min before conducting experiments.

siRNA targeting at the glyceraldehyde 3-phosphate dehydrogenase (GAPDH) gene was purchased from Ambion (Silencer^{TM} GAPDH siRNA: human, mouse, rat). The eGFP siRNA was purchased from Dharmacon, U.S.A, with an extinction coefficient of 362408 L/mol cm. The sense sequence of eGFP siRNA was 5'-GACGUAAACGGCCACAAGUUC-3', and the antisense sequence was 5'-ACUUGUGGCCGUUUACGUCGC-3'. The negative control siRNA with scrambled sequence used in the experiment was also purchased from Ambion.

3.2.2 Gel electrophoresis assay

The interaction of peptide/siRNA complexes was investigated using agarose gel electrophoresis assay. Peptides (C6M1 and DM1) were mixed with siRNA targeting eGFP (peptide/sieGFP complexes) and were prepared as described above, with a final amount of 200

ng siRNA per well. The complexes were incubated at room temperature for 30 min before being loaded onto a 1.2% w/v agarose gel labeled with ethidium bromide in TBE buffer and run at 50 V for 60 min.

3.2.3 Cell culture and peptide mediated siRNA transfection

Transfection experiments were conducted using CHO-K1 cells and C166-GFP cells. All cell lines were obtained from ATCC (Rockville, MD, USA).

The CHO-K1 cells (ATCC: CCL-61) were maintained in F-12K medium (Thermo scientific, Ottawa, Canada) supplemented with 10% fetal bovine serum (FBS, Sigma-Aldrich, Oakville, Ontario, Canada) at 37°C in 5% CO_2. Before transfection, CHO-K1 cells were seeded in 24-well plates with a confluence of 35,000 cells/well and in 96-well plates with a confluence of 6,000 cells/well. After incubating at 37°C for 24 hours, cells were rinsed with phosphate buffered saline (PBS), which was then replaced with Opti-MEM. The peptide/siGAPDH complexes were prepared as described above, diluted in Opti-MEM to a final concentration of 50 nM siRNA and then added to each well. After the cells were incubated at 37°C for 4 hours, medium containing FBS was added to obtain a final concentration of 10% FBS.

The C166-GFP cells (ATCC: CRL-2583) were cultured in Dulbecco's Modified Eagle Medium (DMEM, Thermo scientific, Ottawa, Canada) containing 10% FBS at 37°C in 5% CO_2. The GFP cells were seeded in 24-well plates at 35,000 cells/well and incubated for 24 hours before transfection. The cells were rinsed with PBS, and Opti-MEM was then added. The peptide/sieGFP complexes were prepared as described above and were added to each well

at a final concentration of 50 nM siRNA. To maintain cell growth, FBS was added after 4 hours of incubation to achieve a final concentration of 10%.

3.2.4 Serum stability of complexes

The protection afforded by peptide/siRNA complexes against serum components was evaluated by agarose gel electrophoresis assay. The peptide/sieGFP complexes were prepared as described above, with a final amount of 200 ng sieGFP per well, and incubated for 30 min before the addition of FBS. Active FBS was added to each well at a final concentration of 50% v/v, and inactivated FBS was used as control. Aliquots were taken at different time points, and 1 µl of 0.5 M EDTA was immediately added to each sample to stop serum interactions. Heparin was then added to samples at a final concentration of 1.5% v/v, and the samples were incubated for 30 min before being loaded onto a 1.2% w/v agarose gel labeled with ethidium bromide (EtBr) at and run at 50 V for 60 min. The gel products were then visualized using a UV transilluminator.

3.2.5 Cytotoxicity of complexes

The cytotoxicity of peptide/siGAPDH complexes was evaluated using 3-(4,5-dimethylthiazole-2-yl)-2,5-diphenyl tetrazolium bromide (MTT) assay. CHO-K1 cells were seeded in 96-well plates at 6,000 cells/well and transfected with peptide/siGAPDH complexes, as described above. After 48 hours, cells were rinsed with PBS, and 100 µL of MTT solution (5 mg/mL in PBS) was added to each well. After 2 hours of incubation at 37°C, 100 µL of solubilization solution, composed of 10% Triton X-100 (Sigma) plus 1% HCl (Sigma) in anhydrous isopropanol (Invitrogen), was added to each well to dissolve the formazan crystals.

The optical densities were then measured at 570 nm with a microplate reader (FLUOstar Optima, BMG Labtech, Ortenberg, Germany). Cell viability was calculated as the optical density of each sample divided by the optical density of untreated controls. All measurements were performed in triplicate.

3.2.6 Uptake efficiency of complexes

The cellular uptake efficiency of complexes was studied by flow cytometry (type BD Biosciences, BD FACS Vantage SE Cell Sorter, USA). CHO-K1 cells were seeded in 24-well plates and transfected with peptide/Cy-3-labeled siRNA complexes 24 hours later, as described above. After 4 hours of incubation at 37°C, cells were rinsed with PBS and incubated in 15 U/ml heparin medium for 20 min. This step was repeated 3 times. Cells were then washed twice with PBS, detached from the plate with 0.25% trypsin/EDTA, and then collected in the suspension of 4% PFA in PBS. The collected samples were analyzed by fluorescence acquired cell sorting (FACS), and the data were analyzed by Flowjo software. All measurements were performed in triplicate.

3.2.7 Fluorescence microscopy

The cellular uptake efficiency of complexes was studied by fluorescence microscopy. CHO-K1 cells were seeded in 24-well plates at 60,000 cells/well, and transfected with peptide/Cy-3-labeled GAPDH siRNA complexes 24 hours later, as described above. After 4 hours of incubation at 37°C, cells were rinsed with PBS and incubated in 15 U/ml heparin medium for 20 min. This step was repeated 3 times. Cells were then washed twice with PBS, and fixed with 500 µl/well of 4% PFA in PBS at 37°C. After 30 min, the fixation PBS was

aspirated, and the cells were washed twice with PBS before they were covered with Fluoroshield with DAPI mounting medium (Sigma-Aldrich, Oakville, Ontario, Canada). The samples were visualized on EVOS FL cell imaging system (Life Technology, Carlsbad, USA), with a 40x objective lens. A Sony ICX445 CCD of 1.3 megapixels was installed on the microscope.

3.2.8 GAPDH silencing assay at mRNA level

The efficiency of GAPDH siRNA interference was evaluated using real time RT-PCR that shows the gene knockdown on mRNA level. GAPDH primers used in this experiments are shown below: 5'-TGT GTC CGT CGT GGA TCT GA-3' (F), 5'-TTF CTG TTG AAG TCG CAG GAG-3' (R). CHO-K1 cells were seeded in 24-well plates and transfected with peptide/siGAPDH complexes 24 hours later, as described above. After 48 hours, total RNA was isolated using the RNeasy Mini Kit (Qiagen, Valencia, CA, USA), and the RNA concentration was measured using Nanodrop (Nanodrop spectrophotometer ND-1000, Thermo scientific, Ottawa, Canada). RNA was then reverse transcribed into cDNA using Bio-Rad iScript cDNA synthesis kit (Bio-Rad Laboratories, Ontario, Canada). RT-PCR was performed using the Mx3005P™ Real Time PCR System (Agilent Technologies, Wilmington, DE, USA) with Brilliant II Fast SYBR Green QPCR Master Mix (Agilent Technologies), according to the manufacturer's instructions. All measurements were performed in triplicate. The data was normalized to cyclophilin genes, with primer sequences as: 5'-GGTGATCTTTGGTCTCTTCGG-3' (F), and 5'-TAGATGCTCTTTCCTCCTGTG-3' (R).

Cyclophilin are a family of proteins that catalyzes the isomerization of peptide bonds from trans form to cis form at proline residues and facilitates protein folding.

3.2.9 GAPDH silencing assay at protein level

The amount of GAPDH protein expression was measured using the GAPDH KDalert assay kit (Ambion, Austin, TX, USA). CHO-K1 cells were seeded in 96-well plates and transfected with peptide/siGAPDH complexes 24 hours later, as described above. After 48 hours, cells were rinsed with PBS and lysed with KDalert lysis buffer; they were then processed according to the manufacturer's instructions. Fluorescence was measured at room temperature with microplate reader (FLUOstar Optima, BMG Labtech, Ortenberg, Germany). All measurements were performed in 5 wells in parallel.

3.2.10 eGFP silencing assay

C166 GFP cells were seeded in 24-well plates and transfected with peptide/sieGFP complexes 24 hours later, as described above. After 48 hours of incubation, the cells were rinsed with PBS and collected in 4% PFA solutions. The samples were evaluated by FACS, and the results were analyzed by Flowjo software.

3.2.11 Serum effect on knockdown experiments

24 hours before the transfection experiment, CHO-K1 cells were seeded at 6,000 cells/well into 96-well plates in F-12K medium with 10% FBS. The cells were rinsed with PBS and replaced with fresh F-12K medium containing 10% FBS. The peptide/siGAPDH complexes were prepared as described above and were added to CHO-K1 cells at a final concentration of

50 nM siRNA for 4 hours, followed by the addition of fresh F-12K medium with 10% FBS in the same amount as the previously described transfection experiment. After 48 hours of incubation, the cells were processed using the KDalert GAPDH assay kit, according to the manufacturer's instructions.

3.3 Results and Discussions

In developing an efficient siRNA delivery system, several important factors need to be considered. First, the delivery system must protect siRNA from being affected by its surroundings, which can include degradation caused by RNAse and aggregation caused by proteins. Second, the delivery system should deliver siRNA into cells and facilitate the RNAi process. Moreover, the delivery system should not cause cytotoxicity, either *in vitro* or *in vivo*.

Considering these factors, i.e. peptide siRNA co-assembly, siRNA loading and protection capability, peptide/siRNA complexes transfection efficiency, peptide C6M1 was designed previously by our group. The sequence was listed in Table 3.1. To determine whether DEGylation can improve the complex's serum stability without compromising its transfection efficiency, a diethylene glycol molecule was conjugated to peptide C6M1 at the N-terminus (Table 3.1).

Table 3.1 Sequences and molecular weight of peptide

Name	Sequence	MW (g/mol)	Purity
C6M1	Acetyl-RLWRLLWRLWRRLWRLLR-NH2	2689	96.3%
DM1	DEG-RLWRLLWRLWRRLWRLLR-NH2	2835	95.7%

3.3.1 The interaction of peptide with siRNAs

For effective delivery of siRNA into cells, the anionic charge of siRNA molecules should be neutralized by peptides. To investigate the interaction of peptide with siRNA, increasing

amounts of peptides were mixed with siRNA that targeted the eGFP gene, and the complexes were analyzed by agarose gel electrophoresis assays. For our peptides C6M1 (Figure 3.1A) and DM1 (Figure 3.1B), the peptide/siRNA complexes started to form at a very low molar ratio of 1/1, as evidenced by a decrease in the intensity of the band representing a molar ratio of 1/1 relative to that representing a molar ratio of 0 (siRNA only). siRNA molecules were completely associated with C6M1 (Figure 3.1A) at molar ratios of 10/1 and above and with DM1 (Figure 3.1B) at molar ratios of 15/1 and above.

These results support the hypothesis that the complete association of peptides with siRNA occurs when the molar ratio is greater than 6/1, as there are 7 positively charged arginine residues in 1 molecule of C6M1, as well as DM1, and there are 21 pairs of negatively charged oligonucleotides in one sieGFP molecule.

Note that siRNA molecules were entirely complexed with DM1 at a higher molar ratio, i.e., a molar ratio of 15/1, than that for siRNA with C6M1. This finding suggests that although both peptides have the same number of positively charged arginine residues, more DEGylated peptides are required to form a complex with siRNA. One explanation is that the DEG shield builds a steric hindrance around complexes, which reduces the positive charge density of the peptides.

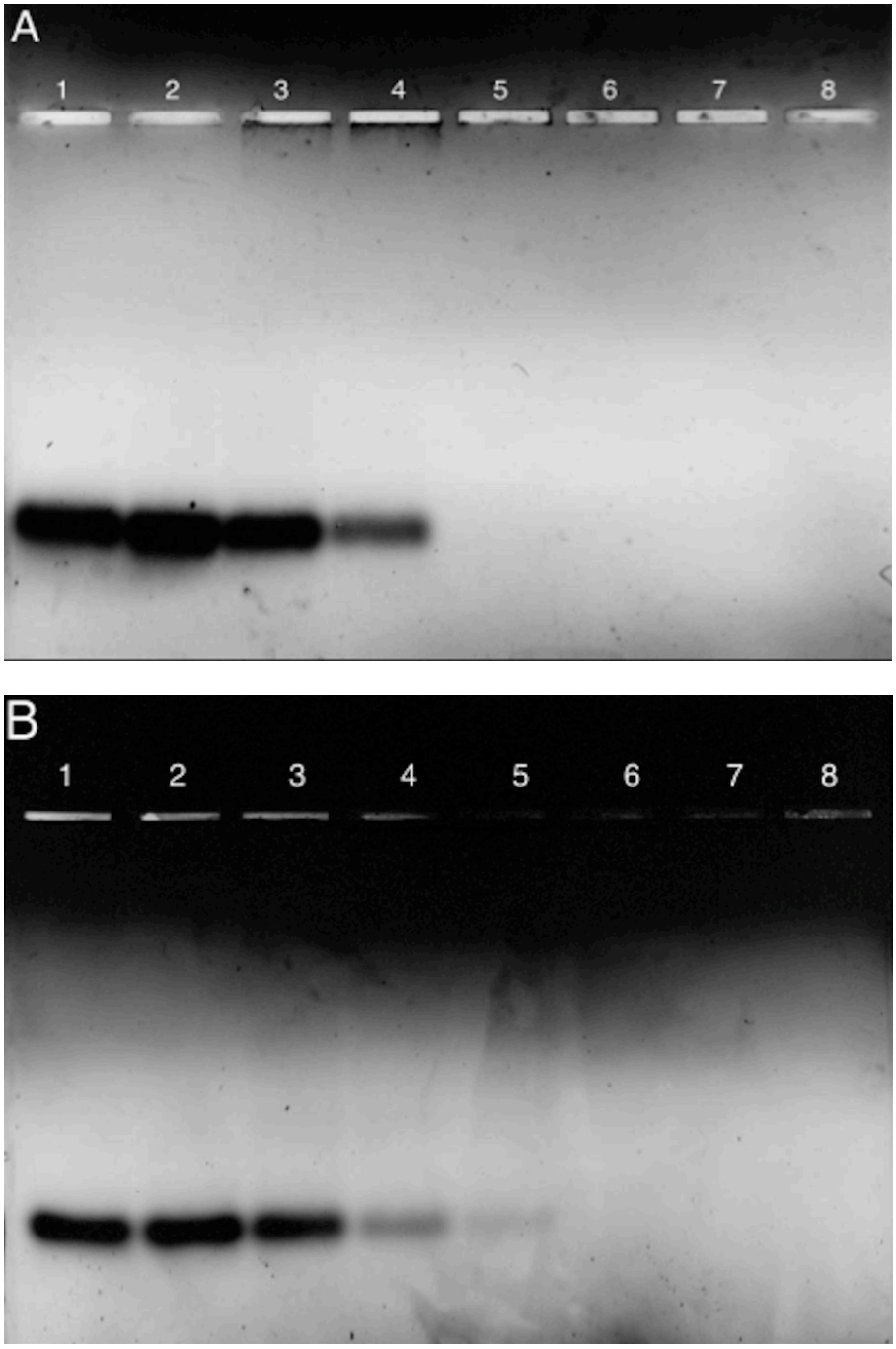

Figure 3.1 Agarose gel electrophoresis assay. A) Complexes C6M1/sieGFP and B) Complexes DM1/sieGFP, at molar ratios 0, 1/1, 5/1, 10/1, 15/1, 20/1, 30/1, and 40/1.

3.3.2 DEGylated peptide complexed siRNA is stable in the presence of serum

Delivery systems should be able to shield and protect siRNA from degradation by nuclease enzymes in the cytoplasm and in serum. These enzymes have been reported to degrade DNA and RNA molecules into small ineffective fragments that lose their therapeutic effects [226-229]. To investigate the stability of two complexes in the presence of serum, an agarose gel electrophoresis assay was conducted.

The complexes formed between peptide and siRNA could be dissembled by the addition of heparin (Figure 3.2). It has been reported that the addition of heparin would competitively disassociate DNA [230, 231] and siRNA [232, 233] from positively charged complexes. After the addition of heparin, the fluorescence intensity of siRNA did not change (Figure 3.2, lane 2). However, when C6M1/siRNA and DM1/siRNA complexes were incubated with heparin for 30 min, a weak band appeared, indicating the release of siRNA (Figure 3.2, lane 4, and lane 6). Naked siRNA without peptides and peptide/siRNA complexes at a molar ratio of 30/1 were incubated in 50% active FBS for various time periods (Figure 3.3). The naked siRNAs were completely degraded within 6 h (Figure 3.3, lane 4, and lane 5), while siRNA complexed with C6M1 and DM1 degraded much more slowly. siRNA was protected by peptide C6M1 for 24 h (Figure 3.3, lane 6-9), but the siRNA was completely degraded within 48 h (Figure 3.3, lane 10). Peptide DM1 achieved higher stability, which was able to protect siRNA for up to 72 h (Figure 3.3, lane 11-16).

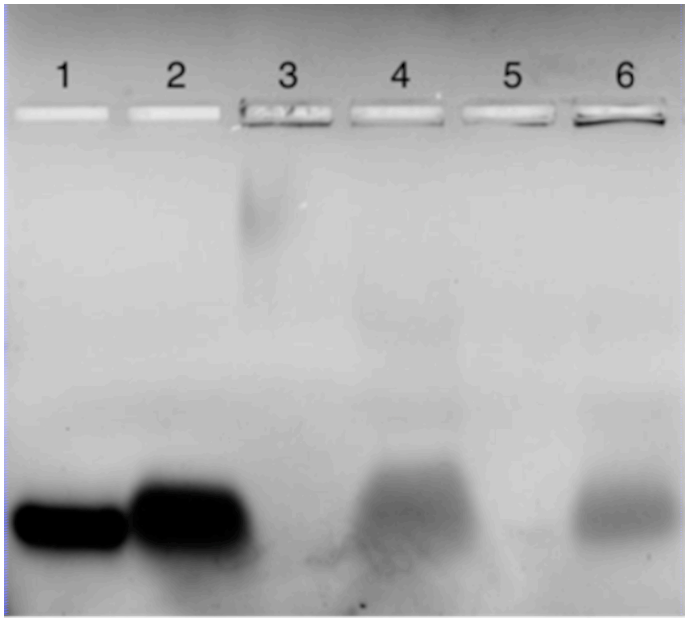

Figure 3.2 Interaction of complexes with heparin. The complexes were formed at molar ratio 30/1, and eGFP targeting gene was used in the experiment. Lane 1: naked siRNA; Lane 2: siRNA incubated with heparin for 30 min; Lane 3 and 5: C6M1/siRNA and DM1/siRNA respectively; Lane 4 and 6: C6M1/siRNA and DM1/siRNA incubated with heparin for 30 min, respectively.

After 6 hours, siRNA protected by C6M1 was partially degraded (Figure 3.3, lane 8-10), as evidenced by its decreased band intensity. It is worth noticing that, within 48 hours, there was no significant change in the band intensity of siRNA protected by DM1 (Figure 3.3, lane 11-16).

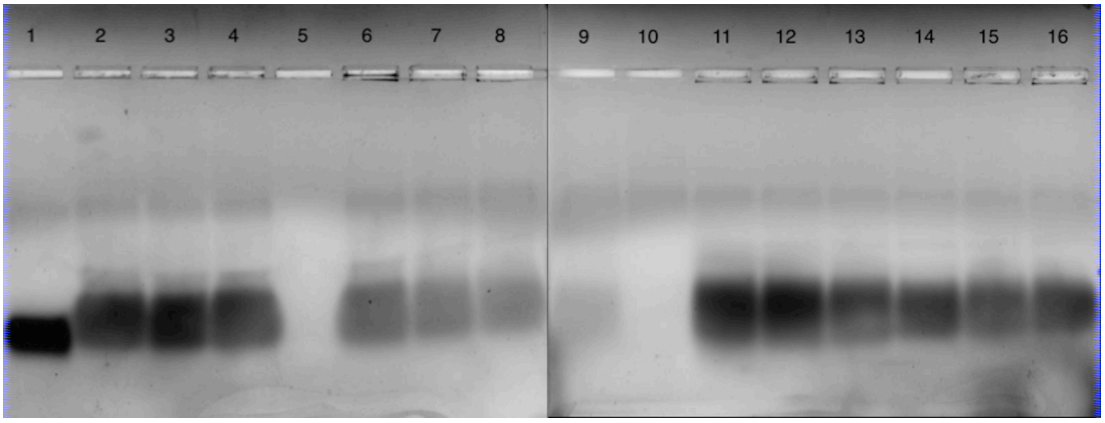

Figure 3.3 Serum stability of complexes in the presence of 50% serum v/v. The complexes were formed at molar ratio 30/1, and eGFP targeting gene was used in the experiment. Heparin was added to each well except lane 1. Lane 1: naked siRNA; Lane 2 and 3: C6M1/siRNA and DM1/siRNA after 30 min without addition of serum, respectively; Lane 4 and 5: naked siRNA incubated with serum for 2 h and 6 h; Lane 6 – 10: C6M1/siRNA incubated with serum for 2 h, 6 h, 12 h, 24 h, and 48 h; Lane 11 – 16: DM1/siRNA incubated with serum for 2 h, 6 h, 12 h, 24 h, and 48 h.

The results presented here suggest that the DEGylation of peptide C6M1 can improve its ability to protect siRNA against degradation by serum nucleases and enzymes. The DEG layer around the complexes might sterically shield siRNA molecules against surrounding molecules. It has been reported that polyethylene glycol plays an important role in stabilizing the structure of gene delivery systems and in protecting the siRNA vector from nuclease attack [234]. Here, we have shown that peptides conjugated with a shorter form of ethylene glycol, i.e., diethylene glycol, can also protect siRNA from degradation and prolong its incubation time within serum-containing medium. This finding suggests a promising *in vivo* application for peptide-assembled siRNA systems.

3.3.3 DEGylation can promote cell viability of cationic peptides

Cell viability is one of the most important factors in selecting gene delivery systems. It has been reported that PEGylation can reduce the cytotoxicity of pDNA [235] and siRNA delivery systems. The effects of various peptide/siRNA complexes on CHO-K1 cell viability were tested using MTT assay.

In Figure 3.4, neither C6M1/siRNA nor DM1/siRNA complexes caused cellular toxicity at molar ratios of 20/1 to 40/1. However, C6M1/siRNA complexes exhibited *in vitro* toxicity at a higher molar ratio of 80/1, resulting in only 69% viability, while DM1/siRNA complexes were not toxic at any molar ratios. It is very encouraging that little cytotoxicity was observed with DM1/siRNA complexes, which might be due to the reduced cationic density induced by DEG chains on the surface of complexes [236]. Highly positively charged C6M1/siRNA complexes at molar ratios of 80/1 might interact with negatively charged cell membranes and cause aggregation on the membrane surface, resulting in membrane rupture and cell death. Therefore, reducing the positive charge density by conjugating the DEG to peptides is a good way to reduce the cytotoxicity of cationic peptides as siRNA carriers.

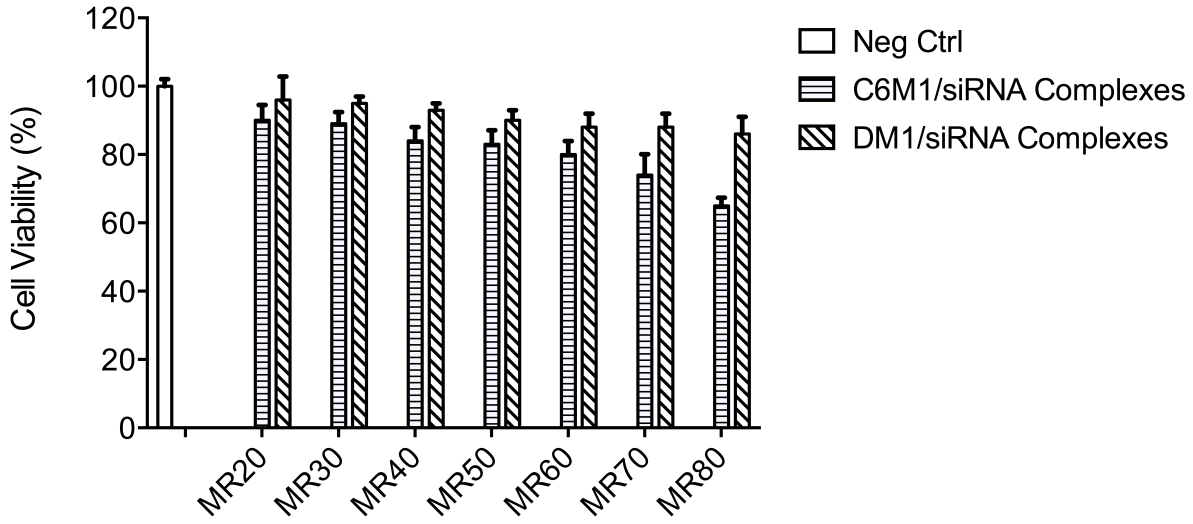

Figure 3.4 Cell toxicity performed by MTT assay on CHO-K1 cells. Complexes C6M1/siGAPDH and DM1/siGAPDH at molar ratios of 20/1, 30/1, 40/1, 50/1, 60/1, 70/1, and 80/1.

3.3.4 Influence of DEGylation on cellular uptake efficiency

One common concern of PEGylation is that it highly reduces charge density and thus decreases cellular uptake efficiency [222, 235]. To investigate the effects of DEGylation on siRNA delivery into cells, we used FACS to compare the cellular uptake potency of Cy-3 labeled siRNA complexed with DM1 and C6M1 (Figure 3.5).

As shown in Figure 3.5A, little naked siRNA was delivered into the cytoplasm. However, when siRNA was complexed with C6M1 and DM1 peptides, over 90% of siRNA was

delivered into the cells. The fluorescence intensity did not increase with the amount of peptide, and a molar ratio of 20/1 was sufficient to deliver siRNA into cells for both C6M1/siRNA and DM1/siRNA complexes. This result was in good agreement with the results obtained using the agarose gel assay, which demonstrated that free siRNA was fully complexed with peptides at a molar ratio of 20/1.

The quantitatively analyzed results (Figure 3.5B) demonstrate that similar amounts of siRNA were delivered by C6M1 and DM1, suggesting that the DEGylation of the delivery system has little effect on cellular uptake efficiency.

Figure 3.5C shows the typical cellular localization of the DM1/Cy-3 labeled siRNA complexes. A red fluorescence signal could be found in almost every cell, and the fluorescent-labeled siRNA molecules were localized close to the nucleus, where siRNA molecules will bind to the RNA-induced silencing complex (RISC) and initiate RNA interference in the cytosol.

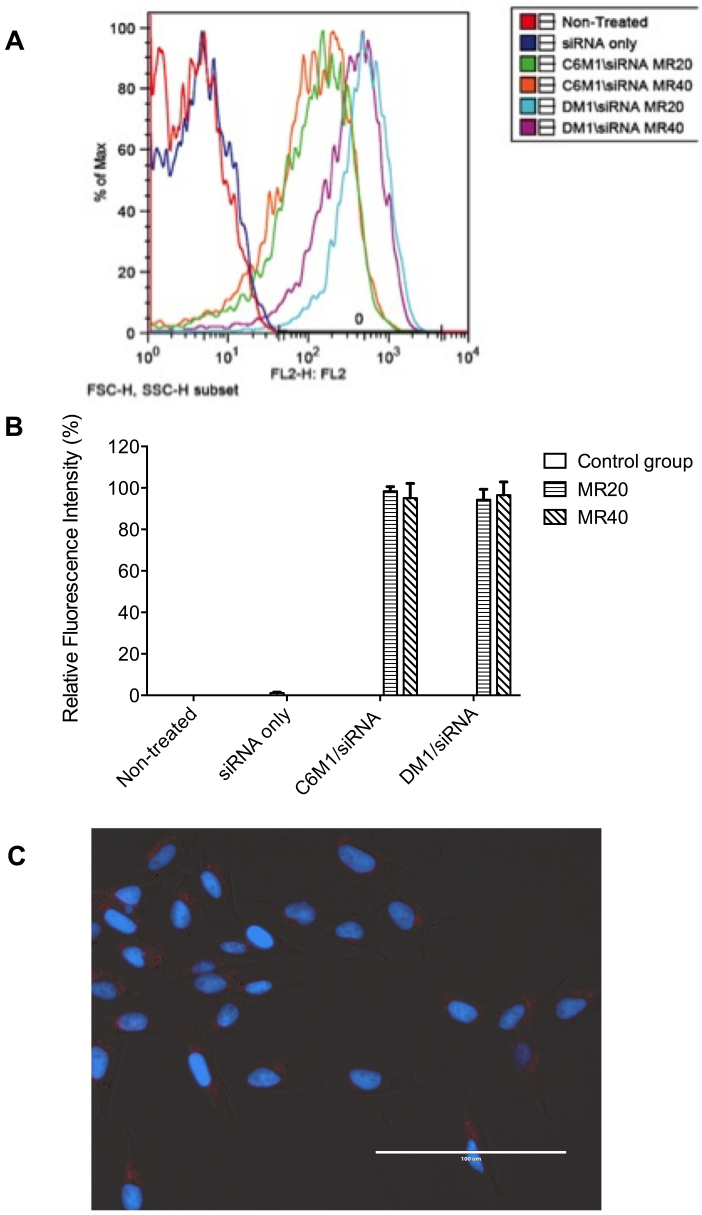

Figure 3.5 Cellular uptake of siRNA mediated by peptides on CHO-K1 cells. Cy-3 labeled siRNA were used in the experiment, and Cy-3 labeled siRNA incubated without transfection agent was used as negative control. Complexes peptide/siRNA were transfected with cells at molar ratios of 20/1 and 40/1. A) Fluorescence intensity measured by FACS, analyzed by FlowJo. B) Percentage of siRNA delivered into the cytoplasm. C) Fluorescence microscope imaging of cellular localization of DM1/siRNA complexes, scale bar = 100 μm

3.3.5 Knockdown efficiency of complexes formed by DEGylated peptide with siRNA in comparison with non-DEGylated peptide

The silencing effect of peptide/siRNA complexes was evaluated on both mRNA and protein levels on different cell lines. First, we conducted RT-PCR on CHO-K1 cells to determine the level of GAPDH mRNA suppression mediated by peptides C6M1 and DM1 (Figure 3.6). Scrambled siRNA was used as a negative control in each treatment group, and the peptide/scrambled siRNA complexes showed no gene silencing effects when compared to non-treated cells (Figure 3.6A).

The relative amount of GAPDH mRNA inhibition was calculated as the peptide/siGAPDH divided by the peptide/scrambled siRNA (Figure 3.6B). Both the C6M1/siRNA and DM1/siRNA complexes demonstrated over 40% gene silencing efficiency, and their inhibitory effects increased as the molar ratio increased. It is worth noting that both the C6M1/siGAPDH and DM1/siGAPDH complexes inhibited GAPDH mRNA expression by more than 50% at a molar ratio of 40/1.

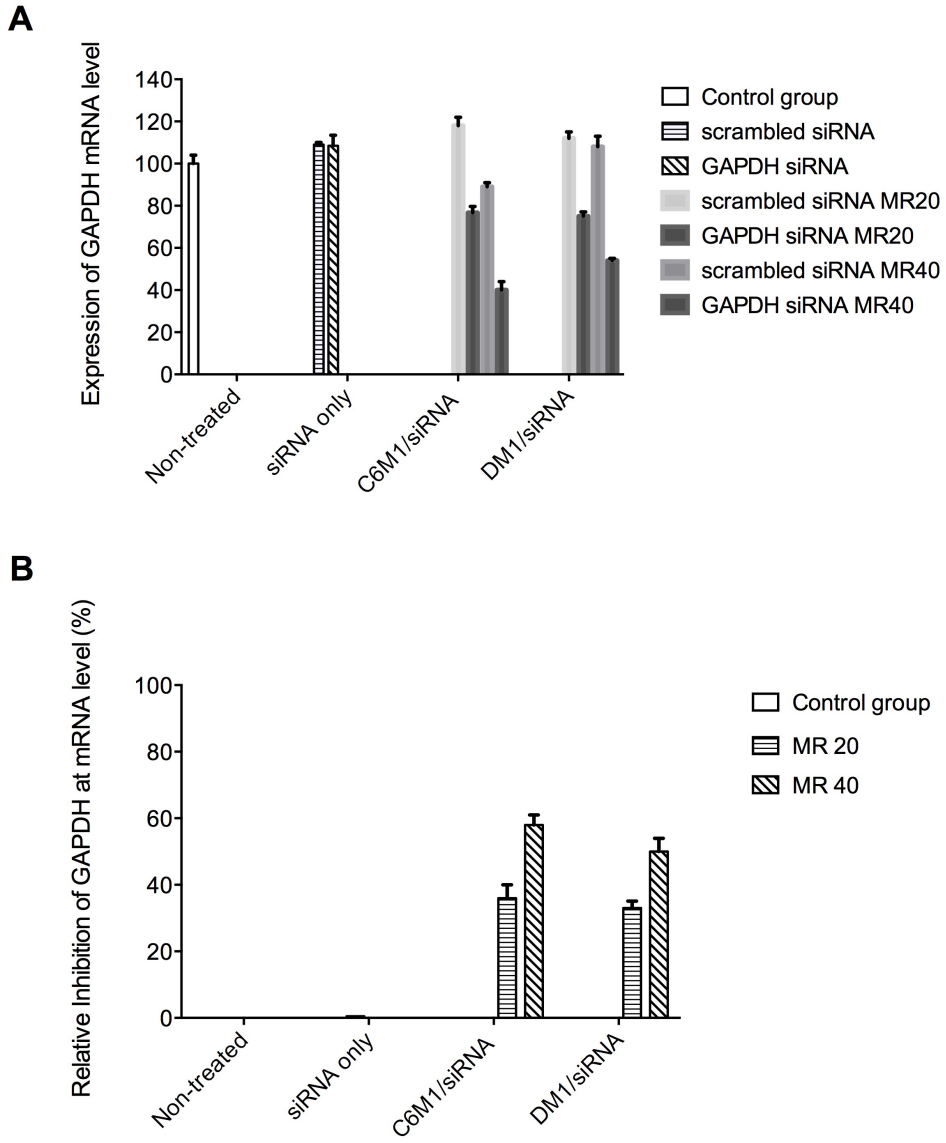

Figure 3.6 Inhibition of GAPDH activity on mRNA level through real time RT-PCR. Peptide/scrambled siRNAs were used as negative control in each group. A) GAPDH gene activity levels regulated with scrambled siRNA and siGAPDH. B) Percentage of GAPDH gene knockdown efficiency, calculated as: (1 – (peptide/siGAPDH expression) / (peptide/ scrambled siRNA expression)) x 100%.

Next, the silencing effects of complexes were confirmed on the protein level using C166 GFP cells that stably expressed the eGFP gene. Fluorescence intensity was measured using FACS and analyzed with FlowJo (Figure 3.7). Complexes of C6M1/sieGFP inhibited the eGFP protein by 35% at a molar ratio of 40/1 and complexes of DM1/sieGFP inhibited the eGFP by 31%. In contrast, cells treated with naked sieGFP did not exhibit any eGFP suppression compared to non-treated samples.

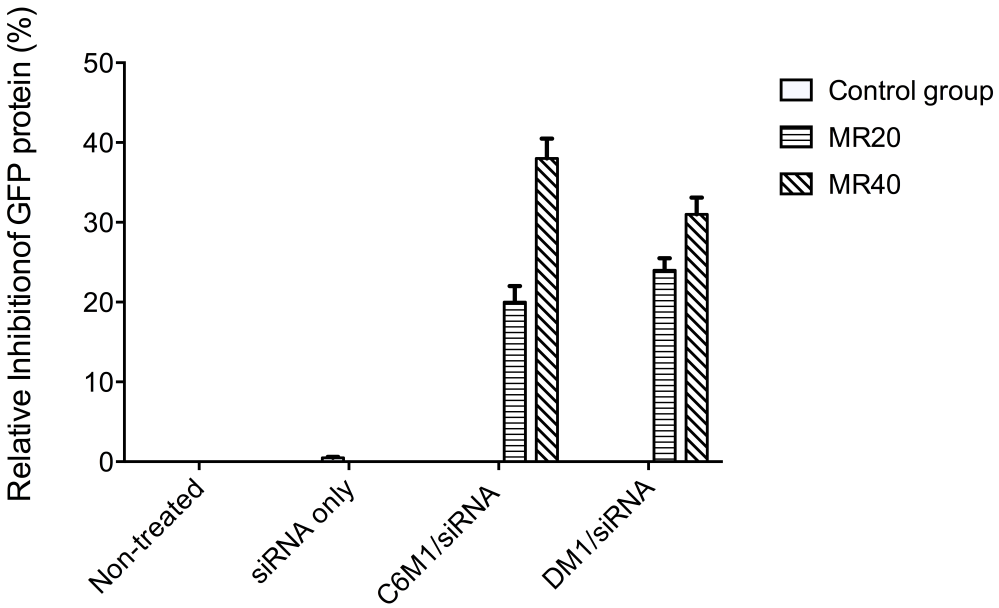

Figure 3.7 Percentage of eGFP gene regulation on protein level through FACS. The results were calculated as: (1- (peptide/sieGFP expression) / (peptide/ scrambled siRNA expression)) x 100%.

The suppression of GAPDH protein activity by peptide/siGAPDH and peptide/scrambled siRNA was measured using the KDalert assay kit (Figure 3.8). GAPDH is an enzyme

catalyzes the sixth step of glycolysis and break down glucose for energy and carbon molecules, and also involved in several non-metabolic processes, including transcription activation, initiation of apoptosis, ER to Golgi vesicle shuttling, and fast axonal, or axoplasmic transport.

In the case of C6M1, complexes reduced GAPDH protein activity by 44% at a molar ratio of 20/1 and by 56% at a molar ratio of 40/1. In the case of DM1, complexes demonstrated a similar efficiency of gene knockdown, i.e., 40% and 61% suppression at molar ratios of 20/1 and 40/1, respectively (Figure 3.8B).

However, it is worth pointing out that C6M1/scrambled siRNA complexes caused a slightly reduction of GAPDH protein expression at a molar ratio of 40/1 (Figure 3.8A). This was the result of C6M1's cytotoxicity on CHO-K1 cells compared to non-treated cells. No significant differences in GAPDH protein expression level were observed between cells treated by DM1/scrambled siRNA compared to non-treated cells.

The GAPDH KDalert kit assay results corresponded well with RT-PCR results, which showed gene knockdown at the mRNA level (Figure 3.6), and the cytotoxicity data (Figure 3.4).

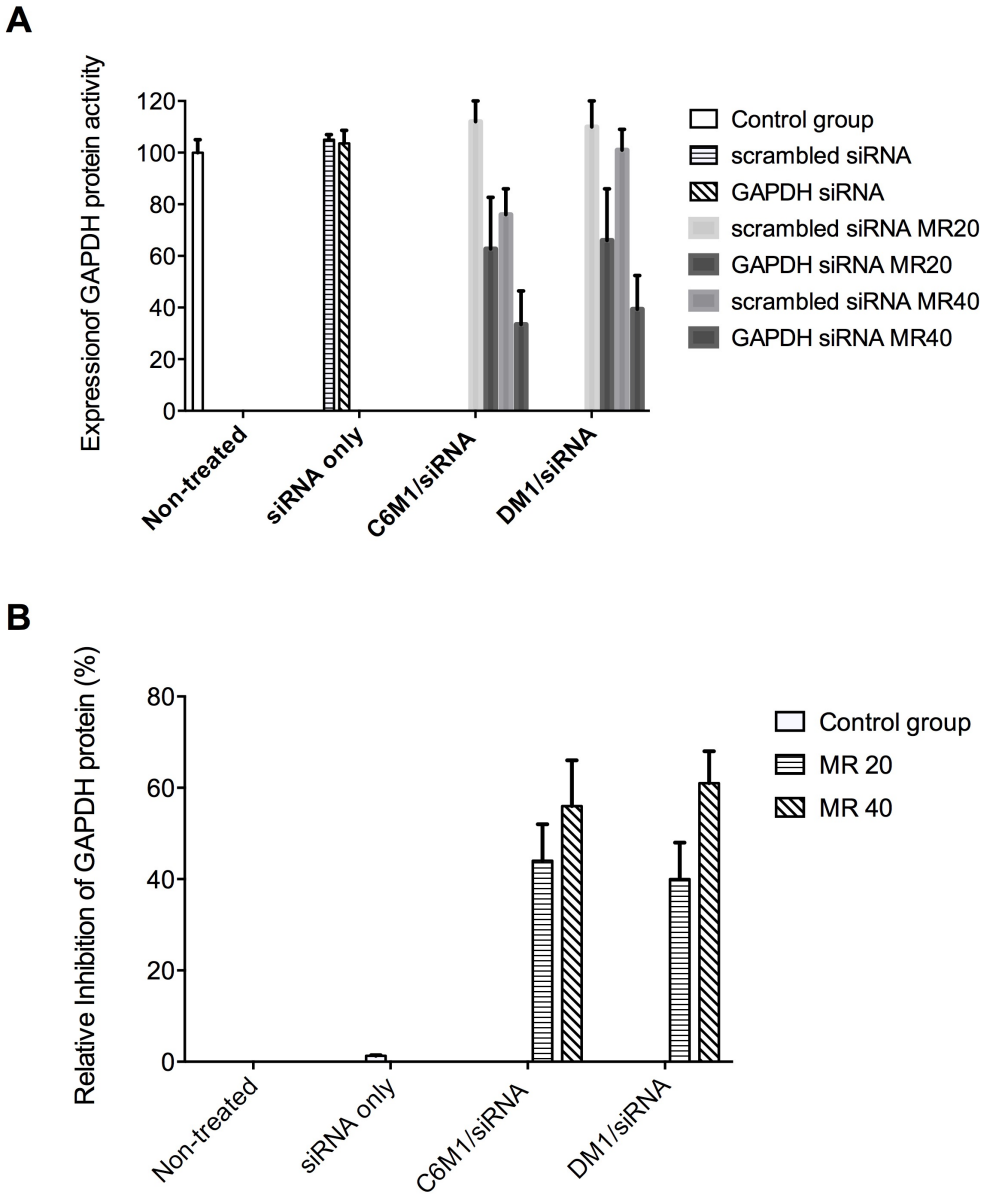

Figure 3.8 Inhibition of GAPDH activity on protein level through real time KDalert assay kit. Peptide/scrambled siRNAs were used as negative control in each group. A) GAPDH gene activity levels regulated with scrambled siRNA and siGAPDH. B) Percentage of GAPDH gene knockdown efficiency, calculated as: (1 – (peptide/siGAPDH expression) / (peptide/ scrambled siRNA expression)) x 100%.

3.3.6 DEGylation on peptides facilitates RNAi efficiency in the presence of high serum concentration

In serum-free medium, the complexes formed by DM1 exhibited a similar level of knockdown efficiency as complexes formed by C6M1. To study the effects of serum on transfection efficiency, we evaluated gene-silencing efficacy on CHO-K1 cells in the presence of increasing amounts of serum (Figure 3.9).

The knockdown efficacies of C6M1/siRNA and DM1/siRNA were comparable at low serum concentration, i.e., 10% of serum, resulting in a reduction of GAPDH protein activity to approximately 50%. However, C6M1/siRNA gradually lost its knockdown capability as the proportion of serum in the medium increased. In the presence of 50% serum, the knockdown efficiency of C6M1/siRNA decreased to 15%, causing 2-fold less suppression of GAPDH protein activity than DM1/siRNA. Both C6M1/siRNA and DM1/siRNA lost their knockdown capability when the proportion of serum reached 90%.

The promising results shown above demonstrate that DEGylation might provide complexes with steric protection to some extent, thus decreasing the ability of complexes to interact with serum components, as previously reported for PEGylation [217, 218]. The presence of massive amounts of albumin in serum has been reported to be the main inhibitor of both DNA [237, 238] and siRNA gene delivery [219, 220]. Negatively charged albumin would compete with siRNA for binding to the positively charged peptides, resulting in the dissociation of the complexes and the degradation of released siRNA [220].

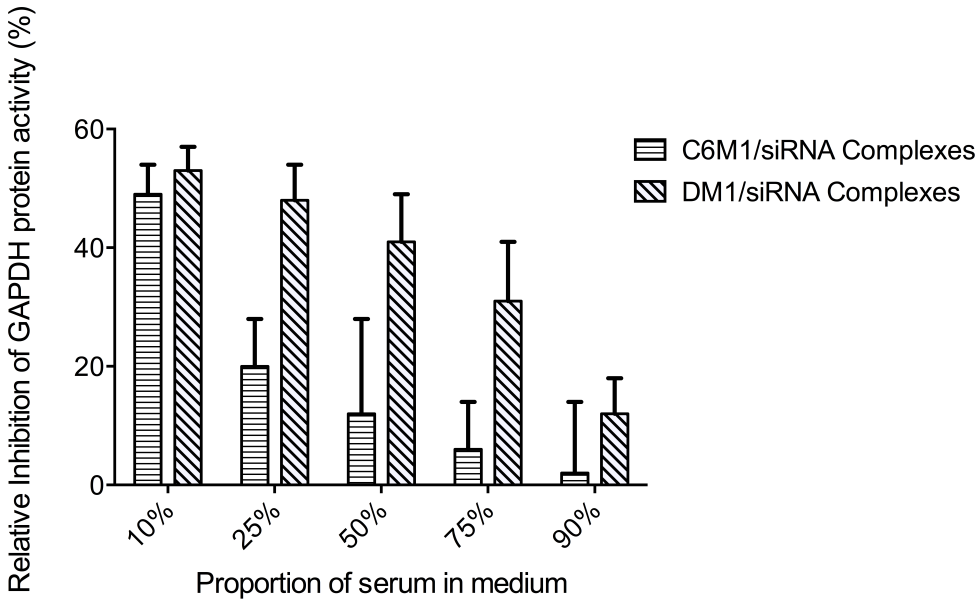

Figure 3.9 Inhibition of GAPDH protein activity in the presence of serum through real time KDalert assay kit. Complexes were formed at molar ratio 40/1, and peptide/scrambled siRNAs were used as negative control in each group.

3.4 Conclusion

RNAi therapy is one of the most promising methods for the treatment of gene-related diseases. However, its application is limited *in vivo* due to the lack of the efficient and safe delivery, where the interactions between siRNA and serum components are a major cause for siRNA degradation during the delivery process [212-214]. To overcome the low efficiency of RNAi caused by serum, we modified our peptide carrier by conjugating it to a short ethylene glycol, i.e., DEG. The DEG-modified peptide/siRNA complexes enhanced cell viability and did not compromise RNAi efficiency. Our data revealed that the peptide conjugated with DEG improved serum resistance while maintaining sufficient gene silencing efficiency. Hence, DEGylated peptide/siRNA complexes may be a promising gene delivery method for *in vivo* gene therapy application.

Despite the improved serum stability, the silencing efficiency of siRNA delivered by C6M1 and the modified DM1 ranged from 40% to 60%, and the less efficient knockdown ability might be due to the entrapment of siRNA in endosome/lysosome vesicles. Therefore, designing new sequences to enhance the endosomal escape of the complexes is required.

Chapter 4

A novel peptide for efficient siRNA delivery *in vitro* and therapeutics *in vivo*

4.1 Introduction

As discussed previously in Chapter3, the application of siRNA has been limited by the anionic nature, relatively large molecular weight, and poor cellular uptake of siRNA molecules [88]. Thus, the development of efficient and safe delivery systems for siRNA has been an important area of research [23]. A variety of delivery strategies have been developed [24], and several strategies stand out. One approach that has attracted wide interest is the use of cell-penetrating peptides (CPPs). CPPs are a class of cationic and/or amphipathic peptides that can deliver siRNA as well as a wide range of small therapeutic molecules for both *in vitro* and *in vivo* applications [155, 156, 247].

To efficiently condense and deliver siRNA, a CPP must have a positive charge [248, 249]; at least eight positive charges are needed for the efficient internalization of cell penetrating peptides [250]. However, excessive positive charges have been reported to cause tissue and cellular toxicity [251]. The use of a nuclear localization sequence (NLS) provides a solution to this dilemma. NLSs are short peptides that can be transported to the nucleus and have fewer than eight positive charges. The first discovered NLS, from simian virus 40 (SV40), is the

sequence PKKKRKV , which has been adopted directly in peptide sequence design for efficient siRNA delivery. For example, MPF (GLAFLGFLGAAGSTMGAWSQPKKKRKV) was derived from SV40 [253].

Based on SV40, we designed a series of amphiphilic peptides composed of a variant of the NLS and a hydrophobic block. The NLS has been modified to PKPKRKV by the single mutation of a lysine residue in SV40 to a proline residue, which aims to limit nuclear translocation and enable the rapid release of the cargo in the cytoplasm [253]. Because only four amino acids in the NLS variant are positively charged at pH 7, we conjugated the sequence PKPKRKV to a hydrophobic moiety to obtain an amphipathic version of CPP for good cellular uptake properties.

Instead of a hydrophobic peptide sequence, we adopted stearic acid as the hydrophobic moiety in our peptides. Stearic acid has been proven to have a high affinity with the cell membrane , and the stearylation of cell-penetrating peptides has been reported to increase the transfection efficiency of both plasmid DNA and siRNA, *e.g.*, STR-R_8, STR-$(RxR)_4$, and STR-$CH_2R_4H_2C$ [254-256]. The amino acid histidine was incorporated as a linker, *i.e.*, HHH. Histidine is a pH-sensitive amino acid and can be protonated at low pH. Through the introduction of histidine moieties, peptides can act as a proton sponge and disrupt endosomal membranes , resulting in the release of siRNA complexes into the cytosol [258].

In this study, we explored a group of five different peptides derived from PKPKRKV for their ability to form siRNA complexes and mediate gene silencing. We revealed that the incorporation of stearic acid and an NLS variant with a selected length of histidine residues

leads to improved transfection efficiency. To investigate the gene-silencing efficiency of the complex, we utilized RT-PCR to examine the knockdown efficiency induced by our peptides with siRNA complexes at the mRNA level. The *in vitro* cytotoxicity was carried out on Human lung cancer cell line (A549, ATCC CCL-185) with an MTT assay before conducting *in vivo* experiments. The results showed that the complexes of siRNA formed with peptide STR-HK were more efficient and displayed lower cytotoxicity than those with peptide H0K, HK, STR-H0K and STR-H6K. The *in vivo* anti-tumor effect of STR-HK/siRNA was determined on a xenograft mouse tumor model. Our results showed that the peptide STR-HK could greatly enhance the internalization of siRNA molecules, achieving a silencing efficiency of 78% *in vitro* and an inhibition rate of 63% *in vivo* without causing toxicity effects.

This Chapter is based on the work published in Acta Biomaterilia, with authorship as: Ran Pan, Wen Xu, Feng Yuan, Dafeng Chu, Yong Ding, Baoling Chen, Mousa Jafari, Yongfang Yuan, Pu Chen.

4.2 Materials and methods

4.2.1 Preparation of complexes

Synthesized by CanPeptide Inc (Quebec, Canada), peptides were dissolved in RNase free water (Thermo scientific, Ottawa, Canada) at a concentration of 1 mM, followed by probe sonication for 10 min, and were stored at -20°C. Synthesized by Sigma, siRNA targeting at the B-cell lymphoma 2 (Bcl-2) gene were dissolved in RNase free water at a concentration of 50 μM, and were store at -80°C.

The peptide/siRNA complexes were prepared in RNase free water for characterization experiments, and were prepared in Opti-MEM (Invitrogen, Carlsbad, CA, USA) for transfection experiments. The peptide/siRNA complexes were prepared at different molar ratio ranged from 1/1 to 80/1 depending on the designed experiment, by slowly manually mixing the peptide solution into siRNA solution with pipette. The complexes were incubated at room temperature for 30 min before conducting experiments.

Lipofectamine 2000, purchased from Life Technologies, was used as positive control in experiments. The lipo 2000/siRNA complexes were prepared in Opti-MEM for transfection experiments, by slowly manually mixing the lipo 2000 solution into siRNA solution with pipette. The ratio of lipo 2000/siRNA remains unknown, since the concentration of lipo 2000 was not revealed by the manufacturer. The amount of lipo 2000 was 1.0 μl/well for 24-well plate, and 0.25 μl/well for 96-well plate, according to the manufacturer's instructions.

4.2.2 Sequence of siRNAs

The siRNA targeting Bcl-2 oncogene was synthesized by Sigma, with a sense sequence of 5'-GGT GGG GTC ATG TGT GTG G-dTdT, and antisense sequence of 5'-CGG TTC AGG TAC TCA GTC ATC C-dTdT. The Silencer^{TM} Cy3-labeled GAPDH siRNA was purchased from Ambion, used in fluorescence microscopy and Fluorescence Activated Cell Sorting (FACS). The eGFP siRNA, used in agarose gel electrophoresis and ribogreen assay, was purchased from Dharmacon with an extinction coefficient of 362408 L/mol cm. The sense sequence of eGFP siRNA was 5'-GAC GUA AAC GGC CAC AAG UUC-dTdT, and antisense sequence was 5'-ACU UGU GGC CGU UUA CGU CGC-dTdT. The negative control siRNA with scrambled sequence used in the experiment was purchased from Ambion.

4.2.3 Gel electrophoresis assay

The interaction of peptide/siRNA complexes was investigated using agarose gel electrophoresis assay. Peptides were mixed with siRNA to form peptides/siRNA complexes as described above with a final amount of 200 ng siRNA per well. The complexes were incubated at room temperature for 30 min before being loaded onto a 1.2% w/v agarose gel labeled with ethidium bromide in TBE buffer and run at 50 V for 60 min.

4.2.4 RiboGreen assay

The amounts of siRNA were quantified by ribogreen assay (Quanti-IT^{TM} RiboGreen, Invitrogen, USA). Peptides were mixed with siRNA to form peptides/siRNA complexes as described above. According to manufacturer's instruction, the complexes solution and ribogreen solution was prepared separately, and the aqueous working solution of ribogreen

assay was slowly added into each sample manually. Each sample was incubated at room temperature for 3 min before measured on UV-Vis spectrometer (Ultrospec 4300 Pro, GE, Canada) with excitation at 480 nm and the emission at 520 nm.

4.2.5 Fourier Transform Infrared (FTIR) spectroscopy

The secondary structure of STR-HK was investigated by a Vertex 70 STIR spectrometer (Bruker Optics, Inc., Billerica, MA, USA) equipped with a liquid nitrogen cooled MCT detector. STR-HK was dissolved in water with different concentration. The spectra of peptides were recorded in the range of 4000-400 cm^{-1} at a spectra resolution of 4 cm^{-1}, and were analyzed with OPUS 5.5 software (Bruker Optics, Inc., Billerica, MA, USA). The absorption spectrum was analyzed between 1700 cm^{-1} and 1600 cm^{-1}.

4.2.6 Particle size

The hydrodynamic diameter of peptide/siRNA complexes were determined on a Zetasizer Nano ZS (Malvern Instruments, U.K.) equipped with a 4 mW He-Ne laser operating at 633 nm. The complexes were prepared as described above at a molar ratio of 40/1, with a final siRNA concentration of 100 nM. The light intensity of complexes were collected at an angle of 173°.

4.2.7 Atomic force microscopy (AFM)

The morphology of STR-HK/siRNA complexes was observed by AFM (Dimension Icon, Bruker, California, USA) at a molar ratio of 40/1. The complexes were prepared as described above, and were loaded on a freshly cleaved-mica surface. The samples were then washed

twice and allowed to air-dry overnight. Standard tips (Bruker, California, USA) were used. Samples were visualized in peak force quantitative nanomechnics (PeakForce QNM) mode, an extension of peak force tapping mode, at 1.0 Hz scanning rate. The scanned image was collected from a 5 x 5 μm area.

4.2.8 Transmission electron microscopy (TEM)

The morphology of STR-HK/siRNA complexes was acquired by transmission electron microscopy (TEM, Philips CM10 TEM, Amsterdam, the Netherlands) at a molar ratio of 40/1. The complexes were prepared as described above with 300 nM of siRNA in 10 ml samples, and were applied to a 400 mesh Formva coated copper grid (Canemco-Marivac, Canton de Gore, Canada). The samples were washed 5 times with RNase free water and dried overnight, and then stained with uranyl acetate (Electron Microscopy Sciences, Hatfiled, USA).

4.2.9 Cell culture and peptide mediated siRNA transfection

Transfection experiments were conducted using Human lung cancer cell line (A549, ATCC CCL-185). The A549 cells were maintained in F-12K medium (Thermo scientific, Ottawa, Canada) supplemented with 10% fetal bovine serum (FBS, Sigma-Aldrich, Oakville, Ontario, Canada) at 37°C in 5% CO_2. Before transfection, A549 cells were seeded in 24-well plates with a confluence of 40,000 cells/well or 60,000 cells/well, and in 96-well plates with a confluence of 7,500 cells/well. After incubating at 37°C for 24 hours, cells were rinsed with phosphate buffered saline (PBS), which was then replaced with Opti-MEM. The STR-HK/siRNA complexes were prepared as described above, diluted in Opti-MEM to a final concentration of 50 nM siRNA and then added to each well. After the cells were incubated at

37°C for 4 hours, medium containing FBS was added to obtain a final concentration of 10% FBS.

4.2.10 Cytotoxicity of complexes

The cytotoxicity of peptide/siRNA complexes was evaluated using 3-(4,5-dimethylthiazole-2-yl)-2,5-diphenyl tetrazolium bromide (MTT) assay, purchased from Sigma. A549 cells were seeded in 96-well plates at 7,500 cells/well and transfected with peptide/siRNA complexes, as described above. After 48 hours, cells were rinsed with PBS, and 100 µL of MTT solution (5 mg/mL in PBS) was added to each well. After 2 hours of incubation at 37°C, 100 µL of solubilization solution, composed of 10% Triton X-100 (Sigma) plus 1% HCl (Sigma) in anhydrous isopropanol (Invitrogen), was added to each well to dissolve the formazan crystals. The optical densities were then measured at 570 nm with a microplate reader (FLUOstar Optima, BMG Labtech, Ortenberg, Germany). Cell viability was calculated as the optical density of each sample divided by the optical density of untreated controls. All measurements were performed in triplicate.

4.2.11 Fluorescence microscopy

The cellular uptake efficiency of complexes was studied by fluorescence microscopy. A549 cells were seeded in 24-well plates at 60,000 cells/well, and transfected with peptide/Cy-3-labeled GAPDH siRNA complexes 24 hours later, as described above. After 4 hours of incubation at 37°C, cells were rinsed with PBS and incubated in 15 U/ml heparin medium for 20 min. This step was repeated 3 times. Cells were then washed twice with PBS, and fixed with 500 µl/well of 4% PFA in PBS at 37°C. After 30 min, the fixation PBS was

aspirated, and the cells were washed twice with PBS before they were covered with Fluoroshield with DAPI mounting medium (Sigma-Aldrich, Oakville, Ontario, Canada). The samples were visualized on a Zeiss Observer Z1 microscope with a 40x objective lens. Images were analyzed using AxioVision software. All measurements were performed in triplicate.

4.2.12 Confocal laser scanning microscopy (CLSM)

A549 cells were seeded in a Nunc Lab-Tek II 4-well chambered coverglass (Thermo scientific, Ottawa, Canada) at 80,000 cells/well, and transfected with peptide/Cy-3-labeled GAPDH siRNA complexes 24 hours later, as described above. After incubation at 37 °C, 75 nM/well of Lysotracker Green (Life Technology, Carlsbad, USA) were added into the medium and incubated for 1 hour. Cells were then washed with 15 U/ml heparin medium for 3 times in one hour at 37 °C, and rinsed twice with PBS. 500 μL of medium were added into each well, with 1 drop of NucBlue Live ReadyProbes Reagent (Life Technology, Carlsbad, USA). Carl Zeiss LSM 700 confocal microscope (Zeiss, Jena, Germany) was used to visualize the cells. The microscope was equipped with Plan-Apochromat 20x/0.8 NA objective lens. The images were analyzed with Olympus FluoView FV1000 software.

4.2.13 Uptake efficiency of complexes

The cellular uptake efficiency of complexes was quantified by flow cytometry (type BD Biosciences, BD FACS Vantage SE Cell Sorter, USA). A549 cells were seeded in 24-well plates at 60,000 cells/well, and transfected with peptide/Cy-3-labeled siRNA complexes 24 hours later, as described above. After 4 hours of incubation at 37°C, cells were rinsed with PBS and incubated in 15 U/ml heparin medium for 20 min. This step was repeated 3 times.

Cells were then washed twice with PBS, detached from the plate with 0.25% trypsin/EDTA, and then collected in the suspension of 4% PFA in PBS. The collected samples were analyzed by fluorescence acquired cell sorting (FACS), and the data were analyzed by Flowjo software. All measurements were performed in triplicate.

4.2.14 Bcl-2 silencing assay at mRNA level

The efficiency of Bcl-2 siRNA interference was evaluated using real time RT-PCR that shows the gene knockdown on mRNA level. The sequences of Bcl-2 primers adopted in this study were: 5'-GGTGGGGTCATGTGTGTGG-3' (F), and 5'-CGGTTCAGGTACTCAGTCATCC-3' (R). A549 cells were seeded in 24-well plates and transfected with peptide/siRNA complexes 24 hours later, as described above. After 48 hours, total RNA was isolated using the RNeasy Mini Kit (Qiagen, Valencia, CA, USA), and the RNA concentration was measured using Nanodrop (Nanodrop spectrophotometer ND-1000, Thermo scientific, Ottawa, Canada). RNA was then reverse transcribed into cDNA using Bio-Rad iScript cDNA synthesis kit (Bio-Rad Laboratories, Ontario, Canada). RT-PCR was performed using the Mx3005P™ Real Time PCR System (Agilent Technologies, Wilmington, DE, USA) with Brilliant II Fast SYBR Green QPCR Master Mix (Agilent Technologies), according to the manufacturer's instructions. The data was normalized to cyclophilin genes, with primer sequences as: 5'-GGTGATCTTTGGTCTCTTCGG-3' (F), and 5'-TAGATGCTCTTTCCTCCTGTG-3' (R). All measurements were performed in triplicate.

4.2.15 *In vivo* experiment

To evaluate the efficacy the antitumor activity of STR-HK/siRNA complexes, six-week-old male BALB/c nude mice were used as mouse xenograft tumor model, with eight mice involved in each group. Animal experiments were carried out with the NIH Guide for the Care and Use of Laboratory Animals, provided by Shanghai Jiao Tong University, Shanghai, China. Obtained from the B&K Universal Group Limited (Shanghai, China), all mice were maintained under 12 hours light/dark cycles at 25°C with 60±10% humidity. The mice were inoculated subcutaneously with 5×10^6 A549 cells at the right armpit to generate the xenograft tumor model. When the tumor volume reached 100-200 mm^3, STR-HK/siRNA targeting Bcl-2 oncogene complexes was injected directly into the tumor at a molor ratio of 60:1. Total nine treatments per mouse were administered at a dose of 4 ug siRNA/mouse, every three days. The diameters of tumors and the body weight of mouse were measured every day. All mice were sacrificed on day 27, and and the tumor volume was calculated as follows: tumor volume=$0.5\times(\text{width})^2\times\text{length}$.

4.2.16 Western blot

Western blot assay were used to analyze Bcl-2 protein expression in tumor tissue. According to the manufacturer's instructions, the proteins were extracted using a total protein extraction kit (Kangchen Biotechnology, Shanghai, China). Protein samples were separated by 12% SDS-PAGE gels and then transferred to nitrocellulose (NC) membranes. After blocking with blocking buffer for 2 hours, the membranes were incubated with polyclonal rabbit anti-Bcl-2 (Santa Cruz, California, USA) with a ratio of 1:1000 overnight at 4 °C.

Horseradish peroxidase (HRP) conjugated goat anti-rabbit IgG (Kangchen Biotechnology, Shanghai, China) was used as a secondary antibody with a ratio of 1:2000 for 2 hours. The bound secondary antibody was detected by enhanced chemiluminescence (Pierce Biotechnology, Rockford, IL, USA). GAPDH (Kangchen Biotechnology, Shanghai, China) was used as an internal standard.

4.3 Results and Discussion

4.3.1 Characterization and interaction of the peptides with siRNA

The peptides were designed to comprise a modified NLS block, which has 3 positive charges and 0, 3 or 6 histidine residues. Optionally, stearic acid was incorporated at the N-terminus of the peptides, as shown in Table 4.1.

Table 4.1 Sequences and molecular weight of peptides

Name	Sequence	MW	Purity
H0K	Acetyl-PKPKRKV-NH2	895.4	97.3%
HK	Acetyl-HHHPKPKRKV-NH2	1304.7	99.4%
STR-H0K	Stearyl-PKPKRKV-NH2	1117.7	94.7%
STR-HK	Stearyl-HHHPKPKRKV-NH2	1529.0	96.2%
STR-H6K	Stearyl-HHHHHHPKPKRKV-NH2	1940.1	95.1%

The sizes of the peptide/siRNA complexes were examined by dynamic light scattering at peptide to siRNA molar ratios of 20/1, 40/1, 60/1 and 80/1. As shown in Table 4.2, the average diameter of the complexes ranged from 47 nm – 184 nm, which has been reported as the optimal size range for nanoparticles internalized by cells [259]. Preferably, the size of carrier/siRNA complexes should be less than 200 nm to ensure optimal diffusion through tumor tissue by the enhanced permeation retention effect (EPR), and to reduce the recognition

and removal by phagocytic cells *in vivo*. Figure 4.1 shows the typical morphology of the STR-HK/siRNA complexes as visualized by atomic force microscopy (AFM) and transmission electron microscopy (TEM) at a molar ratio of 40/1. Although some aggregated complexes are observed in both images, the main population of the complexes was characterized with a width of approximately 40-120 nm, consistent with the DLS results. Additionally, the AFM and TEM images revealed the round shapes of the complexes resulting from the co-assembly of STR-HK and siRNA molecules.

Table 4.2 Particle sizes of peptides with siRNA complexes at different molar ratios

Name	MR20 (nm)	PDI	MR40 (nm)	PDI	MR60 (nm)	PDI	MR80 (nm)	PDI
H0K	151	> 0.5	144	0.48±0.09	129	0.33±0.05	134	0.29±0.07
HK	184	> 0.5	167	0.35±0.11	120	0.22±0.17	131	0.21±0.03
STR-H0K	147	0.31±0.17	129	0.31±0.06	101	0.27±0.02	97	0.23±0.04
STR-HK	132	0.24±0.04	115	0.29±0.05	88	0.18±0.01	64	0.12±0.03
STR-H6K	124	0.29±0.03	109	0.22±0.03	76	0.17±0.05	47	0.19±0.02

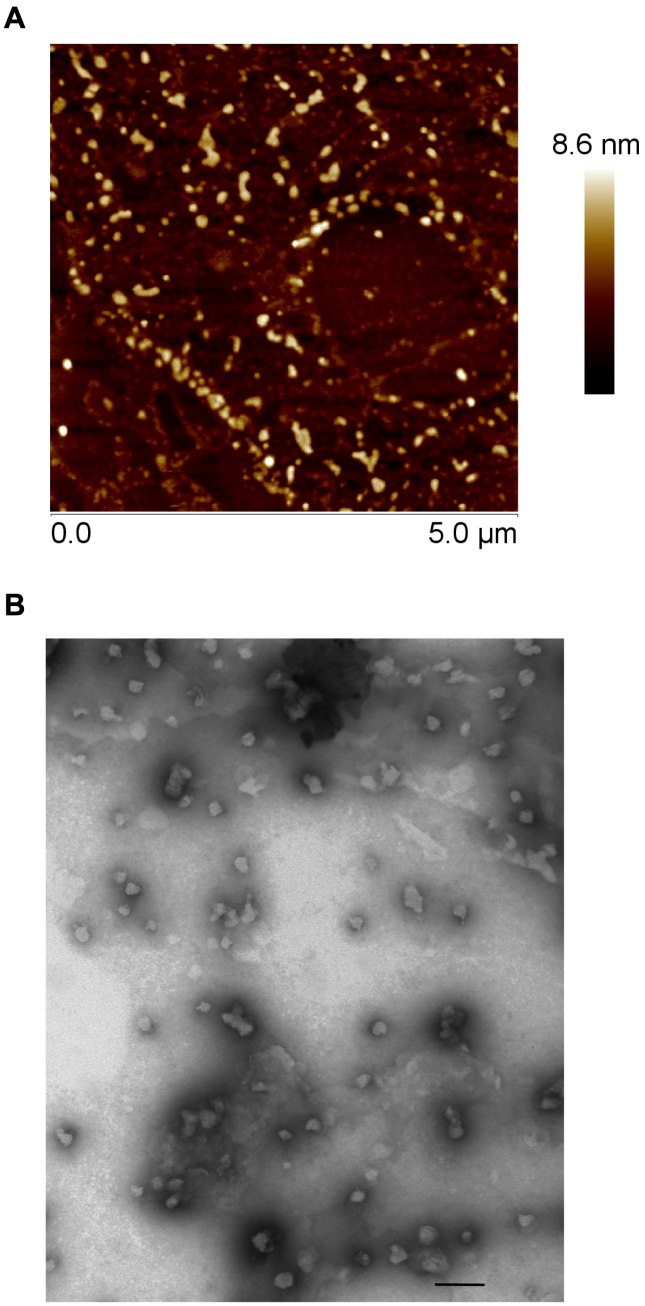

Figure 4.1 Morphology and size investigation of STR-HK/siRNA complexes. A: A typical AFM image of STR-HK/siRNA complexes at MR 40, with a 5 µm x 5 µm scan. B: TEM image of STR-HK/siRNA complexes at MR 40, with a scale bar of 100 nm.

The secondary structure of the peptide STR-HK was studied by Fourier Transform Infrared **(**FTIR) spectroscopy in the range of 1700-1600 cm^{-1}, which is the spectral region most sensitive to peptide secondary structure, where the amide I band is located. The peaks at ~ 1630 cm^{-1} and ~ 1690 cm^{-1} were assigned to β-sheet structures, and the peaks at ~ 1670 cm^{-1} represent β-turn structures [260]. As shown in Figure 4.2, STR-HK showed one peak at approximately 1630 cm^{-}, and another peak at 1670 cm^{-1}, suggesting the presence of a combination of β-sheet and β-turn structures. When the concentration of STR-HK was increased, the intensities of the peaks increased, while the locations of the peaks remained the same, suggesting that the secondary structures were stable and independent of concentration.

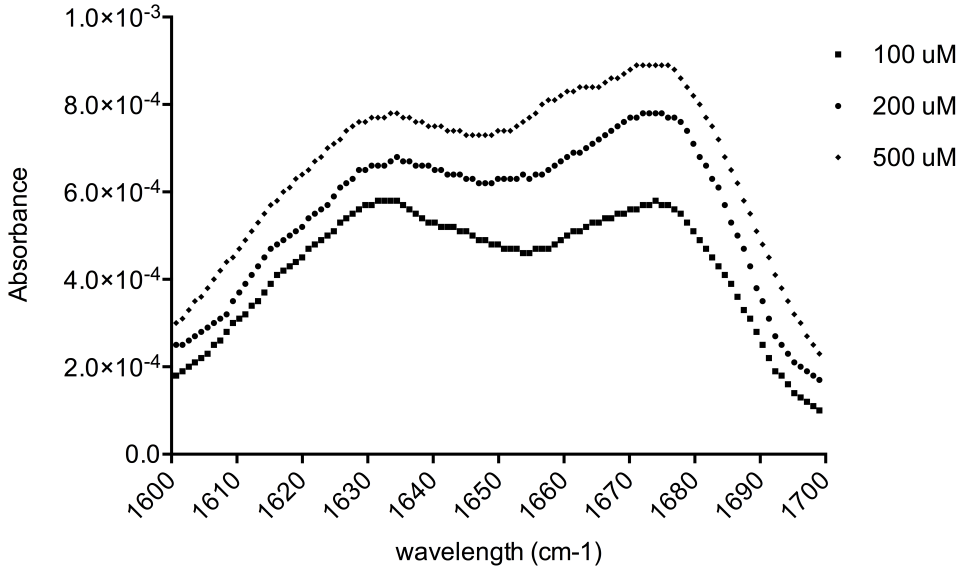

Figure 4.2 FTIR spectra of peptides STR-HK of the amide I region with concentration different concentrations.

To investigate the complexes formed between the peptides and siRNA, a RiboGreen assay was applied to quantitatively characterize the interactions between the peptides and siRNA (Figure 4.3A). The strong fluorescence of RiboGreen intercalates with free siRNA, and the binding capacity of siRNA can be detected and calculated based on the fluorescence of RiboGreen. At a pH of 7, arginine and lysine residues are positively charged and can interact with the phosphate groups on siRNA molecules through electrostatic interactions. There were four positively charged residues in each peptide molecule, *i.e.*, three lysine amino acids and one arginine amino acid. The intensities of the complexes gradually decreased with an increasing molar ratio of peptides/siRNA, and the siRNA molecules were completely complexed with peptides HK, STR-H0K, STR-HK, STR-H6K at a molar ratio of 15/1, and with peptide H0K at a molar ratio of 20/1.

Figure 4.3B shows a typical agarose gel electrophoresis assay for the STR-HK/siRNA complexes at different molar ratios. In Figure 4.3B, the peptide/siRNA complexes started to form at a very low molar ratio (MR) of 1/1, as evidenced by the decrease in the band intensity relative to that for the molar ratio of 0 (siRNA only). The siRNA molecules were completely associated with STR-HK at MR 15 and above, as there was no band for free siRNA detected.

Ideally, siRNA molecules should completely bind to peptides when the molar ratio is greater than 11/1, since in peptide sequence PKPKRKV there are four positively charged residues in one molecule at pH 7, which consisted of three lysine residues and one arginine residue. There were 21 pairs of negatively charged nucleotides in one siRNA molecule, which in theory, could be condensed with these peptides at a molar ratio of approximately 11/1. The experimental results suggest that the peptide/siRNA complexes can be used in transfection

experiments with a molar ratio higher than 15/1 to ensure complete siRNA complexation. In this study, we prepared the complexes in pH 7 environments, and molar ratios of 20/1, 40/1, 60/1 and 80/1 were adopted in the following cellular experiments.

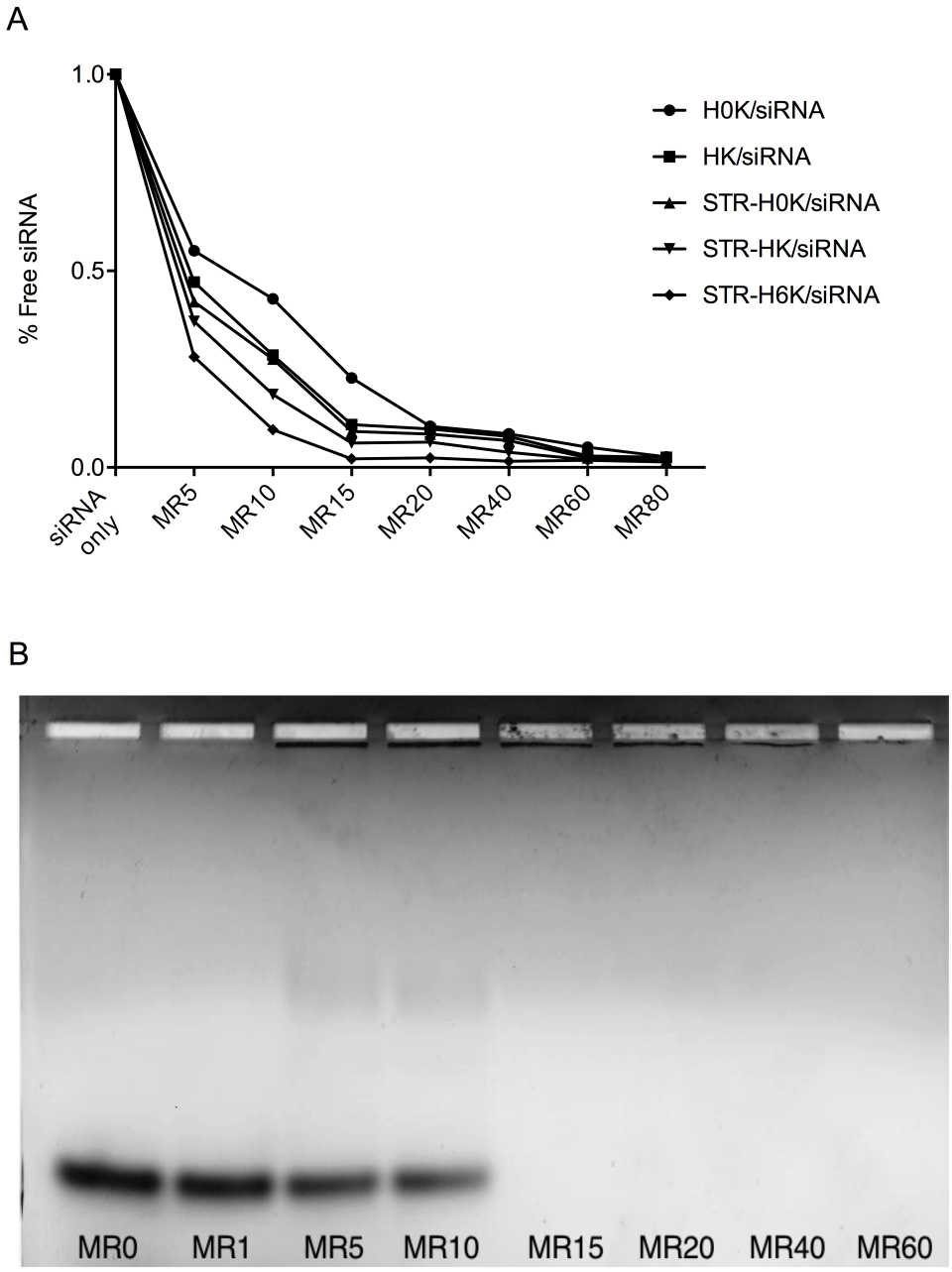

Figure 4.3 Interactions between peptides and siRNA molecules. A: siRNA binding capacity, measured by ribogreen assay with five peptides/siRNA compelxes: H0K/siRNA, HK/siRNA, STR-H0K/siRNA, STR-HK/siRNA, and STR-H6K/siRNA: with molar ratios of 0, 5/1, 10/1, 15/1, 20/1, 40/1, 60/1, and 80/1; B: an agarose gel electrophoresis assay of STR-HK/siRNA complexes: with molar ratios of 0, 1/1, 5/1, 10/1, 15/1, 20/1, 40/1, and 60/1.

4.3.2 Knockdown efficiency of the HK peptide/siRNA complexes *in vitro*

To gain insight into the potential use of our peptides as a delivery agent, we conducted transfection experiments on A549 cells and analyzed the results with RT-PCR (Figure 4.4). The Bcl-2 gene was chosen to evaluate the gene-silencing efficacy of the peptide mediated siRNA transfection. The complexes of scrambled siRNA with peptides (negative control) and the naked Bcl-2 siRNA without peptides showed no knockdown of the Bcl-2 gene at the mRNA level. Comparing the peptides at different molar ratios, the STR-HK/siRNA complexes induced the highest silencing effect of 78% at a molar ratio of 40/1 (Figure 4.4). The complexes of siRNA with STR-H6K induced a silencing efficiency of 36%±4.6% at MR60, while the complexes of siRNA with H0K, HK, STR-H0K showed a less than 30% silencing efficiency.

The STR-HK/siRNA complexes reduced the mRNA level of the Bcl-2 gene to a lesser extent than did lipo2000/siRNA; *i.e.*, 78%±3.4% of STR-HK/siRNA at MR40 and 89%±2.2% of lipo2000/siRNA. However, it was shown above that the high transfection efficiency of lipo2000/siRNA is associated with high cytotoxicity (Figure 4.7, shown in **4.3.4**). Comparing the cell viability profiles of lipo 2000 with those of STR-HK, there was a more than 30% reduction for the lipo2000/siRNA complexes, while there was little toxicity from STR-HK/siRNA at the molar ratios used for the knockdown experiments.

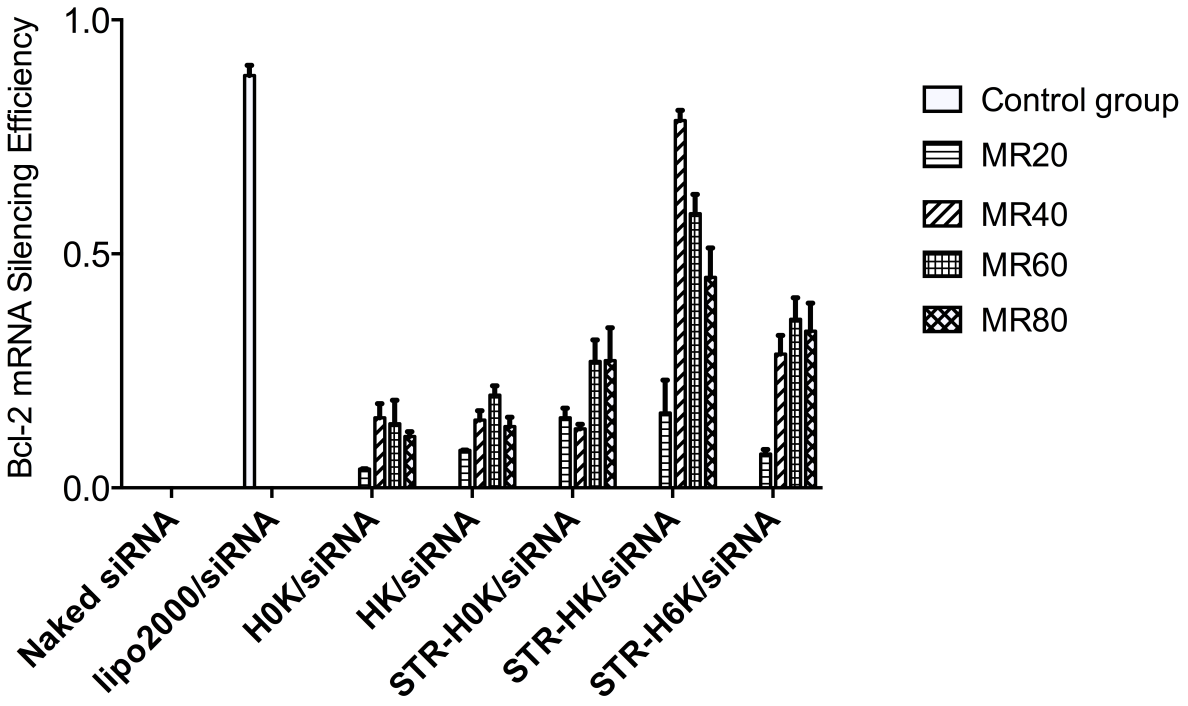

Figure 4.4 Inhibition of Bcl-2 activity on mRNA level through real time RT-PCR, with siRNA conc. = 50 nM/well. Peptide/scrambled siRNA complexes were used as negative control in each group. Lipofectamine 2000 was used as a positive control. Percentage of Bcl-2 gene knockdown efficiency, calculated as: (1 – (peptide/siRNA targeting Bcl-2 gene expression) / (peptide/scrambled siRNA expression)) x 100%.

4.3.3 Cellular uptake and colocalization of the peptide/siRNA complexes

We further evaluated the ability of our peptides to deliver siRNA into cells. To eliminate the effect of the complexes attached to the surfaces of cells [261], 15 U/ml heparin in Opti-MEM was used to wash the cells three times at 37°C to ensure that all the visible siRNA

molecules were localized inside the cells [147]. The uptake efficiency of the Cy-3 labeled siRNA/HK peptide complexes was examined at different molar ratios with fluorescence-activated cell sorting (FACS) (Figure 4.5A).

The uncomplexed siRNA molecules could not be delivered into the cells, while the uptake efficiency of the peptide/siRNA complexes increased significantly. The uptake efficiency of the STR-HK/siRNA complexes at MR 40 was approximately 20% higher than that of the lipo2000/siRNA. However, a lower uptake efficiency of 20%±2.1% was observed in the treatment with the STR-HK/siRNA complexes at MR 20 because the positive charge was involved in the interaction with siRNA, and the net positive charge was insufficient to interact with the cell membranes [138]. The complexes of Cy-3 labeled siRNA with H0K or HK exhibited a 15% cellular uptake rate, while the uptake efficiency increased to 20% - 65% after conjugating with stearic acid, *i.e.*, in the complexes STR-H0K, STR-HK and STR-H6K. These results suggested that stearic acid was essential for the cellular internalization of the peptide/siRNA complexes and that the addition of histidine as a linker was necessary; i.e., the STR-HK/siRNA complexes showed improved uptake efficiency compared with the complexes without histidine, *i.e.*, STR-H0K/siRNA. However, the increased length of the histidine residues resulted in a decreased cellular internalization of the peptides, *i.e.*, of STR-H6K/siRNA relative to STR-HK/siRNA. Furthermore, the low cellular internalization efficiency of the STR-H6K/siRNA complexes might explain their limited gene-silencing performance.

Figure 4.5B shows the typical cellular uptake and localization of the STR-HK/Cy-3 labeled siRNA complexes. As expected, the uncomplexed Cy3-labeled siRNA could not be internalized into the cells (Figure 4.5B1), in accordance with previous results (Figure 4.5A). siRNA internalization occurred only in the presence of STR-HK or lipo2000. A red fluorescence signal could be found in almost every cell and was localized around the nucleus. Moreover, the effects were more pronounced with peptide STR-HK at MR 40 (Figure 4.5B3) than with lipo2000/siRNA (Figure 4.5B2). The fluorescent-labeled siRNA molecules were localized close to the nuclear membrane instead of in the nucleus (Figure 4.5) because siRNA molecules will bind to the RNA-induced silencing complex (RISC) and initiate RNA interference in the cytosol.

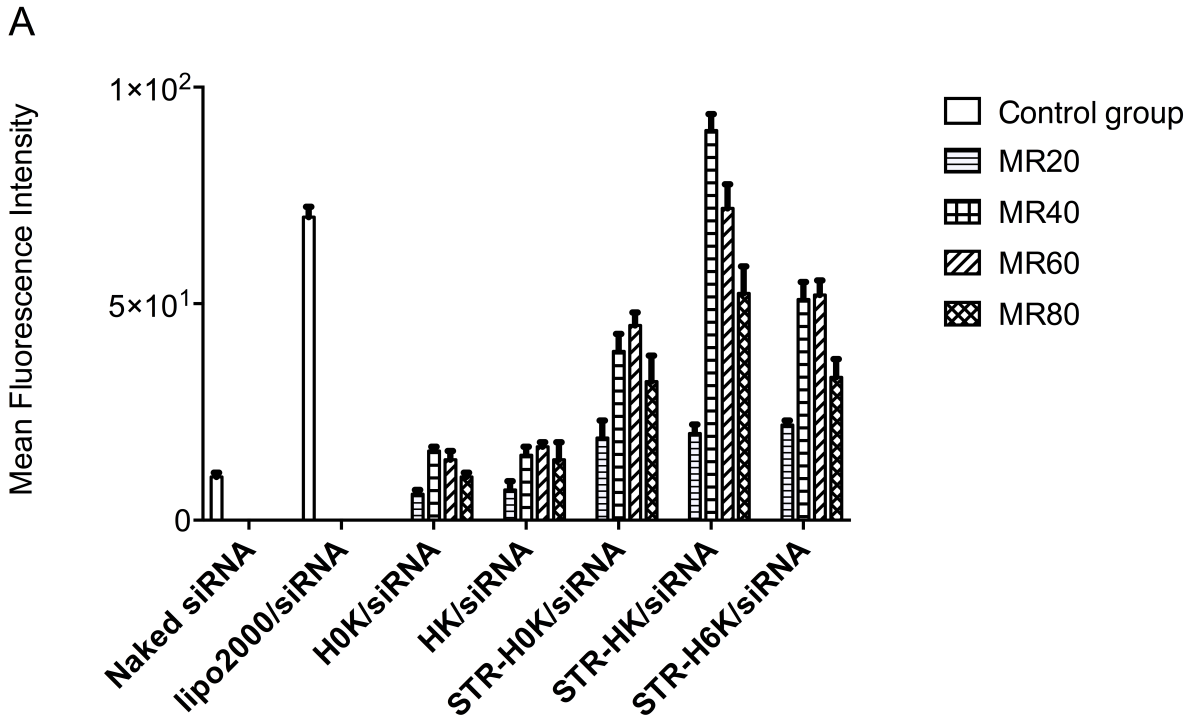

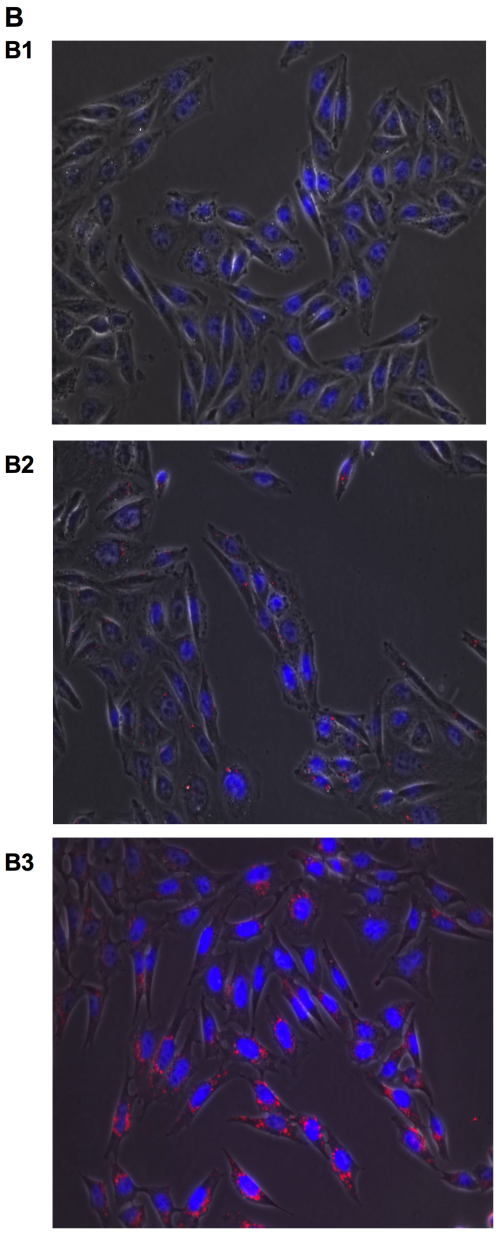

Figure 4.5 Uptake efficiency of peptide/siRNA complexes on A549 cells, with siRNA conc. = 50 nM/well. A: fluorescence intensity of internalized complexes measured by FACS, analyzed by flowjo. B: fluorescence microscopy of STR-HK/siRNA complexes, the blue solid circles: cell nucleus dyed by DAPI; red dots: cy-3 labeled siRNA. B1: siRNA only treated cells; B2: lipo 2000/siRNA treated; B3: STR-HK/siRNA at MR 40.

To observe subcellular localization, A549 cells were treated with peptide/siRNA complexes and visualized with confocal microscopy. Figure 4.6 showed a punctual distribution pattern of peptide/siRNA complexes, which was in accordance with the punctual pattern of endosomal/lysosomal vesicles as labeled with Lysotracker Green. At 3h, the colocalization percentage of siRNAs with endosome/lysosome vesicles were calculated as 87%, visualized as yellow fluorescent spots in Figure 4.6A. This suggested that the peptide/siRNA complexes were internalized within three hours through endocytic pathway. The same colocalization pattern can be visualized clearly in the enlarged cellular image. Endosomal escape of siRNAs can be obsearved at 12 hours after treatment, shown in Figure 4.6B, with the colocalization percentage decreased to 32%.

Figure. 4.6A

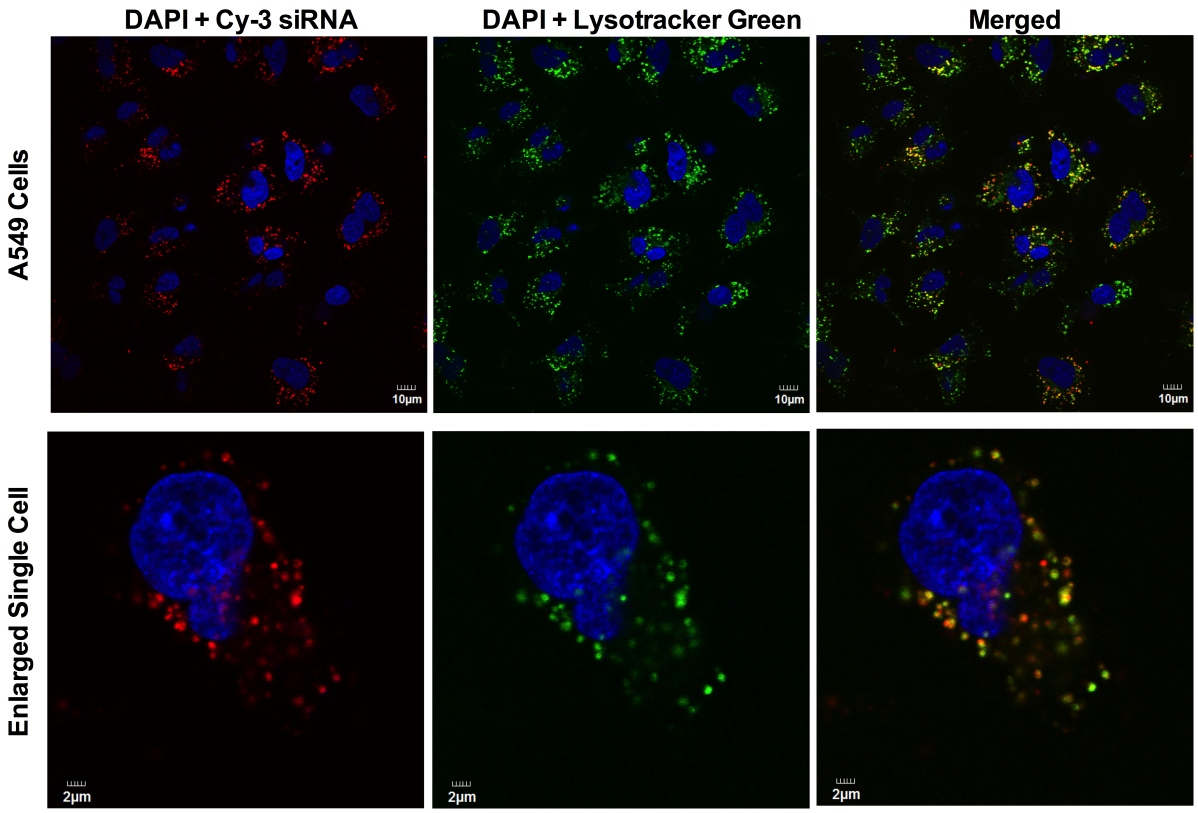
DAPI + Cy-3 siRNA
DAPI + Lysotracker Green
Merged
A549 Cells
Enlarged Single Cell
10µm
2µm

Figure 4.6B

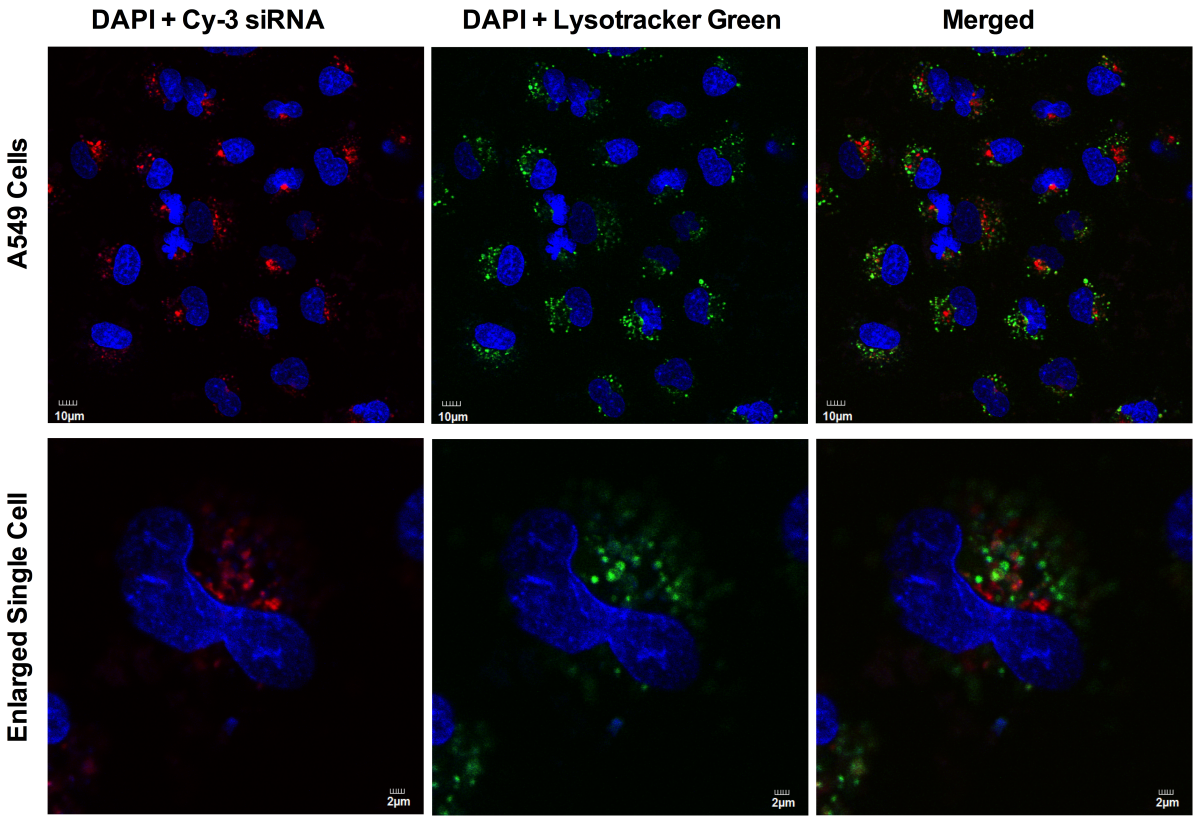

Figure 4.6 Intracellular localization of STR-HK/siRNA complexes on A549 cells, with siRNA conc. = 50 nM/well. Images were visualized by confocal microscopy, and pseudocolored for visualization: blue = DAPI; red = Cy-3 siRNA; green = LysoTracker Green. Co-localization of siRNA with the endosomal/lysosomal marker is in yellow. A: 3 hours incubation time; B: 12 hours incubation time.

4.3.4 Cell viability in the presence of the peptide/siRNA complexes

Safety is one of the most important factors for selecting gene delivery systems. To study the cytotoxicity of peptide/siRNA complexes, an MTT assay was used on A549 cells. The cell

viability profile shown in Figure 4.7A indicated that no cytotoxicity was induced by the siRNA complexes with peptides H0K, HK or STR-H0K. In addition, the cell viability was not significantly affected in the cells treated with STR-HK/siRNA or with STR-H6K/siRNA at MR20 and MR40. There was more than 90% viability at MR 20 and MR 40 after 48 hours of treatment with STR-HK/siRNA and STR-H6K/siRNA, which was higher than the cells treated with the lipo2000/siRNA complexes, which showed only 70% viability. The STR-HK/siRNA and STR-H6K/siRNA treatments at MR60 appeared to induce only slight cytotoxicity compared to the non-treated cells.

Increasing the amounts of STR-HK and STR-H6K greatly influenced the cell viability. At MR80, more than half of the cells died after 48 hours of treatment. A high positive charge density has been reported to result in toxicity because positively charged residues can interact with negatively charged cell membranes and cause aggregation and rupture on the membrane surface . The reduced charge density in STR-HK corresponds to good cell viability results, as expected. This non-toxic nature is important to develop successful gene-silencing reagents and therapeutic agents for *in vivo* applications. The low toxicity shown here suggests that STR-HK is a safe transfection reagent.

The cell viability of peptides only was shown in Figure 4.7B, which was relatively lower than the corresponding complexes. The reason for that might be there are more positive charges in peptides only, while the addition of siRNA molecules neutralizes the charges.

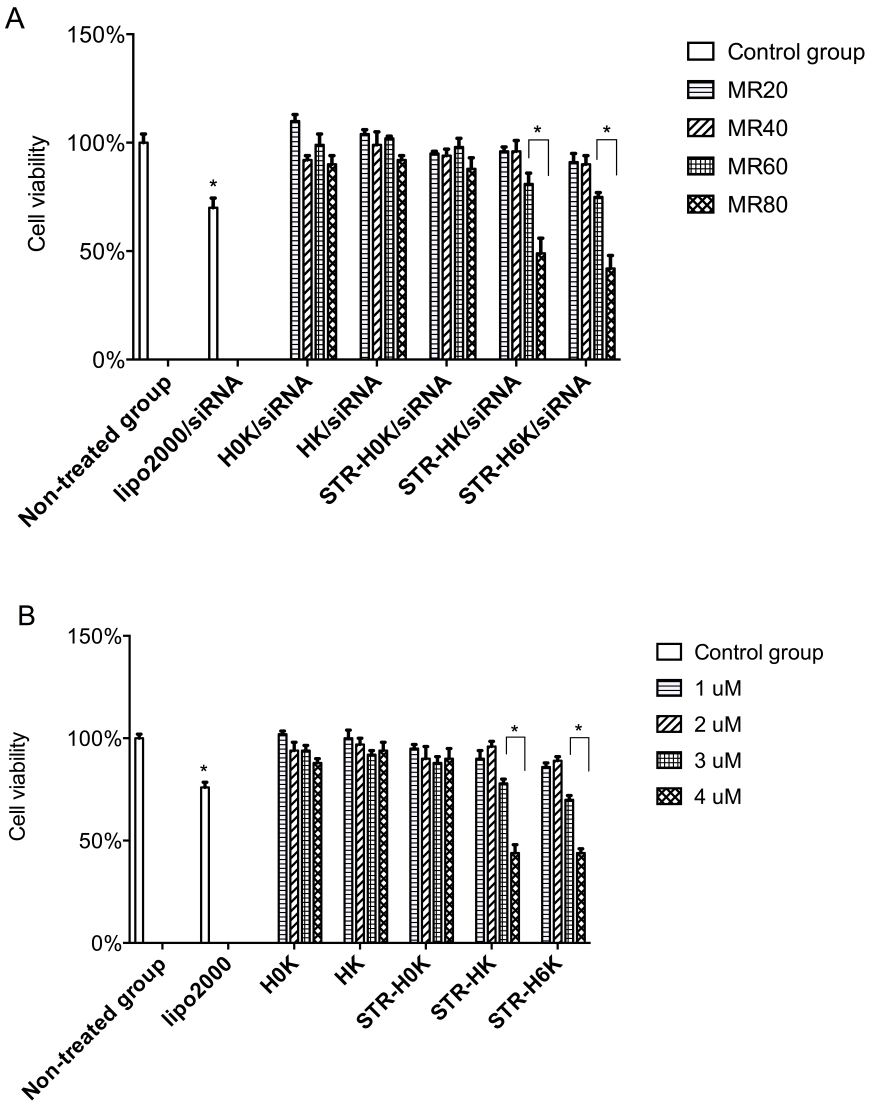

Figure 4.7 Cell toxicity performed by MTT assay on A549 cells, with siRNA conc. = 50 nM/well. Lipofectamine 2000 was used as positive control. A: Peptide/siRNA complexes were tested with 4 different molar ratios: 20/1, 40/1, 60/1, and 80/1. B: Peptide only with addition of peptide amounts equivalent to corresponding complexes: 1 μM/well, 2 μM/well, 3 μM/well, and 4 μM/well. (* vs non-treated group, $p<0.05$)

4.3.5 *In vivo* results with STR-HK/siRNA complexes

siRNA shows great therapeutic potential as a cancer drug in mouse tumor models because of its ability to regulate the activity of oncogenes. In recent years, several studies have reported the *in vivo* application of liposomes as gene delivery agents [263, 264], while the application of peptide-mediated siRNA delivery for *in vivo* applications still remains a challenge, because of the complicated situation in the body, such as the presence of extracellular matrix barriers and the occurrence of serum degradation and immune responses. Therefore, in an effort to demonstrate its clinical potential, we investigated the antitumor activity of the STR-HK/siRNA complexes in a mouse xenograft tumor model.

The Bcl-2 protein is an attractive target for gene therapy because it regulates the mitochondria-mediated apoptosis pathway [265]. Drugs designed to reduce the level of Bcl-2 protein are expected to promote apoptosis and therefore inhibit tumor growth.

To demonstrate their potential for *in vivo* applications, we investigated the antitumor activity of the STR-HK/siRNA complexes in a mouse xenograft Non-small cell line cancer A549 model. The results showed that STR-HK/siRNA at MR 60 could successfully suppress tumor cell proliferation throughout the experimental period (Figure 4.8A) while showing minimal toxicity (Figure 4.8D). Interestingly, the tumor treated with naked Bcl-2 siRNA also showed a decreased size (Figure 4.8). In addition, 62% of silencing efficiency was demonstrated in western blot results of STR-HK/siRNA treated group, while 30% of silencing efficiency was also shown in siRNA only group. The results are in accordance with other researchers on A549 xenograft mouse model , and other types of cancer cells [267]. The

cellular uptake of naked siRNAs *in vitro* was relatively low, compared with the uptake into tissues *in vivo*. The mechanisms remain unknown, but it might be due to the role of the complex extracellular matrices in tissues [267]. However, STR-HK/siRNA complexes clearly induced a better antitumor effects compared with naked siRNA group, shown from the western blot results.

After 27 days of treatment, the tumor tissues were separated and weighed (Figure 4.8B and C). The average tumor volumes of the control group and the STR-HK/siRNA treated group were 1246 mm^3 and 544 mm^3, respectively, demonstrating that the tumor size was significantly reduced upon STR-HK/siRNA treatment. The tumor weight of the STR-HK/siRNA treated group, 0.4714 g, was lower than that of the control group at 1.27 g and than that of the saline treated control group at 1.36 g, demonstrating a tumor inhibition rate of 62.86% (Figure 4.8C). A lack of significant changes in body weight (Figure 4.8D) demonstrated that the STR-HK/siRNA complexes were relatively safe to use. No severe side effects were observed during the experimental periods. A western blot analysis indicated that there was a specific down regulation of the Bcl-2 protein in the STR-HK/siRNA treated group, while the housekeeping protein GAPDH remained unchanged (Figure 4.8E). In summary, STR-HK/siRNA can inhibit tumor growth with an inhibition rate of 62.8% through intratumoral injection in the xenograft mouse tumor model. No significant body weight decreases and no severe side effects were observed over the experimental periods, which suggest that the STR-HK/siRNA complexes are potentially safe for *in vivo* applications.

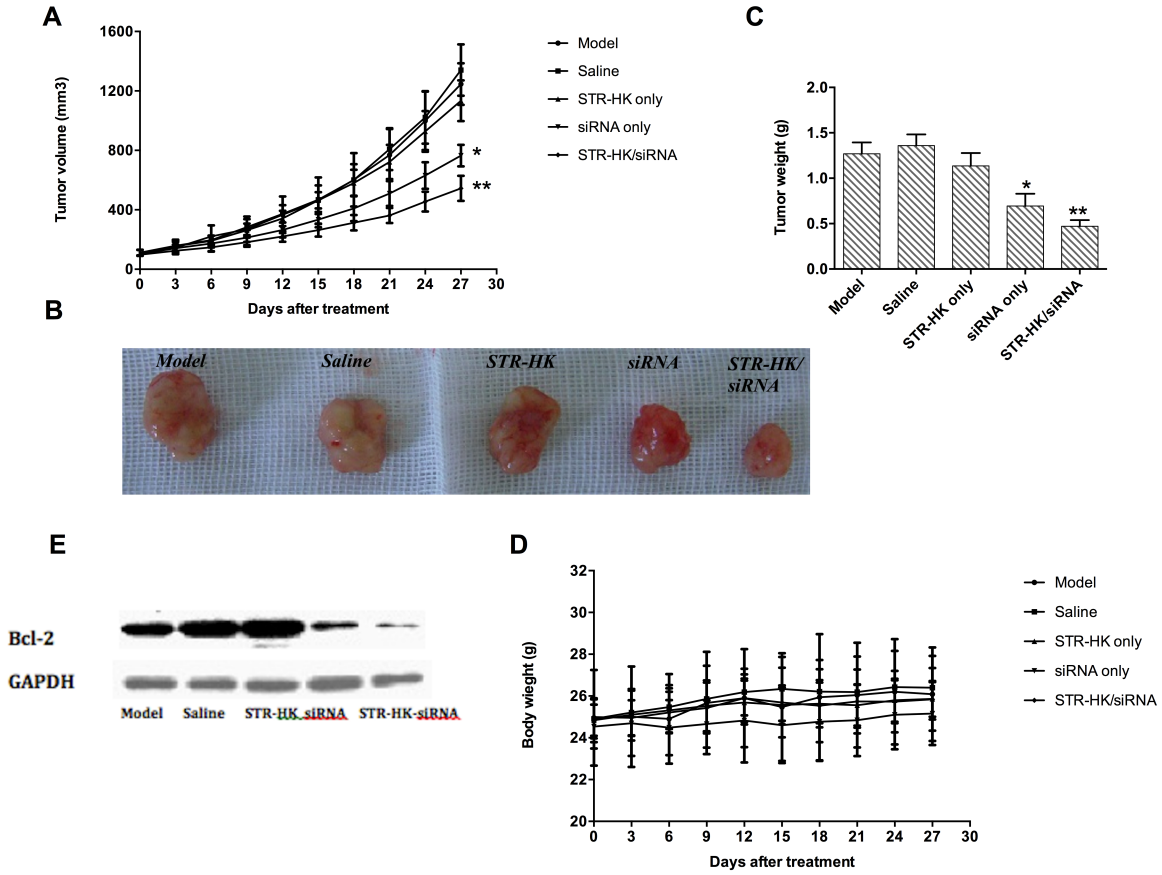

Figure 4.8 *In vivo* results of STR-HK, with 8 mice involved in each group. A: tumor volume of each group (* vs model group, $p<0.05$; ** vs model group and siRNA group, $p<0.05$); B: separated tumor of each group; C: tumor weight of each group; D: body weight of each group; E: Bcl-2 protein expression with western blot.

4.4 Conclusions

Small interfering RNA can inhibit the expression of specific genes and has considerable potential as a therapeutic agent for many diseases. The development of siRNA carriers with good efficiency and low toxicity is highly expected. In this study, we designed a series of peptides and investigated their use as potential siRNA delivery systems. The results revealed that the peptide STR-HK, a new amphiphilic, cationic peptide consisting of a modified NLS block and a stearic acid tail, could efficiently facilitate siRNA delivery. Together with results showing that STR-HK/siRNA possesses the ability to inhibit the expression of specific genes both *in vitro* and *in vivo*, we showed that STR-HK is a successful siRNA delivery carrier and may be used for siRNA therapeutics.

Despite the successful tumor inhibition, peptide STR-HK and the STR-HK/siRNA complexes induced strong cytotoxicity *in vitro* with the increasing amounts of peptide, i.e., the cell viability of STR-HK/siRNA complexes dropped to 50% when the peptide concentration increased to 4 μM. Hence, the modification of peptide sequence and the designing of peptides with less cytotoxicity is highly required.

Chapter 5

Evaluation of Newly Designed Cell Penetrating Peptides with Stearic Acid as siRNA Carriers

5.1 Introduction

As previously discussed in Chapter 3 and Chapter 4, the applications of siRNA depended on the development of delivery systems. In this chapter, we designed a family of cell-penetrating peptides, which formed nano-complexes with siRNA through electrostatic interactions and mediated gene silencing on various cell lines.

Based on the design principles, a selected small number of lysine residues were employed in the sequences, to provide positive charges to bind with the siRNAs while not inducing toxicity due to a high number of positive charges. Second, to overcome the lack of sufficient positive charges to cross the plasma membrane and based on the previous results from Chapter 4 [268] and [269], we adopted stearic acid, which was reported to have a high affinity to the cell membrane. Moreover, we investigated the addition of a histidine group and valine group and the effects on their biological activities. In this chapter, we intended to determine which sequences could increase the gene silencing efficiency without inducing cytotoxicity. The physical chemistry properties of peptide/siRNA complexes were characterized and compared.

The gene silencing efficiency of peptide/siRNA complexes was optimized and then studied in various cell lines. The cytotoxicity and immunogenicity of the complexes was also investigated.

This Chapter is based on the work submitted to Journal of Physical Chemistry B, with authorship as: Ran Pan, Wen Xu, Danyang Zhao, Yong Ding, Sheng Lu, Lei Zhang, Pu Chen.

5.2 Materials and methods

5.2.1 Preparation of complexes

Synthesized by CanPeptide Inc (Quebec, Canada), peptides were dissolved in RNase free water (Thermo scientific, Ottawa, Canada) at a concentration of 500 μM, followed by probe sonication for 10 min, and were stored at -20°C. The peptide sequences were listed in Table 5.1. Synthesized by Sigma, siRNA were dissolved in RNase free water at a concentration of 50 μM, and were store at -80°C.

Table 5.1 Sequences and molecular weight of peptides.

Name	Sequence	MW	Purity
STR-H0K3V6	Stearyl-KKKVVVVVV-NH2	1263.3	96.2%
STR-H3K3V6	Stearyl-HHHKKKVVVVVV-NH2	1676.7	95.3%
STR-H6K3V6	Stearyl-HHHHHHKKKVVVVVV-NH2	2088.1	92.8%
STR-H3K6V6	Stearyl-HHHKKKKKKVVVVVV-NH2	2060.2	95.4%
STR-H3K3V9	Stearyl-HHHKKKVVVVVVVVV-NH2	1972.1	94.3%
STR-H3K9V6	Stearyl-HHHKKKKKKKKKVVVVVV-NH2	2444.8	96.1%

The peptide/siRNA complexes were prepared in RNase free water for characterization experiments, and were prepared in Opti-MEM (Invitrogen, Carlsbad, CA, USA) for transfection experiments. The peptide/siRNA complexes were prepared at different molar ratios depending on the designed experiment, by slowly manually mixing the peptide solution

into siRNA solution with pipette. The complexes were incubated at room temperature for 30 min before conducting experiments.

Lipofectamine 2000, purchased from Life Technologies, was used as positive control in experiments. The lipo2000/siRNA complexes were prepared in Opti-MEM for transfection experiments, by slowly manually mixing the lipo 2000 solution into siRNA solution with pipette. The ratio of lipo 2000/siRNA remains unknown, since the concentration of lipo 2000 was not revealed by the manufacturer. The amount of lipo 2000 was 1.0 μl/well for 24-well plate, and 0.25 μl/well for 96-well plate, according to the manufacturer's instructions.

5.2.2 Sequence of siRNAs

The siRNA targeting Bcl-2 oncogene was synthesized by Sigma, with a sense sequence of 5'-GGT GGG GTC ATG TGT GTG G-dTdT, and antisense sequence of 5'-CGG TTC AGG TAC TCA GTC ATC C-dTdT. The Silencer^{TM} Cy3-labeled GAPDH siRNA was purchased from Life Technologies (Burlington, ON, Canada) and used in Fluorescence Activated Cell Sorting (FACS). Targeting glyceraldehyde 3-phosphate dehydrogenase (GAPDH) gene, the silencer GAPDH siRNA was also purchased from Life Technologies and the sequence was not revealed by the manufacturer. The eGFP siRNA was synthesized by Dharmacon with an extinction coefficient of 362408 L/mol cm. The sense sequence of eGFP siRNA was 5'-GAC GUA AAC GGC CAC AAG UUC-dTdT, and antisense sequence was 5'-ACU UGU GGC CGU UUA CGU CGC-dTdT. The negative control siRNA with scrambled sequence used in the experiment was also purchased from Life Technologies.

5.2.3 Ribogreen assay

The amounts of siRNA were quantified by ribogreen assay (Quanti-IT^{TM} RiboGreen, Invitrogen, USA). Peptides were mixed with siRNA to form peptides/siRNA complexes as described above. According to manufacturer's instruction, the complexes solution and ribogreen solution was prepared separately, and the aqueous working solution of ribogreen assay was slowly added into each sample manually. Each sample was incubated at room temperature for 3 min before measured on UV-Vis spectrometer (Ultrospec 4300 Pro, GE, Canada) with excitation at 480 nm and the emission at 520 nm.

5.2.4 Particle size

The hydrodynamic diameter of peptide/siRNA complexes were determined on a Zetasizer Nano ZS (Malvern Instruments, U.K.) equipped with a 4 mW He-Ne laser operating at 633 nm. The complexes were prepared as described above at a molar ratio of 60/1, with a final siRNA concentration of 100 nM. The light intensity of complexes was collected at an angle of 173°.

5.2.5 Atomic force microscopy (AFM)

The morphology of peptide/siRNA complexes was observed by AFM (Dimension Icon, Bruker, California, USA) at a molar ratio of 60/1. The complexes were prepared as described above, and were loaded on a freshly cleaved-mica surface. The samples were then washed twice and allowed to air-dry overnight. Standard tips (Bruker, California, USA) were used. Samples were visualized in peak force quantitative nanomechnics (PeakForce QNM) mode, an

extension of peak force tapping mode, at 1.0 Hz scanning rate. The scanned image was collected from a 1 x 1 μm area.

5.2.6 Cell culture and peptide mediated siRNA transfection

Transfection experiments were conducted on various cell lines. Human lung cancer cell line (A549, ATCC CCL-185) and Chinese hamster ovary cell line (CHO-K1, ATCC CCL-61) were maintained in F-12K medium (Thermo scientific, Ottawa, Canada) supplemented with 10% fetal bovine serum (FBS, Sigma-Aldrich, Oakville, Ontario, Canada) at 37°C in 5% CO_2. HeLa cells (ATCC CCL-2) were maintained in Minimum Essential Medium (Thermo scientific, Ottawa, Canada) supplemented with 10% FBS at 37°C in 5% CO_2. Human pancreatic cancer cell line (Panc-1, ATCC CCL-1469) were maintained in Dulbecco's Modified Eagle Medium high glucose (Thermo scientific, Ottawa, Canada) supplemented with 10% FBS at 37°C in 5% CO_2.

Before transfection, A549 cells were seeded in 24-well plates with a confluence of 40,000 cells/well or 60,000 cells/well, and in 12-well plates with a confluence of 100,000 cells/well. CHO-K1 cells were seeded in 24-well plates with a confluence of 35,000 cells/well or 60,000 cells/well, and in 96-well plates with a confluence of 6,000 cells/well. HeLa cells were seeded in 24-well plates with a confluence of 40,000 cells/well, and Panc-1 cells were seeded in 24-well plates with a confluence of 45,000 cells/well.

After incubating at 37°C for 24 hours, cells were rinsed with phosphate buffered saline (PBS), and then replaced with Opti-MEM. The peptide/siRNA complexes were prepared as described above, diluted in Opti-MEM to a final concentration of 50 nM siRNA and then

added to each well. After incubated at 37°C for 4 hours, the cells were proceeded to collection for flow cytometry, or supplemented with medium containing FBS to obtain a final concentration of 10% FBS.

The C166-GFP cells (ATCC: CRL-2583) were cultured in Dulbecco's Modified Eagle Medium high glucose containing 10% FBS at 37°C in 5% CO_2. The GFP cells were seeded in 24-well plates at 40,000 cells/well and incubated for 24 hours before transfection. The cells were rinsed with PBS, and Opti-MEM was then added. The peptide/siRNA complexes were prepared as described above and were added to each well at a final concentration of 50 nM siRNA. To maintain cell growth, FBS was added after 4 hours of incubation to achieve a final concentration of 10%.

Macrophage cells (RAW 264.7, ATCC TIB-71) were maintained in Dulbecco's Modified Eagle Medium high glucose supplemented with 10% fetal bovine serum at 37°C in 5% CO_2. Before transfection, RAW 264.7 cells were seeded in 12-well plates with a confluence of 250,000 cells/well. After incubating at 37°C for 24 hours, cells were rinsed with PBS and Opti-MEM was then added. The peptide/siRNA complexes were prepared as described above, diluted in Opti-MEM to a final concentration of 50 nM siRNA and then added to each well. After the cells were incubated at 37°C for 6 hours, cells were harvested and total RNA were isolated.

5.2.7 Cell viability assay

The cytotoxicity of peptide/siRNA complexes was evaluated using 3-(4,5-dimethylthiazole-2-yl)-2,5-diphenyl tetrazolium bromide (MTT) assay, purchased from

Sigma-Aldrich. CHO-K1 ells were seeded in 96-well plates and transfected with peptide/siRNA complexes, as described above. After 48 hours, cells were rinsed with PBS, and 100 μL of MTT solution (5 mg/mL in PBS) was added to each well. After 2 hours of incubation at 37°C, 100 μL of solubilization solution, composed of 10% Triton X-100 (Sigma) plus 1% HCl (Sigma) in anhydrous isopropanol (Invitrogen), was added to each well to dissolve the formazan crystals. The optical densities were then measured at 570 nm with a microplate reader (FLUOstar Optima, BMG Labtech, Ortenberg, Germany). Cell viability was calculated as the optical density of each sample divided by the optical density of untreated controls. All measurements were performed in triplicate.

5.2.8 Fluorescent activated cell sorting (FACS)

The cellular uptake efficiency of complexes was quantified by flow cytometry (type BD Biosciences, BD FACS Vantage SE Cell Sorter, USA). CHO-K1 cells were seeded in 24-well plates at 60,000 cells/well, and transfected with peptide/Cy-3-labeled siRNA complexes 24 hours later, as described above. After 4 hours of incubation at 37°C, cells were rinsed with PBS and incubated in 15 U/ml heparin medium for 20 min. This step was repeated 3 times. Cells were then washed twice with PBS, detached from the plate with 0.25% trypsin/EDTA, and then collected in the suspension of 4% PFA in PBS. The collected samples were analyzed by fluorescence acquired cell sorting (FACS), and the data were analyzed by Flowjo software. All measurements were performed in triplicate.

5.2.9 Gene silencing assay at mRNA level

The efficiency of siRNA interference was evaluated using real time RT-PCR that shows the gene knockdown on mRNA level. Cells were seeded in 24-well plates and transfected with peptide/siRNA complexes 24 hours later, as described above. After 48 hours, total RNA was isolated using the RNeasy Mini Kit (Qiagen, Valencia, CA, USA), and the RNA concentration was measured using Nanodrop (Nanodrop spectrophotometer ND-1000, Thermo scientific, Ottawa, Canada). RNA was then reverse transcribed into cDNA using Bio-Rad iScript cDNA synthesis kit (Bio-Rad Laboratories, Ontario, Canada). RT-PCR was performed using the Mx3005P™ Real Time PCR System (Agilent Technologies, Wilmington, DE, USA) with Brilliant II Fast SYBR Green QPCR Master Mix (Agilent Technologies), according to the manufacturer's instructions. GAPDH primers used in this experiment are: 5'-TGT GTC CGT CGT GGA TCT GA-3' (F), and 5'-TTG CTG TTG AAG TCG CAG GAG-3' (R). Bcl-2 primers used in this experiment are: 5'-GGT GGG GTC ATG TGT GTG G-3' (F), and 5'-CGG TTC AGG TAC TCA GTC ATC C-3' (R). The data was normalized to cyclophilin genes, with primer sequences as: 5'-GGTGATCTTTGGTCTCTTCGG-3' (F), and 5'-TAGATGCTCTTTCCTCCTGTG-3' (R). All measurements were performed in triplicate.

5.2.10 Western blot

Western blot assay were used to analyze Bcl-2 protein expression. A549 cells were seeded in 6-well plate with density of 10,000 cells/well, and treated after 24 hours incubation as described before. Cells were harvested 72 hours after treatment and samples were separated by 12% SDS-PAGE gels and then transferred to nitrocellulose (NC) membranes. After blocking

with blocking buffer for 2 hours, the membranes were incubated with polyclonal rabbit anti-Bcl-2 (Santa Cruz, California, USA) with a ratio of 1:1000 overnight at 4 °C. Horseradish peroxidase (HRP) conjugated goat anti-rabbit IgG was used as a secondary antibody with a ratio of 1:2000 for 2 hours. The bound secondary antibody was detected by enhanced chemiluminescence (Pierce Biotechnology, Rockford, IL, USA). β-actin was used as an internal standard. The images were quantified with Image J software.

5.2.11 eGFP silencing assay

C166 GFP cells were seeded in 24-well plates and transfected with peptide/siRNA targeting GFP protein complexes 24 hours later, as described above. After 48 hours of incubation, the cells were rinsed with PBS and collected in 4% PFA solutions. The samples were evaluated by FACS, and the results were analyzed by Flowjo software.

5.2.12 *In vitro* complement activation assay

The ELISA-based method for quantification of serum S-protein bound C terminal complex (SC5b-9) was performed. Peptides and control compound Zymosan (Sigma, Oakville, ON, Canada) were incubated with human serum (Quidel, San Diego, CA, USA) for 1 hour at 37 °C. The serum was then diluted 150-fold by specimen diluent (provided in the ELISA kits). The SC5b-9 levels of samples were evaluated with MicroVue SC5b-9 plus kit (Quidel, San Diego, CA, USA) according to the manufacturer's instruction. All measurments were performed in duplicate.

5.2.13 Cytokine activation assay

RAW 264.7 cells were seeded in 12-well plate and transfected as described above. 6 hours after transfection, total RNA was isolated as described above. RT-PCR was performed with different primers, shown in Table 5.2. All measurements were performed in duplicate.

Table 5.2 Sequences of primers for RT-PCR with cytokine activation assay

Gene	Sequences of primer
β-actin	F: AGAGGGAAATCGTGCGTGAC
	R: CAATAGTGATGACCTGGCCGT
iNOS	F: CAGCTGGGCTGTACAAACCTT
	R: CATTGGAAGTGAAGCGTTTCG
COX-2	F: AGAAGGAAATGGCTGCAGAA
	R: CTCAATACTGGAAGCCGAGC
IL1-β	F: CCCAAGCAATACCCAAAGAA
	R: GCTTGTGCTCTGCTTGTGAG
TNF-α	F: AGACCCTCACACTCAGATCATCTTC
	R: TTGCTACGACGTGGGCTACA
IL6	F: AAGTGCATCATCGTTGTTCAT
	R: GAGGATACCACTCCCAACAGA

5.3 Results and Discussion

5.3.1 Incorporation of stearic acid and valine group with positively charged lysine group

The STR-KV family peptides were designed with a stearic acid moeity, a positive lysine amino acid block, and a hydrophobic valine block. In addition, a selected number of histidine residues were also included in the peptide sequences. It has been reported that the stearylation of cell-penetrating peptides could increase the transfection efficiency of plasmid DNAs or siRNAs [254-256] because stearic acid had a high affinity to cellular membranes [254]. It has also been demonstrated in our previous work that the addition of stearic acid helps the formation of complexes [269, 270].

To co-assemble with siRNA molecules via electrostatic interactions, positively charged lysine residues were adopted in the peptide sequences. The number of lysine residues was limited to avoid cytotoxicity and immunogenicity caused by high positive charge density [271, 272]. The structure of two hydrophobic blocks that are present in the ends of peptides has been employed in lipid-based gene delivery for a long time. Lipids that consisted of two hydrophobic tails were considered to have a lower critical aggregation concentration than those with a single chain : thus, they could reduce the amounts of nanoparticles that are needed. To adopt these advantages while reducing the cytotoxicity and avoiding possible immune responses, a hydrophobic valine block was incorporated in the STR-KV family of peptides. Histidine was employed as a linker group. Moreover, the pH-sensitive histidine

residues were always employed in peptide or polymer designs to provide protonable groups [274].

Based on the above designing principles, a library of six peptides was designed and studied to investigate the role of: 1) the positively charged lysine group, 2) the hydrophobic valine groups, and 3) the number of protonable hisitidine residues on the peptide-mediated siRNA gene silencing efficiency.

5.3.2 Interaction of peptides with siRNAs and the size distribution of complexes

To study the peptides from the STR-KV family that formed stable complexes with siRNA, a Ribogreen RNA intercalation assay was performed to quantitatively characterize the interactions between the peptides and siRNAs (Figure 5.1). The highly sensitive fluorescent reagent was designed to bind to free RNA, with an excitation of approximately 500 nm and an emission of approximately 525 nm [275]. As shown in Figure 5.1, the Ribogreen fluorescence intensities gradually decreased with the increasing amounts of peptides. At a pH of 7, the positively charged lysine residues interacted with siRNA molecules through electrostatic interactions. Considering 21 pairs of negatively charged nucleotides in one siRNA molecule, peptides with three lysine residues should at least theoretically, completely condense siRNA at a molar ratio of 14/1. In addition, peptide STR-H3K6V6 and STR-H3K9V6 can have a stronger binding affinity with siRNA molecules because there are more positively charged lysine amino acids in one peptide molecule: thus, there should be a sufficient charge to encapsulate siRNA at the lower molar ratio of 7/1 and 5/1. In Figure 5.1, the percentage of

free siRNAs decreased to less than 10% when the molar ratio was above 20/1 for all six peptides.

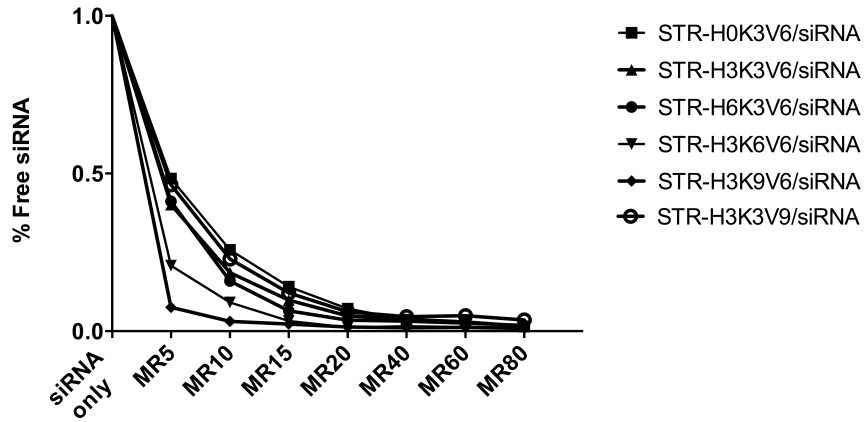

Figure 5.1 siRNA binding capacity with peptides, measured by RiboGreen assay. siRNA concentration was 50 nM, and formed complexes with molar ratios ranged from 0 to 80/1.

The size distributions of the peptide/siRNA complexes were examined by dynamic light scattering at various molar ratios. As shown in Table 5.3, the average diameter of the complexes ranged from 80 nm to 170 nm. Ideally, the nanoparticles with sizes below 200 nm was considered to be as the optimal size for the cellular internalization of nanoparticles [276]. Particles that were larger than 200 nm would be recognized and removed by phagocytic cells *in vivo*. Meanwhile, it worth noticed that the size distribution of STR-H3K3V9/siRNA complexes was wide with PDI larger than 0.5, while other peptides formed complexes uniformly at molar ratios larger than 20/1 with PDI ranges from 0.1 to 0.3.

Table 5.3 Particle sizes of peptides with siRNA complexes at different molar ratios

Name	MR20 (nm)	PDI	MR40 (nm)	PDI	MR60 (nm)	PDI	MR80 (nm)	PDI
STR-H0K3V6	151	> 0.5	144	0.38±0.09	129	0.33±0.05	134	0.29±0.07
STR-H3K3V6	174	> 0.5	167	0.35±0.11	107	0.22±0.17	131	0.21±0.03
STR-H3K6V6	147	0.31±0.17	129	0.31±0.06	101	0.27±0.02	97	0.23±0.04
STR-H6K3V6	132	0.24±0.04	115	0.29±0.05	88	0.18±0.01	64	0.12±0.03
STR-H3K3V9	162	> 0.5	168	> 0.5	170	> 0.5	152	> 0.5
STR-H3K9V6	124	0.29±0.03	109	0.22±0.03	76	0.17±0.05	47	0.19±0.02

5.3.3 *In vitro* effects of peptide/siRNA complexes on different cell lines

To evaluate the siRNA delivery efficacy by STR-KV peptides, quantitative RT-PCR was utilized to measure the mRNA levels in various cell lines. Scrambled siRNA was adopted as a negative control and the most commonly used siRNA transfection reagent, lipofectamine 2000, was adopted as a positive control in the following experiments. To optimize the transfection conditions and determine the potency of the STR-KV family peptides, the siRNA targeting GAPDH gene was utilized in CHO-K1 cells (Figure 5.2A). A total of six peptides were complexed with siRNA at four molar ratios, i.e., the molar ratios of 20/1, 40/1, 60/1 and 80/1. The expression of GAPDH mRNA percentage mediated by lipo2000/siRNA was 19.2%±3.2%, and the STR-KV peptides with siRNA complexes showed different extents of silencing efficacy. When compared at the optimal molar ratios of STR-KV peptides, STR-H3K3V6/siRNA induced the highest silencing effect with mRNA expression percentages of

25.4%±8.1% at a molar ratio of 60/1, and STR-H3K9V6/siRNA reduced the mRNA expression level to a lesser extent, i.e., 42.7%±4.2% at a molar ratio of 40/1, whereas others showed mRNA levels higher than 65%.

To further confirm the gene silencing efficiency, STR-H3K3V6/siRNA complexes were transfected in A549 cells with Bcl-2 genes at various molar ratios. As shown in Figure 5.2B, the scrambled siRNA could not reduce the Bcl-2 mRNA levels in the cells, regardless of whether they were complexed with lipo2000 or peptides. In contrast, the mRNA reduction percentage of the STR-H3K3V6/siRNA complexes at a molar ratio of 60/1 was, at most, 19.7%±5.9%, which was comparable to the lipo2000/siRNA results, i.e., 14.9%±3.5%. Interestingly, the knockdown efficiency that was induced by STR-H3K3V6/siRNA decreased when increasing the number of complexes during transfection, i.e., the Bcl-2 mRNA level was 39.2%±4.3% at a molar ratio of 80/1. The transfection results for HeLa and Panc-1 cells demonstrated the same trend (Figure 5.2C and 2D respectively), which showed a similarly highest silencing efficiency at a molar ratio of 60/1, i.e., 18.6%±5.7% and 20.2%±6.8% respectively, and then decreased at MR80.

A

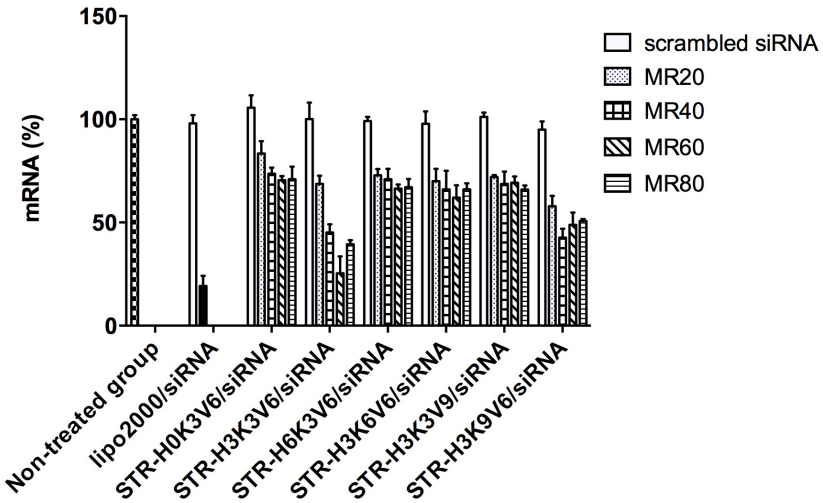
150
100
50
0
mRNA (%)
scrambled siRNA
MR20
MR40
MR60
MR80
Non-treated group
lipo2000/siRNA
STR-H0K3V6/siRNA
STR-H3K3V6/siRNA
STR-H6K3V6/siRNA
STR-H3K6V6/siRNA
STR-H3K3V9/siRNA
STR-H3K9V6/siRNA

B

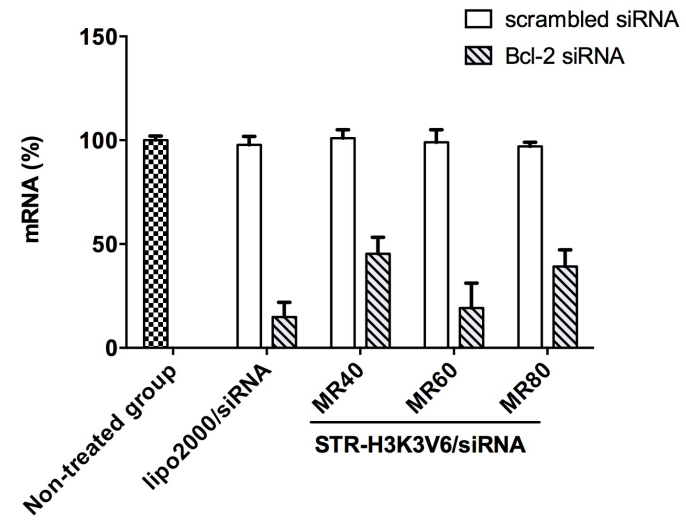
150
100
50
0
mRNA (%)
scrambled siRNA
Bcl-2 siRNA
Non-treated group
lipo2000/siRNA
MR40
MR60
MR80
STR-H3K3V6/siRNA

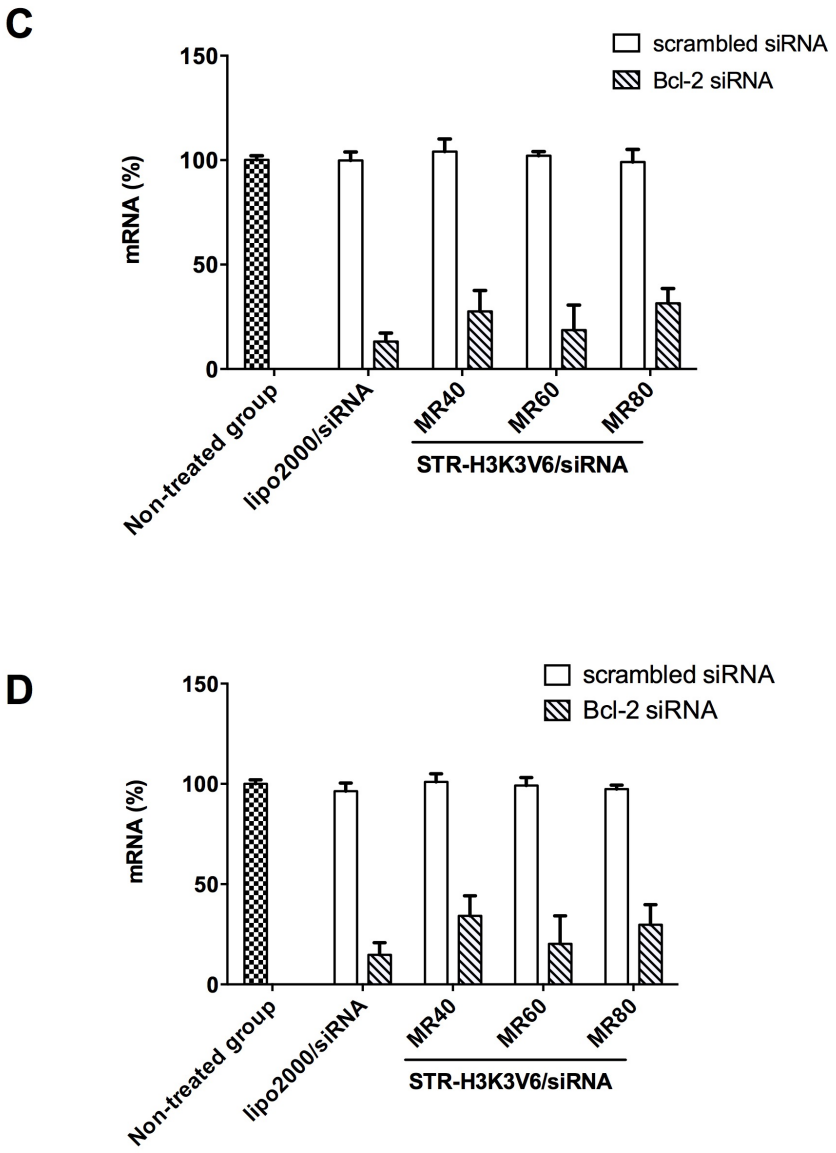

Figure 5.2 Inhibition of GAPDH or Bcl-2 activity on mRNA level through real time RT-PCR, with siRNA conc. = 50 nM/well. Peptide/scrambled siRNA complexes were used as negative control in each group. Lipofectamine 2000 was used as a positive control. Percentage of targeting gene knockdown efficiency calculated as: (1 – (peptide/siRNA targeting gene expression) / (peptide/scrambled siRNA expression)) x 100%. The experiments are carried on CHO-K1 cells with GAPDH siRNA (A), A549 cells with Bcl-2 siRNA (B), HeLa cells with Bcl-2 siRNA (C), and Panc-1 cells with Bcl-2 siRNA (D).

The results obtained with the STR-KV peptides demonstrated that the gene-silencing efficiency not only was linked to the amount of positively charged residues but was also affected by the number of histidine groups, e.g., STR-H3K3V6 and STR-H6K3V6 had the same number of lysine residues, but the efficiencies varied. There was the same number of histidine groups and positively charged lysines in STR-H3K3V6 and STR-H3K3V9, but STR-H3K3V6/siRNA complexes achieved much better knockdown efficiency than STR-H3K3V9/siRNA, which suggested that the combination of histidine, lysine and valine might also be essential to a high transfection efficiency. Based on DLS results in Table 5.3, the average size of STR-H3K3V9/siRNA complexes was larger than the one of STR-H3K3V6, which might suggest the increase of valine residues result in morphology changes of complexes. Visualized by atomic force microscopy (AFM), the results were consistent with DLS results. As shown in Figure 5.3A, the diameter of the main particles of STR-H3K3V6/siRNA in AFM imaging was approximately 100 nm, with a typical morphology of round shape. However, aggregation of complexes was observed in AFM images of STR-H3K3V9/siRNA (Figure 5.3B), which led to difficulty to observe the actual morphologies of STR-H3K3V9/siRNA complexes. These results suggested a possible explanation of low silencing efficiency of STR-H3K3V9/siRNA: the addition of valine resulted in aggregation of complexes that was not favor for cellular transfection. The increased size would affect the functionality of the nanoparticles in various aspects, e.g., the cellular internalization pathway might vary , the cellular uptake efficiency might decrease when the size increases [278, 279], and the siRNA encapsulation ability and release from nanoparticles might vary [280].

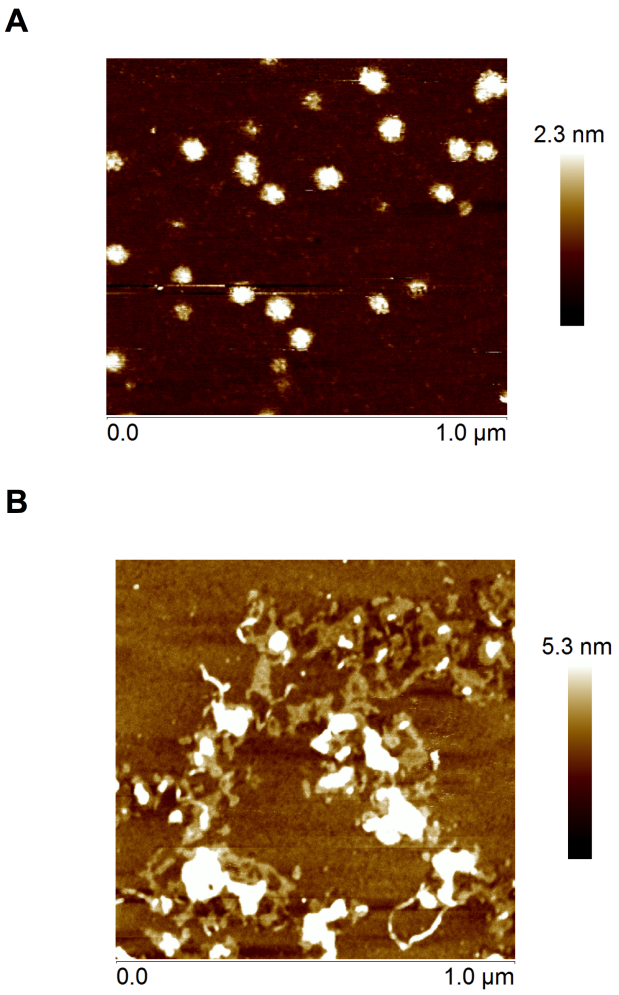

Figure 5.3 Morphology investigation of peptide/siRNA complexes. A: A typical AFM image of STR-H3K3V6/siRNA complexes at MR 60, with a 1 µm x 1 µm scan. B: A typical AFM image of STR-H3K3V9/siRNA complexes at MR 60, with a 1 µm x 1 µm scan

The siRNA delivery efficiency by STR-KV peptides was investigated at the protein level with KDalert™ GAPDH assay kit. As shown in Figure 5.4A, the GAPDH protein activity reduction profile was in accordance with the previous gene-silencing results observed at the

mRNA level. STR-H3K3V6/siRNA and STR-H3K9V6/siRNA showed GAPDH protein silencing efficiency as 63%±27% and 49%±12% respectively. The results were further confirmed with employing STR-H3K3V6 peptide with eGFP siRNA on C166-GFP cells (Figure 5.4B). Again, STR-H3K3V6/siRNA showed highest knockdown efficiency at a molar ratio of 60/1. No suppression of GAPDH protein was observed with peptide/scrambled siRNA treated cells, whereas STR-H3K3V6/siRNA (MR60) inhibited GFP protein to 41%±3.9%, a lesser extent than lipo2000/siRNA complexes, i.e., 49%±4.4%.

The protein reduction activity was further analyzed on A549 cells that were transfected with peptide/Bcl-2 siRNA complexes by the western blotting technique. β-actin was adopted as an internal control in this experiment. As shown in Figure 5.4C, the naked Bcl-2 siRNA without peptides and the scrambled siRNA with STR-H3K3V6 complexes did not change the Bcl-2 protein level. In contrast, STR-H3K3V6/siRNA at the molar ratio of 60/1 significantly reduced the level of Bcl-2 protein. These results suggest that the peptide STR-H3K3V6 is an effective siRNA delivery reagent at both the mRNA level and protein level on various cell lines.

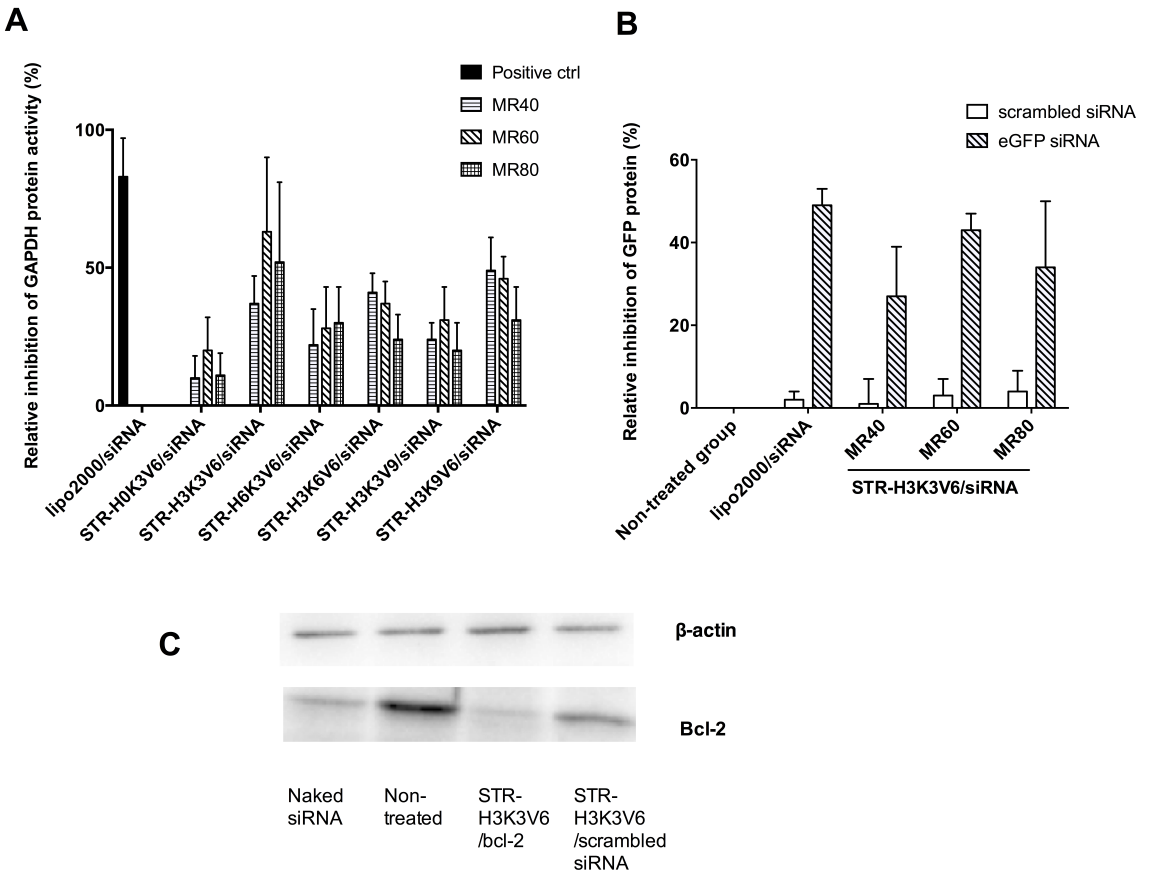

Figure 5.4 Inhibition of GAPDH, eGFP, or Bcl-2 activity on protein level, with siRNA conc. = 50 nM/well. The experiments were carried out on CHO-K1 cells evaluating GAPDH protein activity with GAPDH KDalert kit assay (A), C166-GFP cells evaluating GFP protein activity with flow cytometry (B), and A549 cells evaluating Bcl-2 protein activity with Western Blotting assay (C).

To determine the cellular uptake efficiency of the complexes, fluorescence-activated cell sorting (FACS) was adopted to measure the fluorescence intensity of the cells that were treated with carrier/Cy-3 labeled siRNA. Before analyzing the results by FACS, the cells were

washed with 15 U/ml heparin in Opti-MEM three times at 37°C [147] to eliminate the effect of the complexes that were attached to the surfaces of the cells [261]. As expected, the uncomplexed siRNA could not be delivered into the cells, whereas the uptake efficiency was significantly improved when the siRNA formed complexes with peptides (Figure 5.5). The FACS results were in accordance with the gene silencing results shown previously (Figure 5.2 and 5.4); the STR-H3K3V6/Cy-3 siRNA exhibited the highest uptake efficiency at the molar ratio of 60/1, while both STR-H3K3V9/Cy-3 siRNA and STR-H3K6V6/Cy-3 siRNA complexes showed large amounts of uptake at the molar ratio of 40/1. Although lipo2000/siRNA demonstrated an excellent gene-silencing ability, the cellular uptake efficiency of the complexes was relatively lower than STR-H3K3V6, or comparably with STR-H3K3V9 and STR-H3K6V6.

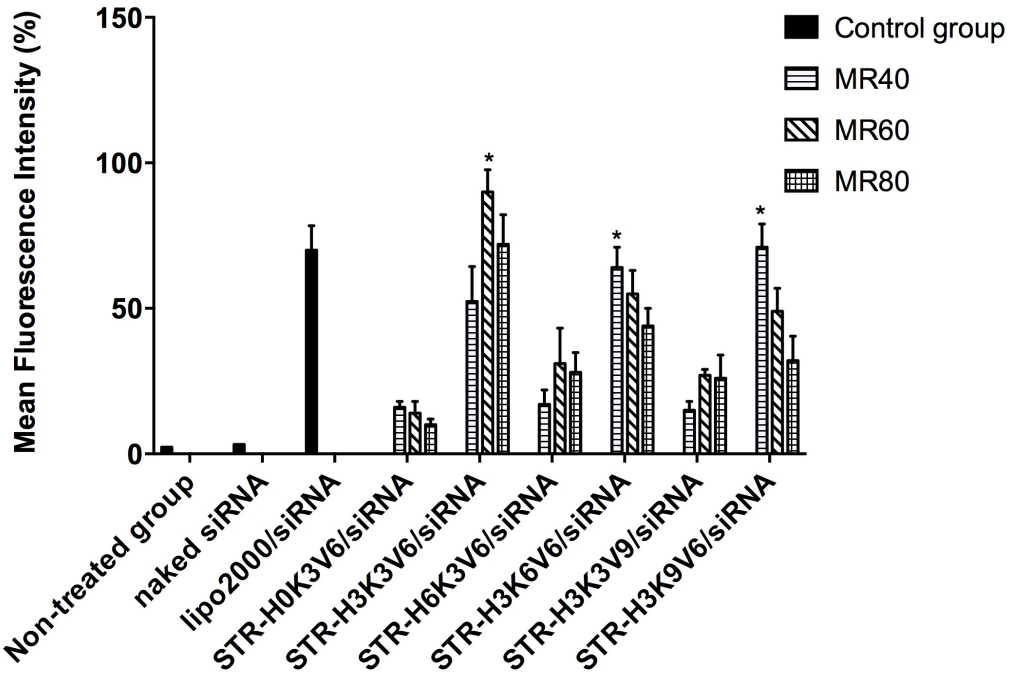

Figure 5.5 Uptake efficiency of peptide/siRNA complexes on CHO-K1 cells with siRNA conc. = 50 nM/well. The fluorescence intensity of internalized complexes measured by FACS, analyzed by flowjo in the Cy-3 channel.

5.3.4 *In vitro* cell viability and complement activation assay

A good gene delivery system should be safe, and should not induce cytotoxicity or stimulate the immune system. To investigate the cell viability of the peptide/siRNA complexes, an MTT assay was conducted on CHO-K1 cells. As shown in Figure 5.6A, a less than 10% cell death was detected for most peptide/siRNA complexes. Under transfection conditions, i.e., a molar ratio of 60/1, STR-H3K9V6/siRNA induced an approximately 20% cell death, which was higher than any other peptide/siRNA complexes but still lower than the lipo2000/siRNA complexes, which had with a 30% of cell death. A possible explanation was

the higher number of lysine groups that were present in STR-H3K9V6. It has been reported that highly positively charged nanoparticles might induce cytotoxicity because the positively charged residues would interact with the cell membranes and cause aggregation or rupture of the membrane surfaces [262].

To investigate the immune recognition of the peptide/siRNA complexes in involving the proinflammatory cytokines, the mRNA levels of various cytokines were evaluated by quantitative RT-PCR. Macrophages RAW 264.7 cells were adopted in this experiment because macrophages first interact with external particles in the bloodstream with respect to the immune system [281], and they are one of the most common cells that are involved in innate and adaptive immune systems. Bacterial endotoxin LPS at a concentration of 0.1 μg/mL were used as a positive control. As shown in Figure 5.6B, the expression of TNF-α induced by LPS was 6 times higher than in non-treated cells, whereas other cytokines induced by LPS were more than 50 times higher. In contrast, no significant cytokine expression was induced by the treatment of STR-H3K3V6/siRNA complexes.

The complement activation assay was then evaluated the safety of the system, and high levels of complement activation was demonstrated related to a variety of diseases. The complement system defends the human body for the foreign objects invasion, which can be activated through various pathways, i.e., classical, lectin, and alternative pathways. After activation, the complement system will generate terminal complement complexes, i.e., TCC and SC5b-9 by the assembly of C5 to C9. The ELISA assay was adopted to measure the concentration of Sprotein-bound C terminal complex (SC5b-9) in serum. As shown in Figure 5.6C, STR-H3K3V6 did not exhibit SC5b-9 activation, compared with positive control

Zymosan and negative control serum alone. Thus, the STR-H3K3V6 based siRNA delivery system was biocompatible without causing cytotoxicity, or showing any complement or cytokines stimulations.

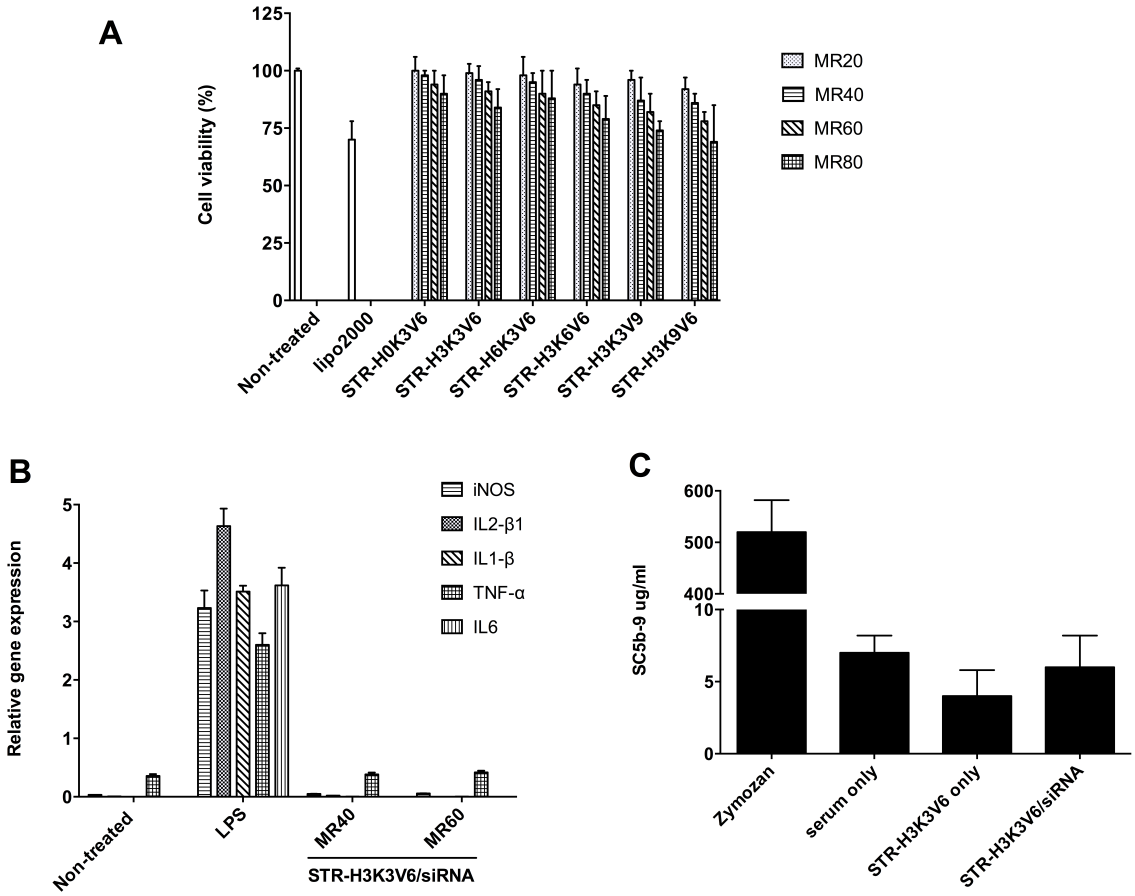

Figure 5.6 *In vitro* toxicity and biocompatibility of peptide/siRNA complexes, with siRNA conc. = 50 nM/well. A: Cell viability of peptide/siRNA complexes were performed on CHO-K1 cells with MTT assay. B: Cytokine mRNA expression of peptide/siRNA complexes were performed on RAW 264.7 cells, 0.1 μg/mL LPS was adopted as positive control. C: SC5b-9 formation in human serum was quantified by ELISA kit assay, 5 μg/mL Zymosan was adopted as positive control.

5.4 Conclusions

In this chapter, a series of peptides was designed and investigated for their use as potential siRNA delivery systems. Various numbers of lysine and valine residues were selected and combined with histidine residues and stearic acid in an effort to improve siRNA delivery and cell viability. The results revealed that the peptide STR-H3K3V6, a new cell-penetrating peptide that consists of a stearic acid moiety with a sequence of STR-HHHKKKVVVVVV, could efficiently facilitate siRNA delivery. The peptide STR-H3K3V6 efficiently encapsulated siRNAs from molar ratio 20/1, and the formed complexes were around 100 nm in diameter, which was suitable for nanoparticle devliery. The STR-H3K3V6/siRNA complexes induced 80%-90% gene-silencing efficiency at mRNA level on four cell lines. In addition, this peptide-based delivery system is safe and biocompatible, as no obvious cytotoxicity or immune responses observed *in vitro*, in terms of complement or cytokine activation assay. Our data suggested that peptide STR-H3K3V6 improved siRNA delivery on various cell lines with low cytotoxicity, and can be used as delivery carriers for siRNA therapeutics.

Chapter 6

Investigation of uptake mechanisms and direct translocation properties of a new CPP for siRNA delivery

6.1 Introduction

Since their discovery, the CPP uptake mechanism has been extensively studied, and several hypotheses have been proposed [137, 282-284]. No universal uptake pathway can be applied to all CPPs, and the internalization route can be affected by various factors, including the CPP concentration and structure, the physical properties of cell membranes, the interaction between CPPs and cell membranes, and the nanoparticles carried by CPPs.

Direct penetration and endocytosis have been suggested as the two main uptake mechanisms. CPPs that can enter cells at a low temperature are considered internalized via a direct translocation pathway [285]. However, several studies report that increasing the concentration of CPPs might trigger direct penetration [139, 286, 287]. Tat and penetratin have both been internalized through endocytosis under most conditions, but they were also taken up via direct translocation at high concentrations [137, 139, 146]. However, several studies show that triggering direct penetrating by increasing the CPP concentration might lead to high cytotoxicity of nanoparticles due to biological membrane damage [146, 288].

Endocytosis is the other common mechanism for nanoparticle internalization, including clathrin-dependent endocytosis, macropinocytosis and caveolae-dependent endocytosis. In uptake through an endocytic pathway, CPPs first interact with extracellular components via electrostatic interactions, such as heparin sulfate proteoglycans and chondroitin sulfate proteoglycans [289, 290]. These anionic proteoglycans are abundant on the cellular membrane surface and are receptors for nanoparticle internalization [289, 290]. However, the nanoparticles internalized through endocytosis pathways may be trapped in endosomes and then degraded in late lysosomes, which reduces the biological potency of these nanoparticles. Moreover, evidence shows that direct translocation and endocytosis can coexist for the same CPP [291, 292]. Despite differences in their mechanisms, direct translocation and endocytosis might initiate the internalization process through interactions with the same components at cellular membranes [293]. For instance, heparan sulfate proteoglycans on the cell membrane surface are involved in both endocytosis and direct penetration of CPPs [294].

To facilitate siRNA cellular uptake and gene silencing efficiency, we previously developed a cell-penetrating peptide for siRNA delivery in the form of STR-H3K3V6/siRNA complexes (abbreviated to STR-KV/siRNA in this chapter). With the sequence STR-HHHKKKVVVVVV, the peptide STR-KV has shown 90% gene knockdown efficiency in various cell lines with limited cytotoxicity, discussed in Chapter 5. To further improve our delivery system for *in vivo* applications, a comprehensive study on the cellular uptake mechanism and intracellular trafficking of STR-KV/siRNA complexes is necessary.

Herein, we investigated the cellular internalization mechanism for STR-KV/siRNA complexes using different biochemical probes/methods. Several endocytosis inhibitors were

used to block certain pathways, and the impact of temperature and the mitochondrial process inhibitor were also evaluated in detail. Moreover, the interaction between the complexes and cell membrane components was investigated. Confocal microscopy was also used to study co-localization of the delivery system with endosome/lysosome compartments and intracellular trafficking of the STR-KV/siRNA complexes.

This Chapter is based on the work submitted to Molecular Pharmaceutics, with authorship as: Ran Pan, Wen Xu, Yong Ding, Sheng Lu, Lei Zhang, Pu Chen.

6.2 Materials and methods

6.2.1 Formulation of peptide/siRNA complexes

Synthesized by CanPeptide Inc (Quebec, Canada), peptides were dissolved in RNase free water (Thermo scientific, Ottawa, Canada) at a concentration of 1 mM, followed by probe sonication for 10 min, and were stored at -20°C. Synthesized by Sigma-Aldrich (Oakville, Ontario, Canada) or Life Technologies (Burlington, Ontario, Canada), siRNAs were dissolved in RNase free water at a concentration of 50 μM, and were store at -80°C.

The peptide/siRNA complexes were prepared in RNase free water for characterization experiments, and were prepared in Opti-MEM (Invitrogen, Carlsbad, CA, USA) for transfection experiments. The peptide/siRNA complexes were prepared at different molar ratios depending on the designed experiment, by slowly manually mixing the peptide solution into siRNA solution with pipette. The complexes were incubated at room temperature for 30 min before conducting experiments.

6.2.2 Sequence of siRNAs

The Silencer^{TM} Cy3-labeled GAPDH siRNA with excitation/emission as 547/563 nm was purchased from Life Technologies, used in Confocal Laser Scanning Microscopy (CLSM) and Fluorescence Activated Cell Sorting (FACS). The MISSION^{TM} Cy-5 labeled Negative Control #1 siRNA with excitation/emission as 650/670 nm was purchased from Sigma-Aldrich, used in Confocal Laser Scanning Microscopy. Silencer GAPDH siRNA, targeting glyceraldehyde 3-phosphate dehydrogenase (GAPDH) gene, was purchased from Life Technologies and the

sequence was not revealed by the manufacturer. The negative control siRNA with scrambled sequence used in the experiment was also purchased from Life Technologies.

6.3 RiboGreen assay

The amounts of free siRNA were quantified by RiboGreen assay (Quanti-IT^{TM} RiboGreen, Invitrogen, USA). Peptides were mixed with siRNA to form peptides/siRNA complexes as described above. Different concentrations of heparin were added to the complexes and incubated for 1 hour before conducting RiboGreen assay. According to manufacturer's instruction, the complexes solution and ribogreen solution was prepared separately, and the aqueous working solution of ribogreen assay was slowly added into each sample manually. Each sample was incubated at room temperature for 3 min before measured on UV-Vis spectrometer (Ultrospec 4300 Pro, GE, Canada) with excitation at 480 nm and the emission at 520 nm.

6.3.1 Cell culture and peptide mediated siRNA transfection

Transfection experiments were conducted on various cell lines. Human lung cancer cell line (A549, ATCC CCL-185) and Chinese hamster ovary cell line (CHO-K1, ATCC CCL-61) were maintained in F-12K medium (Thermo scientific, Ottawa, Canada) supplemented with 10% fetal bovine serum (FBS, Sigma-Aldrich, Oakville, Ontario, Canada) at 37°C in 5% CO_2. HeLa cells (ATCC CCL-2) were maintained in Minimum Essential Medium (Thermo scientific, Ottawa, Canada) supplemented with 10% FBS at 37°C in 5% CO_2. Before transfection, A549 cells were seeded in 24-well plates with a confluence of 60,000 cells/well for uptake experiments, and 40,000 cells/well for knockdown experiments. CHO-K1 cells

were seeded in 24-well plates with a confluence of 60,000 cells/well for uptake experiments and 35,000 cells/well for knockdown experiments. HeLa cells were seeded in 24-well plates with a confluence of 50,000 cells/well for uptake experiments and 30,000 cells/well for knockdown experiments.

After incubation at 37°C for 24 hours, cells were rinsed with phosphate buffered saline (PBS), and then replaced with Opti-MEM. The peptide/siRNA complexes were prepared as described above, diluted in Opti-MEM and added to each well with a final concentration of 50 nM siRNA and 3 μM peptide. After incubated at 37°C for 4 hours, the cells were proceeded to collection for flow cytometry, or supplemented with medium containing FBS to obtain a final concentration of 10% FBS and incubated for a total of 48 hours before analyzing with RT-PCR.

6.3.2 Heparin competition assay

Cells were seeded and transfected with peptide/siRNA complexes in 24 hours, as described above. 30 min prior to and 4 hours after transfection, 3 μg/ml of heparin containing medium was added to each well. The cells were incubated at 37°C for 4 hours and then collected for flow cytometry.

6.3.3 GAG lyases assay

The cells were seeded and incubated as described above. Washed with PBS, cells wer pre-treated with 5 mIU/ml of heparinase III from *Flavobacterium heparinum* reconstituted in 20 mM Tris-HCl buffer (pH 7.5 with 0.1 mg/ml BSA and 4 mM $CaCl_2$), or with 20 mIU/ml of chondroitinase ABC from *Proteus vulgaris* in 50 mM Tris buffer (pH 8.0 with 60 mM sodium

acetate and 0.02% BSA) [295]. After 2 hours incubation with heparinase III or chondroitinase ABC, the cells were rinsed gently 6 times with PBS and then transfected with peptide/Cy-3-labeled siRNA complexes as described above. 4 hours later, the cells were washed and collected to analyze with flow cytometry.

6.3.4 Treatments of the cells with endocytic inhibitors

The cells were seeded and incubated as described above. 1 hour before transfection, the medium was discarded and cells were rinsed with PBS, which was then replaced with Opti-MEM. The freshly prepared chemical inhibitors were then added to each well and incubated for 1 hour. The cells were then transfected with peptide/siRNA as described above. After 4 hours incubation at 37°C, the medium was discarded, then the cells were washed with 0.5 mg/ml trypsin in PBS for 5 min, and 0.5 mg/ml heparin in Opti-MEM for 20 min to remove the complexes attached on cell membranes. This step was repeated for 3 times before collection for flow cytometry.

For positive control, the cells were treated with 18 μg/ml of Transferrin for 15 min, or with 0.75 μM of LacCer for 15 min. After 3 hours incubation, the cells were washed 3 times with ice-cold Opti-MEM, then incubated in ice-cold washing buffer for 2 min (0.2 M acetic acid with 0.2 M NaCl in PBS) to remove Transferrin, or incubated in ice-cold 5% BSA for 10 min for 4 times to remove LacCer. The cells were then washed with ice-cold PBS and Opti-MEM before collection for flow cytometry.

6.3.5 Effects of cellular energy state on internalization

The temperature dependent uptake experiments were conducted both at 37°C and 4°C. The cells were seeded in 24-well plates as described above 24 hours before transfection. For low temperature experiments, cells were incubated at 4°C 1 hour prior to, and 4 hours after treated with peptide/Cy-3 labeled siRNA complexes. 4 hours after transfection, the cells were washed and collected to analyze with flow cytometry.

Alternatively, cells were pre-treated with sodium azide (200 μM) for 30 min prior to and 4 hours after transfected with peptide/Cy-3 labeled siRNA. 4 hours after transfection, the cells were washed and collected to analyze with flow cytometry.

6.3.6 Flow cytometry

The cellular uptake efficiency of complexes was quantified by flow cytometry (type BD Biosciences, BD FACS Vantage SE Cell Sorter, USA). 4 hours after transfection, cells were rinsed with PBS and incubated in 15 U/ml heparin containing medium for 20 min. This step was repeated for 3 times. Cells were then washed twice with PBS, detached from the plate with 0.25% trypsin/EDTA, and then collected in the suspension of 4% PFA in PBS. The collected samples were analyzed by fluorescence acquired cell sorting (FACS), and the data were analyzed by Flowjo software. All measurements were performed in triplicate.

6.3.7 GAPDH silencing assay at mRNA level

The efficiency of GAPDH siRNA interference was evaluated using real time RT-PCR that shows the gene knockdown on mRNA level. Cells were seeded in 24-well plates and transfected with peptide/siRNA complexes 24 hours later, as described above.

After 48 hours, total RNA was isolated using the RNeasy Mini Kit (Qiagen, Valencia, CA, USA), and the RNA concentration was measured using Nanodrop (Nanodrop spectrophotometer ND-1000, Thermo scientific, Ottawa, Canada). RNA was then reverse transcribed into cDNA using Bio-Rad iScript cDNA synthesis kit (Bio-Rad Laboratories, Ontario, Canada). RT-PCR was performed using the Mx3005P™ Real Time PCR System (Agilent Technologies, Wilmington, DE, USA) with Brilliant II Fast SYBR Green QPCR Master Mix (Agilent Technologies), according to the manufacturer's instructions. All measurements were performed in triplicate.

6.3.8 Confocal laser scanning microscopy (CLSM)

A549 cells were seeded in a Nunc Lab-Tek II 4-well glass chamber slides (Thermo scientific, Ottawa, Canada) at 60,000 cells/well, and transfected with peptide/Cy-3-labeled GAPDH siRNA, or peptide/Cy-5-labeled Negative Control siRNA complexes 24 hours later, as described above.

For endosome/lysosome co-localization experiments, 75 nM/well of Lysotracker Green (Life Technology, Carlsbad, USA) were added into the medium 3 hours after transfection and incubated at 37 °C for 1 hour. 3 hours after transfection, cells were then incubated in 15 U/ml heparin containing medium for a total one hour at 37 °C, and rinsed twice with PBS. 500 μL of medium were added into each well, with 1 drop of NucBlue Live ReadyProbes Reagent (Life Technology, Carlsbad, USA). Carl Zeiss LSM 700 confocal microscope (Zeiss, Jena, Germany) was used to visualize the cells. The microscope was equipped with Plan-

Apochromat 20x/0.8 NA objective lens. The images were analyzed with Olympus FluoView FV1000 software.

For multi-positioned time-lapse imaging, cells were treated with peptide/Cy-5 labeled siRNA complexes for 10 min, and then rinsed with PBS. Fresh 500 μL of Opti-MEM were added into each well, and 10 μL of 1X CellMask™ Green Plasma Membrane Stain (with excitation/emission as 522/535 nm, purchased from Life Technologies) were added to each well. Before visualize the samples with Nikon A1R confocal microscope system, equipped with Nikon Eclipse Ti Advanced PFS for time-lapse imaging station, 1 drop of NucBlue Live ReadyProbes Reagent (purchased from Life Technologies) was added to each well. The microscope was equipped with Nikon T-P2 objective lens. The images were analyzed and complied into movie clips with Nikon NIS Elements Viewer software.

6.4 Results and Discussion

6.4.1 Study the interactions between complexes and cell surface proteoglycans

Whether though endocytosis or direct translocation, universally, interactions with the cellular membrane are first involved in the CPP internalization process [296, 297]. Most CPPs initiate the internalization processes through electrostatic interactions with the anionic heparan sulphate proteoglycans (HSPGs) located on the cell membrane [298, 299]. Studies show that HSPGs are essential for defining cationic nanoparticle uptake by the cells. For example, the level of uptake for certain peptides was reduced or inhibited in glycosaminoclycans-deficient cell lines [300-302], which demonstrates that the CPP uptake process depends on interaction between CPPs and certain HSPGs. In addition, the HSPG expression levels differ based on cell type, e.g., the glycosaminoclycan (GAG) HSPGs are overexpressed on most cancer cell membranes [303-305] and might regulate or favor uptake of certain CPPs in specific cell lines [304, 306, 307]. Thus, to investigate interactions with HSPGs and the role of HSPGs in STR-KV/siRNA complex internalization, heparin interaction assays and GAG lyases assays were performed using CHO-K1, A549 and HeLa cells.

As shown in Figure 6.1A, co-incubating various cells with the HSPG analogue heparin decreased uptake of STR-KV/siRNA complexes, which implies that the presence of heparin hinders transfection of STR-KV/siRNA complexes. This result also suggests that the STR-KV/siRNA complexes interact with and bind to HSPGs. The uptake efficiency might be reduced for 2 reasons: 1) a heparin analogue competing with the HSPGs at the cell surface for binding to the STR-KV/siRNA complexes, or 2) the heparin analogue caused dissociation of

our complexes. To better understand the role of heparin in uptake of the STR-KV/siRNA complexes, a RiboGreen assay was used to quantify the complex dissociation percentage due to heparin, and a GAG lyases assay was used to investigate the influence of HSPGs on STR-KV/siRNA complex internalization.

The RiboGreen reagent is designed to intercalate with free siRNA and emit a strong fluorescence signal at 525 nm; thus, the percentage of dissociated siRNA can be detected and calculated based on fluorescence intensity [308]. The siRNA-Ribogreen fluorescence intensity is shown in Figure 6.1B. The complexes began to dissociate with 1 μg/ml of heparin and reached a plateau at 7.5 μg/ml of heparin, which implies complete dissociation of the complexes. Calculated from Figure 6.1B, ~ 15% of the complexes dissociated at the concentration of heparin from the previous experiment, assuming a linear relationship between the dissociation percentage and increased level of heparin. Thus, the presence of a heparin analogue caused partial dissociation of the complexes, and more than 80% of complexes remained intact in the previous experiment. This result implies that the decrease in complex uptake shown in Figure 6.1A might be mainly due to the complexes binding with exogenous negatively charged components.

The negatively charged glycosaminoglycans are a group of cell surface receptors covalently linked to cell surface proteins, e.g., HSPGs [309] and chondroitin sulfate proteoglycans (CSPGs) [310]. In the following experiments, two types of GAG lyases were used to remove the GAGs at the cell membrane surface. Heparinase III from *Flavobacterium heparinum* was used to remove the HS glycosaminoglycans, and chondroitinase ABC from *Proteus vulgaris* was used to remove the CS glycosaminoglycans (CS-A, -B, -C) [311]. As

shown in Figure 6.1C, internalization of STR-KV/siRNA complexes was not affected by the heparinase III pretreatment, and a slight decrease was observed with the chondroitinase ABC-treated cells. This result suggests that enzymatic removal of cell surface HSPGs and CSPGs does not affect the quantity of complexes taken up by the cells. In other words, the HSPG interactions are not essential for cellular uptake of our complexes.

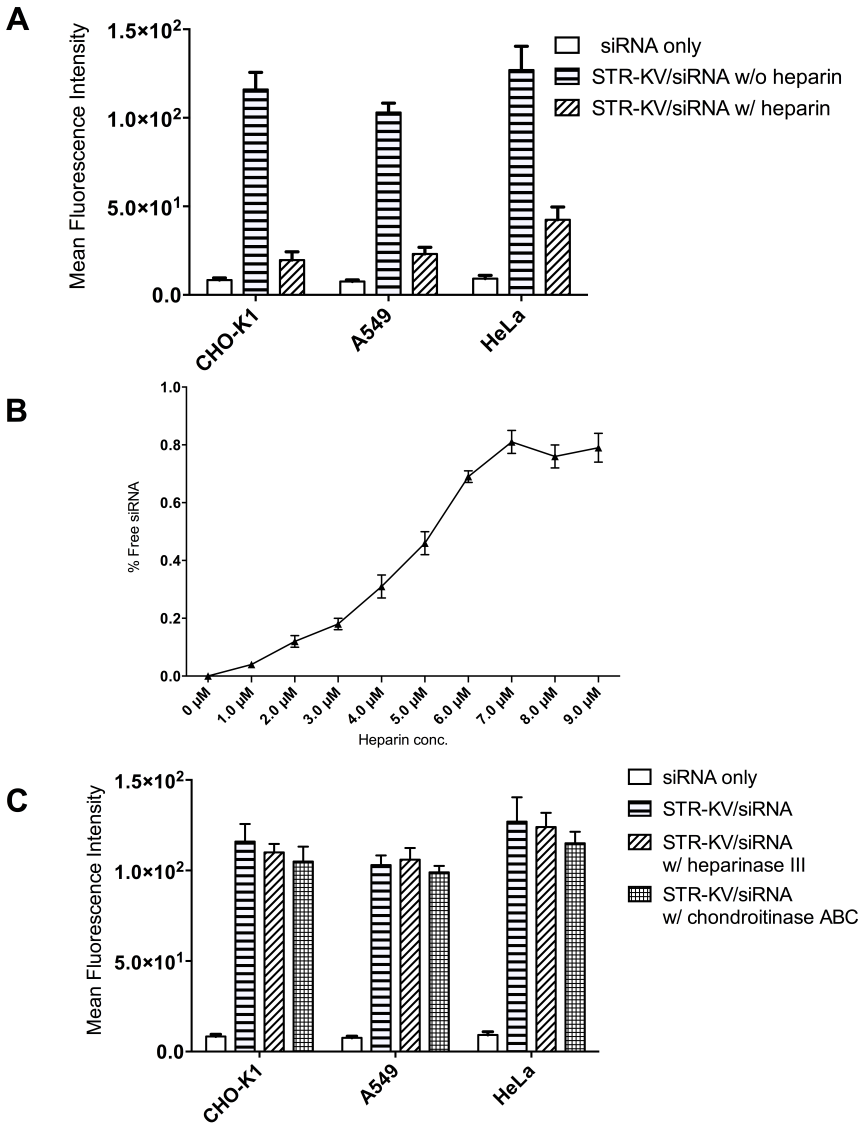

Figure 6.1 Interactions between complexes and cell surface proteoglycans, with siRNA conc. = 50 nM/well. (A), Interactions between complexes and HSPGs analogue heparin on CHO-K1 cells, A549 cells and HeLa cells. (B), Addition of heparin on peptide/siRNA binding affinity; (C), Effects of removal cell surface proteoglycans on complexes uptake efficiency on CHO-K1 cells, A549 cells, and HeLa cells.

6.4.2 Explore the involvement of different endocytic pathways in the complex uptake

To better understand the uptake mechanisms, various chemical endocytosis inhibitors were used to study the STR-KV/siRNA complex internalization route. Chlorpromazine was used to block the clathrin-mediated pathway, which inhibits formation of the endocytosis sag coated with clathrin [312]. EIPA (5-(N-ethyl-N-isopropyl) amiloride) was used to block macropinocytosis and phagocytosis by inhibiting the Na+/H+ exchanger [313]. The multiple inhibitor methyl-β-cyclo-dextrin (MBCD) depletes the cholesterol required for both macropinocytosis and caveolae-mediated endocytosis [314]. Filipin and nystatin were employed to inhibit caveolae-mediated pathways; the former impaired caveolae invagination by distorting the structure and function of cholesterol-rich caveolae membrane domains [315]. The latter interacts with lipid cholesterol and inhibits sag formation [316]. In addition, two fluorescently labeled endocytic markers were used as positive controls in experiments to ensure the effectiveness of inhibitors. Transferrin, which is taken up by cells exclusively through the clathrin-mediated pathway, was used as a marker for clathrin-mediated endocytosis [317], and lactosylceramide (LacCer) was used for the caveolae-mediated pathway [318].

As shown in Figure 6.2, a minor decrease in transferrin and LacCer fluorescence intensity was observed in the presence of EIPA, while STR-KV/siRNA complex internalization remained unchanged, which indicates that the complexes were not internalized through macropinocytosis. Similar results were obtained using MBCD-treated cells with no significant reduction in transferrin and STR-KV/siRNA complex uptake, while the LacCer uptake efficiency decreased to less than 50%.

Inhibition of the clathrin-mediated pathway by chlorpromazine (Cpz) dramatically decreased transferrin internalization. However, only a slight reduction was observed for LacCer uptake, which suggests that Cpz successfully inhibited clathrin-mediated endocytosis but did not affect the caveolae-mediated pathway. With a Cpz pre-treatment, a minor reduction (7%-18%) in Cy-3 fluorescence intensity was observed, which indicates that a small fraction of the complexes were internalized through the clathrin-mediated endocytic pathway.

Filipin and nystatin are widely used to inhibit caveolae-mediated endocytosis. As expected, LacCer uptake decreased to less than 30% in the filipin- or nystatin-treated cells, while no significant effects were observed for transferrin internalization. However, a weak increase (5%-12%) in siRNA uptake is shown in Figure 6.3A with nystatin pre-treatment, perhaps because other uptake pathways can be activated as compensation when one is inhibited [319]. The other possible reason for the Cy-3 fluorescence intensity increase might be that the presence of Nystatin enhances cell membrane permeability, which sequesters the cholesterol at the cell membrane surface [320]. Overall, no significant differences were observed for the STR-KV/siRNA complex uptake intensities in the presence of any inhibitors. These observations suggest that the complex internalization process does not depend on macropinocytosis, phagopinocytosis, clathrin-mediated or caveolae-mediated endocytosis, which implies uptake through direct translocation.

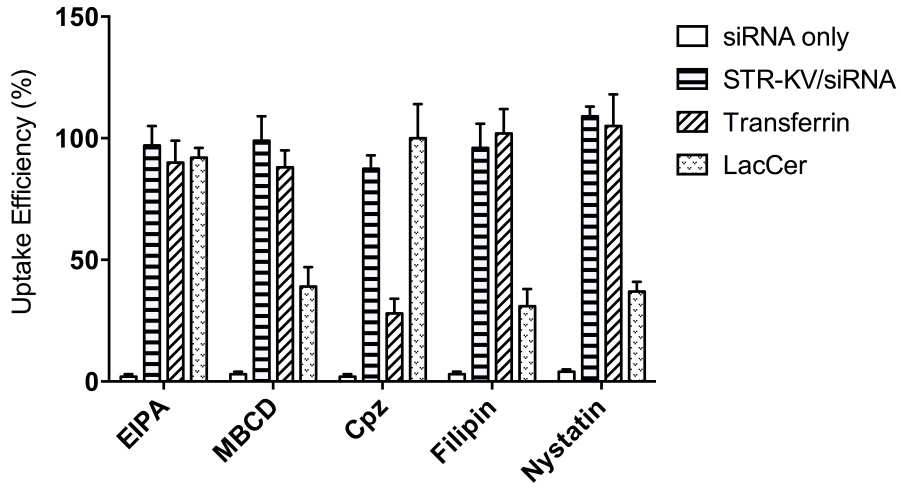

Figure 6.2 Effects of different inhibitors on complexes uptake efficiency on A549 cells. Transferrin, marker of clathrin-mediated endocytosis, and LacCer, marker of caveolae-mediated endocytosis, were used as positive controls. Final Concentrations used here is EIPA = 20 μg/ml, MBCD = 5 mg/ml, Cpz = 5 μg/ml, Fillipin = 4 μg/ml, and Nystatin = 40 μg/ml.

6.4.3 Investigate the influence of cellular energy state on complexes transfection efficiency

To study the impact of the cellular energy state on uptake efficiency of STR-KV/siRNA complexes, low temperature (4 °C) experiments were performed, and the results were compared with experiments at 37 °C. As shown in Figure 6.3A, a minor decrease in fluorescence intensity was observed for HeLa cells at 4 °C, and Cy-3-labeled siRNA uptake with other cell lines was not significantly affected by lowering the cell temperature. Because endocytosis is commonly inhibited at 4 °C, this result suggests that our complexes are internalized via a non-endocytic pathway. Moreover, studies also show that direct translocation might also be affected when the cell energy state is lowered due to the decrease

in cellular membrane fluidity at low temperatures , which explains the slight reduction in siRNA uptake at 4 °C shown in Figure 6.3A. Thus, an alternative means to assess direct CPP translocation through the membranes is necessary.

Sodium azide is a potent mitochondrial oxidative phosphorylation inhibitor that abolishes the ATP-dependent processes and, consequently, active uptake of nanoparticles [322]; it has been commonly used as an endocytosis inhibitor to investigate nanoparticle cellular uptake pathways [323]. The cells were treated with different concentrations of sodium azide prior to and after transfection with STR-KV/siRNA complexes as described in **6.3.5**; the mRNA levels were evaluated using RT-PCR. As shown in Figure 6.3B, the GAPDH levels were equally reduced in the presence and absence of sodium azide for various cell lines. These data are consistent with previous uptake results at low temperatures; both demonstrate that transfection efficacy is independent of the energy state of the cells.

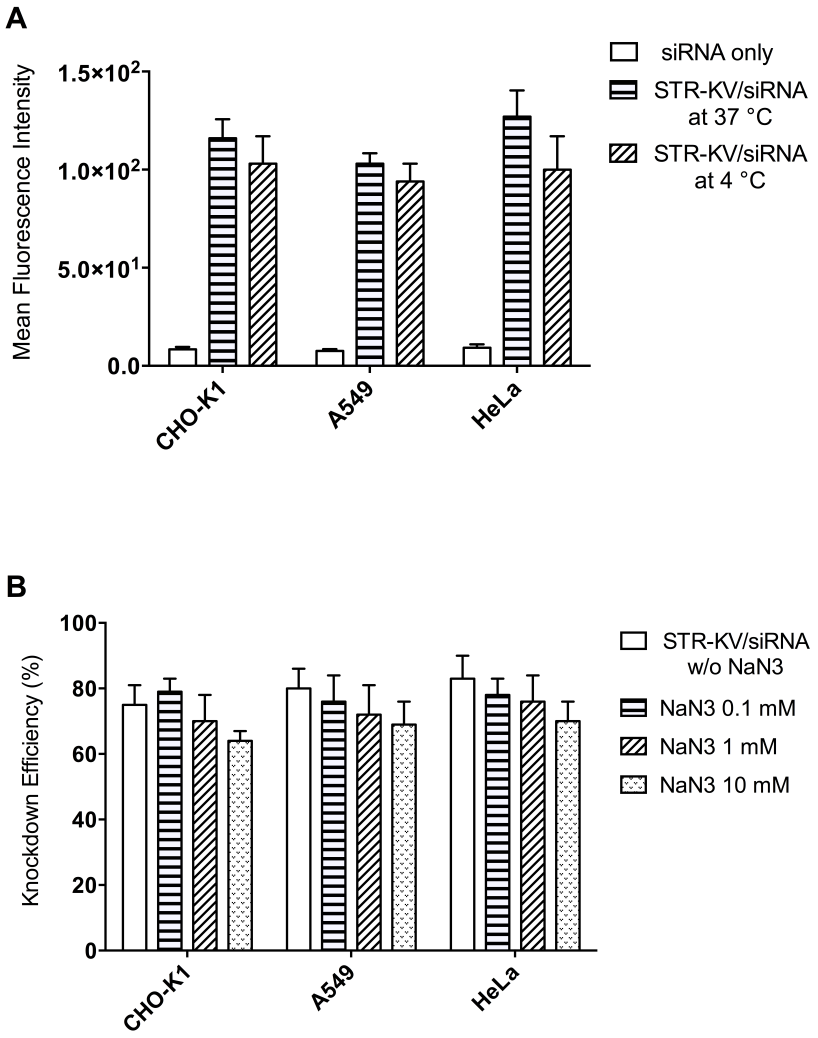

Figure 6.3 Effects of cellular energy state on complexes transfection efficiency on CHO-K1 cells, A549 cells, and HeLa cells. (A), Cells were incubated at both 37°C and 4°C during transfection experiments. (B), Variable concentrations of sodium azide were added to cells before and after transfection experiments.

6.4.4 Examine the internalization process of STR-KV/siRNA complexes

Based on the above results, STR-KV/siRNA complex internalization was not affected by inhibitors and independent of the cellular energy levels. Before drawing the conclusion that the complexes were internalized through direct translocation, live cell confocal microscopy was used to investigate co-localization of the complexes with endosome/lysosome vesicles.

As shown in Figure 6.4A, the endosomes/lysosomes were labeled with Lysotracker, which was visualized as green signals, and the Cy-3-labeled siRNAs are shown as red signals and are localized close to the nucleus. The merged image, as shown in the right panel of Figure 6.4A, yielded a yellow fluorescent signal when siRNAs co-localized with endosomes/lysosomes. Most Cy-3 siRNAs did not co-localize with endosomal/lysosomal vesicles; the software calculated less than 20% co-localization. This result is consistent with the previous results, which indicate that a small quantity of STR-KV/siRNA complexes use endocytosis, while most do not (Figure 6.2).

Multiple points scanning confocal microscopy was used to investigate the dynamic internalization process of the complexes. Image collection began 10 min after transfection and stopped 2 h later with an interval of 2 min. This time series captured 0.16 frames per second, composed from 59 images. As shown in Movie 6.4B, an in situ accumulation of Cy-5 siRNAs was observed around nucleus in different cells, which is evidence that the STR-KV/siRNA complexes entered the cells.

Time-lapse imaging can also be used for visualization with Nikon Eclipse Ti confocal microscope with a Z-stack viewing options, which shows a continuous process, wherein the

complexes internalize into cells. As shown in Movie 6.4C, the complexes in upper right (Cy-5 was visualized as magenta) first accumulated on the cell membranes (green), yielded a white fluorescence signal when complexes co-localized with cell membrane. The complexes then entered the cells as clustered particles, and the particles accumulated around nucleus (blue), where the RNAi process takes place. The same internalization process can be visualized more clearly in Movie 6.4E with a larger area of view, the complexes were entered the cells as clustered particles accumulated around nucleus with diameters at approximately 300 nm 1.5 hours after transfection. The aggregation of complexes on cell membranes was visualized in Movie 6.4C, as well as in Figure 6.4A and 4D; this might explain why the STR-KV/siRNA complexes use a direct translocation pathway but do not cause cytotoxicity. Studies show that increasing the CPP concentration induces direct translocation or physical endocytosis [139, 283, 331], such as MPG [146], PEP [332], CADY [183], and others. STR-KV/siRNA complex aggregation increased the local complex concentration at cell membrane; thus, direct penetration was favored with an overall low concentration.

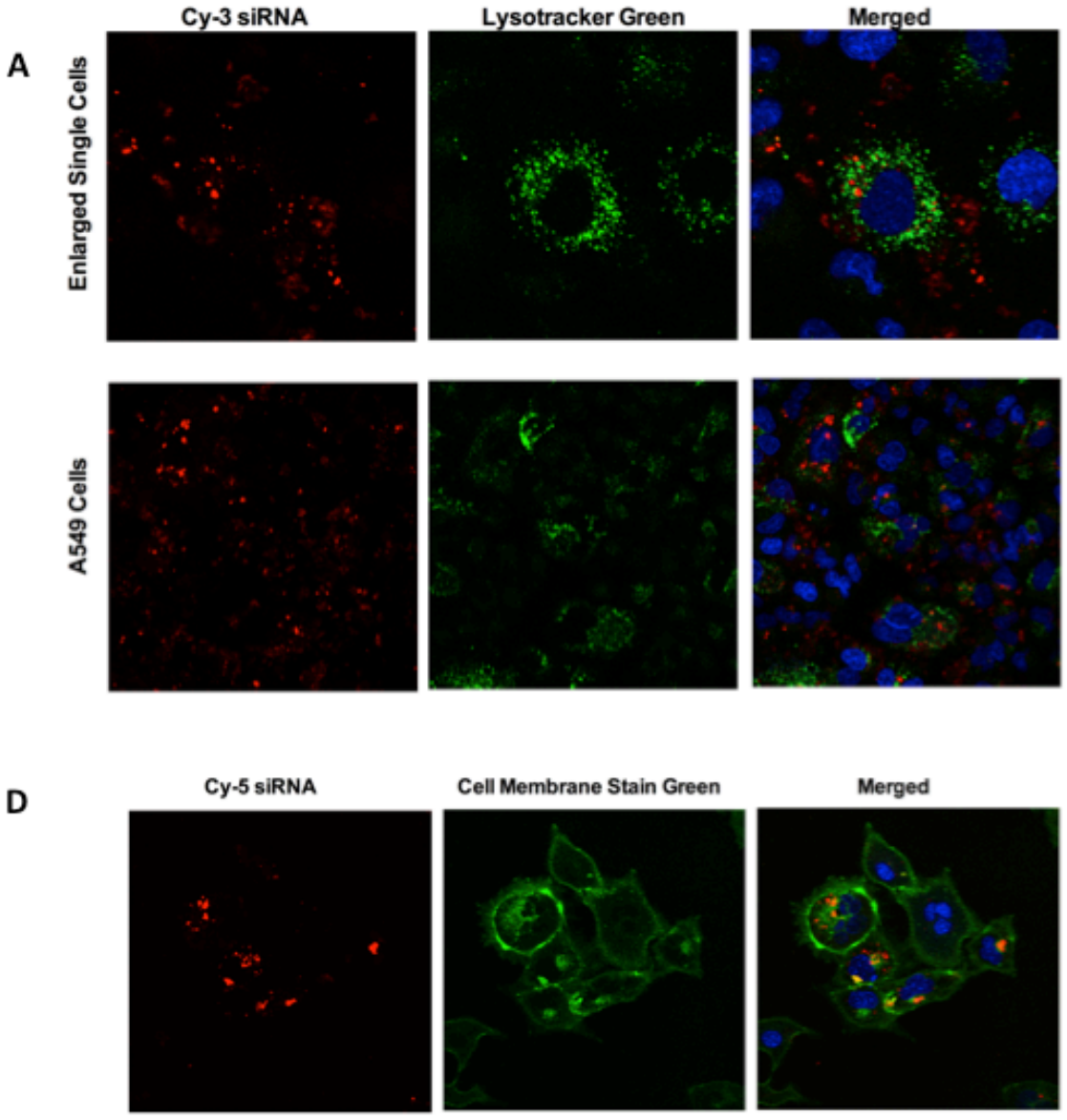

Figure 6.4 Intracellular localization of STR-KV/siRNA complexes on A549 cells, with siRNA conc. = 50 nM/well. Images were visualized by confocal microscopy, and pseudocolored for visualization. (A), Co-localization of STR-KV/ Cy-3 siRNA complexes with endosome/lysosome vesicles: blue = nucleus; red = Cy-3 siRNA; green = LysoTracker Green. Co-localization of siRNA with the endosomal/lysosomal marker is in yellow. (D), Co-localization of STR-KV/Cy-5 siRNA complexes with cell membranes: blue = nucleus; red = Cy-5 siRNA; green = cell membrane.

Movie 6.4 Dynamic internalization process of STR-KV/siRNA on A549 cells. (B), Image collection began 10 min after transfection with 0.16 frames per second, composing from 59 images with 120s interval of each. Images were pseudocolored for visualization: blue = nucleus; red = Cy-5 siRNA; green = cell membrane. (C) and (E), Image collection began 10 min after transfection with a Z-stack viewing options. Z range is 11.40 μm with Z step as 0.5 μm each. Images were pseudocolored for visualization: blue = nucleus; magenta = Cy-5 siRNA; green = cell membrane. Co-localization of siRNA with the cell membrane is in white.

6.5 Conclusion

In this chapter, the STR-KV/siRNA uptake pathway was examined using four different cell lines. The results show a small fraction of complex dissociation, co-incubation of the complexes with the HSPG analogue heparin indicates that our complexes interact with cell surface HSPGs, while a GAG lyase assay suggests this interaction is not essential for complex internalization. Applying different endocytic inhibitors to the cells showed that endocytosis was not the major uptake pathway for our complexes, i.e., less than 20% of the complexes used the clathrin-mediated pathway. Changing the cell energy state by lowering the temperature or adding sodium azide exhibited no minor effects on complex uptake, which indicates that a direct translocation route is most likely. Furthermore, confocal microscopy revealed that the high local complex concentration might be the trigger for complex internalization through an endocytosis-independent pathway.

Chapter 7

Original Contributions and Recommendations

7.1 Contributions

This dissertation presents a thorough of study of peptides as potential siRNA carriers in various aspects. Several cell-penetrating, co-assembling peptides were designed or modified, and the possibility of using these peptides for safe and efficient delivery of siRNAs was evaluated both *in vitro* and *in vivo*. The following aspects are included in this thesis: (1) the modification of the original co-assembling, cell-penetrating peptide C6M1 by conjugating with diethylene glycol into peptide DM1, which improved serum stability without decreasing the gene-silencing efficiency (Chapter 3); (2) the design of a series of stearylated peptides with modified nuclear localization sequences, in which, the most promising candidate STR-HK showed around 78% knockdown efficiency *in vitro* and 62% tumor inhibition rate *in vivo*, with major cytotoxicity observed at molar ratio 80/1 (Chapter 4); (3) the design of a series of stearylated peptides, which showed improved cell viability and biocompatibility achieving 80% - 90% gene-silencing efficiency by peptide STR-H3K3V6/siRNA complexes in various cell lines (Chapter 5); (4) the exploration of the internalization pathway of peptide STR-H3K3V6 in the previous chapter, and its uptake mechanisms, which provided information for future design of peptide-based delivery vehicles for siRNA (Chapter 6). The original contributions to research are summarized in the following sections.

Conjugation of diethylene glycol to a CPP to improve its serum stability:

The development of a library of peptide-based siRNA carriers was previously reported by our group, which induced gene knockdown without inducing cellular toxicity. However, a major limitation of these carriers was that the transfection efficacy was reduced by the presence of serum, resulting in reduced gene knockdown efficiency. To improve the serum stability of the cargo while not decrease the gene-silencing efficacy, one of the most promising peptides C6M1 was conjugated with diethylene glycol. It was demonstrated that the incorporated/co-assembled siRNA complexes increased its stability in serum from less than 24 hours to up to 72 hours, with highly efficient cellular uptake and more than 90% cell viability profile. In addition, the gene-silencing ability of diethylene glycol conjugated-peptide/siRNA complexes was comparable to that of non-conjugated peptide/siRNA at both mRNA and protein levels.

Peptide STR-HK family as siRNA delivery carriers *in vitro* and *in vivo*:

A series of co-assembling, cell-penetrating peptides was designed, including a variant of a nuclear localization sequence, i.e. PKPKRKV, 0-6 histidine residues and an optional stearic acid group. Among the candidates, the most promising one was STR-HK with sequence as STR-HHHPKPKRKV. Stearic acid was adopted as hydrophobic moiety, which improved the uptake efficacy of peptide. The variant of nuclear localization sequence limited nuclear translocation and enhanced the release of cargo into cytoplasm. The incorporation of histidine was aimed to improve the capability of endosomal membrane disruption, which resulted in a

better endosmal escape ability. The STR-HK/siRNA coassembly showed a size distribution ranged from 50 nm to 180 nm, confirmed by dynamic light scattering and atomic force microscopy. The secondary structure of STR-KV was examined by FTIR, showing a combination of β-sheet and β-turn structures. The gene-silencing efficiency induced by STR-HK/siRNA complexes on A549 cells was confirmed by RT-PCR on mRNA level with the highest silencing effect of 78% at a molar ratio of 40/1. The CLSM images suggested that STR-HK/siRNA complexes were internalized within 3 hours through an endocytic pathway, and endosomal escape of siRNAs happened within 12 hours after treatment. Furthermore, the therapeutic potential of STR-HK mediated siRNA delivery was examined *in vivo* for cancer treatment by targeting Bcl-2 gene in a mouse tumor model, and demonstrated that tumor growth was inhibited by 62%, as a result of the downregulation of Bcl-2 protein.

Peptide STR-KV family with improved cell viability and gene-silencing efficiency and its internalization mechanisms:

The STR-KV family peptides were designed with a stearic acid block, a positive lysine amino acids block, and a hydrophobic valine block. Positively charged lysine residues were adopted in the sequences in order to co-assemble with siRNA molecules via electrostatic interactions. Stearic acid was introduced to improve the cellular uptake of complexes. The pH-sensitive histidine residues were employed in the designs to provide protonable groups. Valine groups were added to improve the interactions with cell membrane while reduce the possible cytotoxicity and immunogenicity. The number of lysine, histidine and valine amino acids was

carefully examined on its binding affinity with siRNA molecules, and its gene-silencing efficacy induced by the corresponding peptide/siRNA complexes on a range of cell lines. Within the newly designed peptide family, the most pronounced gene silencing could be achieved with the peptide STR-H3K3V6, which showed a high knockdown efficiency (80% - 90% on various cell lines) rarely reported before. No obvious cytotoxicity was observed with peptide or peptide/siRNA complexes on the four cell lines we chose. The biocompatibility of the peptide STR-H3K3V6 was evaluated in terms of complement activation and cytokine activation, and no obvious responses were observed *in vitro*.

Understanding the uptake mechanisms of cell-penetrating peptide-based siRNA delivery systems will facilitate the development of safe and efficient gene delivery vectors. Thus, the internalization process and intracellular trafficking of the STR-H3K3V6/siRNA (in short as STR-KV/siRNA) complexes was explored. It was confirmed that the electrostatic interaction of peptide/siRNA complexes with heparan sulphate proteoglycans (HSPGs) at the cell surface was essential to triggering the uptake process. In addition, conducting uptake experiments at both 4 °C and 37 °C confirmed that STR-KV/siRNA complexes were internalized through an energy-independent mechanism, most likely involving direct translocation. Utilizing physical and chemical endocytic inhibitors, i.e. Chlorpromazine, EIPA, MBCD, Filipin and Nystatin, was further approved this point. The confocal images were revealed that our complexes were uptake within 2 hours through a non-endocytic pathway on CHO-K1, A549 and HeLa cells.

7.2 Recommendations

Recommended future work to develop peptide-based nanocarriers for efficient and safe siRNA delivery can be divided into following major parts:

Addition of targeting ligands into peptide sequences to further improve the *in vivo* silencing efficiency

Further modification could be applied to its sequence with addition of cell targeting ligands. Moreover, a conjugation with targeting ligands is the most commonly adopted methods to reduce systemic toxicity while improving therapeutic efficiency. Such modifications can be done by one of the following methods: 1) the targeting moiety is attached to one end of the original peptide chain if it is relatively short; 2) the targeting moiety is incorporated into the peptide assemblies by being attached onto the complex surface after the complexation. The commonly adopted targeting ligands involved antibodies, aptamers, small molecules, chemical modified polymers, short peptides, fatty acids, and others. Possible targeting moieties include the followings, depending on the desired targeting sites: 1) Transferrin. The conjugated nanoparticles might accumulate in targeting site 20 min after intravenous injection. 2) Human epidermal growth factor receptor-2 (Her2) antibody. The conjugated siRNA delivery systems resulted an inhibited breast tumor cell proliferation. 3) Tumor homing peptides was another useful targeting strategy in developing siRNA delivery system, e.g., Arg-Gly-Asp (RGD) peptide can effectively employed as targeting ligands.

Evaluate therapeutic effect of peptide/siRNA complexes through intravenous injection *in vivo*:

Preliminary *in vivo* results showed in Chapter 4 that intratumoral injection of Bcl-2 siRNA delivered by STR-HK significantly reduced the tumor proliferation rate in a xenograft NSCLC model with nude mice. To further investigate the possibility of systemic delivery, the complexes of Bcl-2 siRNA with promising peptides with high transfection efficiency and low toxicity *in vitro* can be applied intravenous injections, i.e., STR-HK and STR-KV. The potential animal model could be established as the same one used for intratumoral injection in Chapter 4, i.e., subcutaneous inoculation of 5×10^6 NSCLC A549 cells at the right armpit of six-week-old BALB/c nude mice. Tumor growth and treatments will be monitored and performed on alternative days. After injection, the circulating complexes in bloodstream will be accumulating in tumor either through EPR effects, or through conjugating with a targeting moiety. The mice will be sacrificed after the treatment periods. Several examinations will be performed to evaluate the knockdown efficiency of peptide/siRNA complexes: 1) Tumor tissue will be studied through microscopy for vascularization and angiogenesis; 2) The knockdown efficiency at protein level will be evaluated by western blotting; 3) The non-evasive imaging of biodistribution and pharmacokinetics of complexes will be studied with fluorescently-labeled siRNAs with fluorescent optical microscopy.

Reference

[1] A. Fire, S. Xu, M.K. Montgomery, S.A. Kostas, S.E. Driver, C.C. Mello, Potent and specific genetic interference by double-stranded RNA in Caenorhabditis elegans, Nature, 391 (1998) 806-811.
[2] N.G. Bologna, O. Voinnet, The diversity, biogenesis, and activities of endogenous silencing small RNAs in Arabidopsis, Annual review of plant biology, 65 (2014) 473-503.
[3] Y.U. Konca, K. Kirshenbaum, R.N. Zuckermann, Nanometer-scale siRNA carriers incorporating peptidomimetic oligomers: physical characterization and biological activity, International Journal of Nanomedicine, 9 (2014) 2271-2285.
[4] J. Zhang, X. Li, L. Huang, Non-viral nanocarriers for siRNA delivery in breast cancer, Journal of Controlled Release, 190 (2014) 440-450.
[5] A. Fukuda, J. Badaut, siRNA Treatment: "A Sword-in-the-Stone" for Acute Brain Injuries, Genes, 4 (2013) 435-456.
[6] S. Bakhtiyari, K. Haghani, G. Basati, M.H. Karimfar, siRNA therapeutics in the treatment of diseases, Therapeutic delivery, 4 (2013) 45-57.
[7] J.C. Burnett, J.J. Rossi, RNA-based therapeutics: current progress and future prospects, Chem Biol, 19 (2012) 60-71.
[8] V. Mishra, P. Kesharwani, N.K. Jain, siRNA nanotherapeutics: a Trojan horse approach against HIV, Drug Discovery Today, 19 (2014) 1913-1920.
[9] I. Melnikova, Wet age-related macular degeneration, Nat Rev Drug Discov, 4 (2005) 711-712.
[10] D. Haussecker, Current issues of RNAi therapeutics delivery and development, Journal of Controlled Release, 195 (2014) 49-54.
[11] A. Bouchie, Markets, venture investors and big pharma interest in RNAi soars, Nat Biotech, 32 (2014) 203-204.
[12] E. Bender, The Second Coming of RNAi, Estados Unidos: The Scientist. Exploring life, inspiring innovation, (2014).
[13] M.J. Haas, Alnylam interrupts preeclampsia, SciBX: Science-Business eXchange, 7 (2014).
[14] W. Shiri, P. Dan, RNAi nanomedicines: challenges and opportunities within the immune system, Nanotechnology, 21 (2010) 232001.
[15] Y. Deng, C.C. Wang, K.W. Choy, Q. Du, J. Chen, Q. Wang, L. Li, T.K. Chung, T. Tang, Therapeutic potentials of gene silencing by RNA interference: principles, challenges, and new strategies, Gene, 538 (2014) 217-227.
[16] C.-f. Xu, J. Wang, Delivery systems for siRNA drug development in cancer therapy, Asian Journal of Pharmaceutical Sciences.
[17] S.Y. Wu, X. Yang, K.M. Gharpure, H. Hatakeyama, M. Egli, M.H. McGuire, A.S. Nagaraja, T.M. Miyake, R. Rupaimoole, C.V. Pecot, M. Taylor, S. Pradeep, M. Sierant, C. Rodriguez-Aguayo, H.J. Choi, R.A. Previs, G.N. Armaiz-Pena, L. Huang, C. Martinez, T. Hassell, C. Ivan, V. Sehgal, R. Singhania, H.-D. Han, C. Su, J.H. Kim, H.J. Dalton, C. Kovvali, K. Keyomarsi, N.A.J. McMillan, W.W. Overwijk, J. Liu, J.-S. Lee, K.A. Baggerly, G. Lopez-Berestein, P.T. Ram, B. Nawrot, A.K. Sood, 2′-OMe-phosphorodithioate-modified siRNAs show increased loading into the RISC complex and enhanced anti-tumour activity, Nat Commun, 5 (2014).

[18] G.M. Gordillo, A. Biswas, S. Khanna, X. Pan, M. Sinha, S. Roy, C.K. Sen, Dicer Knockdown Inhibits Endothelial Cell Tumor Growth via MicroRNA 21a-3p Targeting of Nox-4, Journal of Biological Chemistry, 289 (2014) 9027-9038.
[19] T. Takahashi, S. Zenno, O. Ishibashi, T. Takizawa, K. Saigo, K. Ui-Tei, Interactions between the non-seed region of siRNA and RNA-binding RLC/RISC proteins, Ago and TRBP, in mammalian cells, Nucleic Acids Research, 42 (2014) 5256-5269.
[20] M. Sioud, Overcoming the Challenges of siRNA Activation of Innate Immunity: Design Better Therapeutic siRNAs, in: RNA Interference, Springer, 2015, pp. 301-319.
[21] G. Cuccato, A. Polynikis, V. Siciliano, M. Graziano, M. di Bernardo, D. di Bernardo, Modeling RNA interference in mammalian cells, BMC systems biology, 5 (2011) 19.
[22] L. Huang, Y. Liu, In vivo delivery of RNAi with lipid-based nanoparticles, Annu Rev Biomed Eng, 13 (2011) 507-530.
[23] K.A. Whitehead, R. Langer, D.G. Anderson, Knocking down barriers: advances in siRNA delivery, Nat Rev Drug Discov, 8 (2009) 129-138.
[24] M. Jafari, M. Soltani, S. Naahidi, D. N. Karunaratne, P. Chen, Nonviral Approach for Targeted Nucleic Acid Delivery, Current Medicinal Chemistry, 19 (2012) 197-208.
[25] B. Anish, K.T. Amanda, M. Anupama, R. Rajagopal, Nanoparticle-based drug delivery for therapy of lung cancer: progress and challenges, J. Nanomaterials, 2013 (2013) 14-14.
[26] J.-M. Williford, J. Wu, Y. Ren, M.M. Archang, K.W. Leong, H.-Q. Mao, Recent Advances in Nanoparticle-Mediated siRNA Delivery, Annual Review of Biomedical Engineering, 16 (2014) 347-370.
[27] J.-M. Lee, T.-J. Yoon, Y.-S. Cho, Recent Developments in Nanoparticle-Based siRNA Delivery for Cancer Therapy, BioMed Research International, 2013 (2013) 10.
[28] K.L. Kozielski, S.Y. Tzeng, B.A. Hurtado De Mendoza, J.J. Green, Bioreducible Cationic Polymer-Based Nanoparticles for Efficient and Environmentally Triggered Cytoplasmic siRNA Delivery to Primary Human Brain Cancer Cells, ACS Nano, 8 (2014) 3232-3241.
[29] J. Gilleron, W. Querbes, A. Zeigerer, A. Borodovsky, G. Marsico, U. Schubert, K. Manygoats, S. Seifert, C. Andree, M. Stoter, H. Epstein-Barash, L. Zhang, V. Koteliansky, K. Fitzgerald, E. Fava, M. Bickle, Y. Kalaidzidis, A. Akinc, M. Maier, M. Zerial, Image-based analysis of lipid nanoparticle-mediated siRNA delivery, intracellular trafficking and endosomal escape, Nat Biotech, 31 (2013) 638-646.
[30] Y. Hattori, T. Nakamura, H. Ohno, N. Fujii, Y. Maitani, siRNA delivery into tumor cells by lipid-based nanoparticles composed of hydroxyethylated cholesteryl triamine, International Journal of Pharmaceutics, 443 (2013) 221-229.
[31] G. Navarro, S. Essex, V. Torchilin, The “Non-viral” Approach for siRNA Delivery in Cancer Treatment: A Special Focus on Micelles and Liposomes, in: V.A. Erdmann, J. Barciszewski (Eds.) DNA and RNA Nanobiotechnologies in Medicine: Diagnosis and Treatment of Diseases, Springer Berlin Heidelberg, 2013, pp. 241-261.
[32] P. Arukuusk, L. Pärnaste, N. Oskolkov, D.-M. Copolovici, H. Margus, K. Padari, K. Möll, J. Maslovskaja, R. Tegova, G. Kivi, A. Tover, M. Pooga, M. Ustav, Ü. Langel, New generation of efficient peptide-based vectors, NickFects, for the delivery of nucleic acids, Biochimica et Biophysica Acta (BBA) - Biomembranes, 1828 (2013) 1365-1373.
[33] T. Lehto, O.E. Simonson, I. Mager, K. Ezzat, H. Sork, D.-M. Copolovici, J.R. Viola, E.M. Zaghloul, P. Lundin, P.M.D. Moreno, M. Mae, N. Oskolkov, J. Suhorutsenko, C.I.E. Smith, S.E.L. Andaloussi, A Peptide-based Vector for Efficient Gene Transfer In Vitro and In Vivo, Mol Ther, 19 (2011) 1457-1467.

[34] S. Deshayes, K. Konate, A. Rydström, L. Crombez, C. Godefroy, P.-E. Milhiet, A. Thomas, R. Brasseur, G. Aldrian, F. Heitz, M.A. Muñoz-Morris, J.-M. Devoisselle, G. Divita, Self-Assembling Peptide-Based Nanoparticles for siRNA Delivery in Primary Cell Lines, Small, 8 (2012) 2184-2188.
[35] K.K. Hou, H. Pan, G.M. Lanza, S.A. Wickline, Melittin derived peptides for nanoparticle based siRNA transfection, Biomaterials, 34 (2013) 3110-3119.
[36] L.B. Couto, K.A. High, Viral vector-mediated RNA interference, Current opinion in pharmacology, 10 (2010) 534-542.
[37] H. Petrs-Silva, D. Yasumura, M. Matthes, M. LaVail, A. Lewin, W. Hauswirth, Suppression of rds Expression by siRNA and Gene Replacement Strategies for Gene Therapy Using rAAV Vector, in: M.M. LaVail, J.D. Ash, R.E. Anderson, J.G. Hollyfield, C. Grimm (Eds.) Retinal Degenerative Diseases, Springer US, 2012, pp. 215-223.
[38] C. Erdal, Ç. Emre Şefik, S. Ali Demir, Gene Delivery Systems: Recent Progress in Viral and Non-Viral Therapy, 2012.
[39] B. Ozpolat, A.K. Sood, G. Lopez-Berestein, Liposomal siRNA nanocarriers for cancer therapy, Advanced Drug Delivery Reviews, 66 (2014) 110-116.
[40] S.M. Farkhani, A. Valizadeh, H. Karami, S. Mohammadi, N. Sohrabi, F. Badrzadeh, Cell penetrating peptides: Efficient vectors for delivery of nanoparticles, nanocarriers, therapeutic and diagnostic molecules, Peptides, 57 (2014) 78-94.
[41] R. Yu, G. Jih, N. Iglesias, D. Moazed, Determinants of Heterochromatic siRNA Biogenesis and Function, Molecular Cell, 53 (2014) 262-276.
[42] Q.F. Boese, S.A. Scaringe, W.S. Marshall, siRNA as a tool for streamlining functional genomic studies, TARGETS, 2 (2003) 93-100.
[43] H.L. McLeod, Cancer Pharmacogenomics: Early Promise, But Concerted Effort Needed, Science, 339 (2013) 1563-1566.
[44] M. Tomek, T. Akiyama, C.R. Dass, Role of Bcl-2 in tumour cell survival and implications for pharmacotherapy, Journal of Pharmacy and Pharmacology, 64 (2012) 1695-1702.
[45] G.-F. Fu, X.-H. Lin, Q.-W. Han, Y.-F. Xu, D. Guo, G.-X. Xu, Y.-Y. Hou, RNA interference remarkably suppresses bcl-2 gene expression in cancer cells in vitro and in vivo, Cancer Biology & Therapy, 4 (2005) 822-829.
[46] Z. Niu, X. Li, B. Hu, R. Li, L. Wang, L. Wu, X. Wang, Small interfering RNA targeted to secretory clusterin blocks tumor growth, motility, and invasion in breast cancer, Acta biochimica et biophysica Sinica, (2012) gms091.
[47] H. Chen, X. Ma, Z. Li, Q. Shi, W. Zheng, Y. Liu, P. Wang, Functionalization of single-walled carbon nanotubes enables efficient intracellular delivery of siRNA targeting MDM2 to inhibit breast cancer cells growth, Biomedicine & pharmacotherapy = Biomedecine & pharmacotherapie, 66 (2012) 334-338.
[48] M. Wang, A.L. Gartel, The suppression of FOXM1 and its targets in breast cancer xenograft tumors by siRNA, Oncotarget, 2 (2011) 1218-1226.
[49] S.A. Santi, H. Lee, Ablation of Akt2 Induces Autophagy through Cell Cycle Arrest, the Downregulation of p70S6K, and the Deregulation of Mitochondria in MDA-MB231 Cells, PLoS ONE, 6 (2011) e14614.
[50] B. Huang, L. Sun, J. Cao, Y. Zhang, Q. Wu, J. Zhang, Y. Ge, L. Fu, Z. Wang, Downregulation of the GnT-V gene inhibits metastasis and invasion of BGC823 gastric cancer cells, Oncology reports, 29 (2013) 2392-2400.
[51] G. Gasparini, R. Longo, M. Toi, N. Ferrara, Angiogenic inhibitors: a new therapeutic strategy in oncology, Nature clinical practice. Oncology, 2 (2005) 562-577.

[52] M.W. Laschke, M.D. Menger, Anti-angiogenic treatment strategies for the therapy of endometriosis, Human reproduction update, 18 (2012) 682-702.
[53] Y. Shi, M. Tong, Y. Wu, Z. Yang, R.M. Hoffman, Y. Zhang, Y. Tian, M. Qi, Y. Lin, Y. Liu, L. Dai, Y. Sun, Z. Wang, VEGF-C ShRNA inhibits pancreatic cancer growth and lymphangiogenesis in an orthotopic fluorescent nude mouse model, Anticancer research, 33 (2013) 409-417.
[54] E. Salva, L. Kabasakal, F. Eren, N. Ozkan, F. Cakalagaoglu, J. Akbuga, Local delivery of chitosan/VEGF siRNA nanoplexes reduces angiogenesis and growth of breast cancer in vivo, Nucleic acid therapeutics, 22 (2012) 40-48.
[55] Q. Zhang, F. Li, Combating P-glycoprotein-Mediated Multidrug Resistance Using Therapeutic Nanoparticles, Current pharmaceutical design, 19 (2013) 6655-6666.
[56] G. Szakacs, J.K. Paterson, J.A. Ludwig, C. Booth-Genthe, M.M. Gottesman, Targeting multidrug resistance in cancer, Nat Rev Drug Discov, 5 (2006) 219-234.
[57] Y. Donmez, U. Gunduz, Reversal of multidrug resistance by small interfering RNA (siRNA) in doxorubicin-resistant MCF-7 breast cancer cells, Biomedicine & pharmacotherapy = Biomedecine & pharmacotherapie, 65 (2011) 85-89.
[58] Y. Chen, S.R. Bathula, J. Li, L. Huang, Multifunctional Nanoparticles Delivering Small Interfering RNA and Doxorubicin Overcome Drug Resistance in Cancer, Journal of Biological Chemistry, 285 (2010) 22639-22650.
[59] Z. Wu, X. Li, Y. Zeng, X. Zhuang, H. Shen, H. Zhu, H. Liu, H. Xiao, In Vitro and In Vivo Inhibition of MRP Gene Expression and Reversal of Multidrug Resistance by siRNA, Basic & Clinical Pharmacology & Toxicology, 108 (2011) 177-184.
[60] S.T. DeKosky, K. Marek, Looking backward to move forward: early detection of neurodegenerative disorders, Science, 302 (2003) 830-834.
[61] M.B. Youdim, J.J. Buccafusco, Multi-functional drugs for various CNS targets in the treatment of neurodegenerative disorders, Trends in pharmacological sciences, 26 (2005) 27-35.
[62] P.D. Meek, K. McKeithan, G.T. Schumock, Economic considerations in Alzheimer's disease, Pharmacotherapy, 18 (1998) 68-73; discussion 79-82.
[63] S. Prakash, M. Malhotra, V. Rengaswamy, Nonviral siRNA delivery for gene silencing in neurodegenerative diseases, Methods in molecular biology (Clifton, N.J.), 623 (2010) 211-229.
[64] S.Q. Harper, P.D. Staber, X. He, S.L. Eliason, I.H. Martins, Q. Mao, L. Yang, R.M. Kotin, H.L. Paulson, B.L. Davidson, RNA interference improves motor and neuropathological abnormalities in a Huntington's disease mouse model, Proceedings of the National Academy of Sciences of the United States of America, 102 (2005) 5820-5825.
[65] S.C. Kao, A.M. Krichevsky, K.S. Kosik, L.H. Tsai, BACE1 suppression by RNA interference in primary cortical neurons, The Journal of biological chemistry, 279 (2004) 1942-1949.
[66] C.S. Hong, W.F. Goins, J.R. Goss, E.A. Burton, J.C. Glorioso, Herpes simplex virus RNAi and neprilysin gene transfer vectors reduce accumulation of Alzheimer's disease-related amyloid-beta peptide in vivo, Gene Ther, 13 (2006) 1068-1079.
[67] P. Gonzalez-Alegre, Therapeutic RNA interference for neurodegenerative diseases: From promise to progress, Pharmacology & Therapeutics, 114 (2007) 34-55.
[68] S. Yang, Y. Chen, R. Ahmadie, E.A. Ho, Advancements in the field of intravaginal siRNA delivery, Journal of Controlled Release, 167 (2013) 29-39.
[69] J. Lisziewicz, E.R. Tőke, Nanomedicine applications towards the cure of HIV, Nanomedicine: Nanotechnology, Biology and Medicine, 9 28-38.
[70] M.A. Kolber, Development of drug resistance mutations in patients on highly active antiretroviral therapy: does competitive advantage drive evolution, AIDS reviews, 9 (2007) 68-74.

[71] R.M. Surabhi, R.B. Gaynor, RNA interference directed against viral and cellular targets inhibits human immunodeficiency virus type 1 replication, Journal of virology, 76 (2002) 12963-12973.
[72] A. Banerjea, M.J. Li, G. Bauer, L. Remling, N.S. Lee, J. Rossi, R. Akkina, Inhibition of HIV-1 by lentiviral vector-transduced siRNAs in T lymphocytes differentiated in SCID-hu mice and CD34+ progenitor cell-derived macrophages, Mol Ther, 8 (2003) 62-71.
[73] G.A. Coburn, B.R. Cullen, Potent and specific inhibition of human immunodeficiency virus type 1 replication by RNA interference, J Virol, 76 (2002) 9225-9231.
[74] J.M. Jacque, K. Triques, M. Stevenson, Modulation of HIV-1 replication by RNA interference, Nature, 418 (2002) 435-438.
[75] C.D. Novina, M.F. Murray, D.M. Dykxhoorn, P.J. Beresford, J. Riess, S.K. Lee, R.G. Collman, J. Lieberman, P. Shankar, P.A. Sharp, siRNA-directed inhibition of HIV-1 infection, Nat Med, 8 (2002) 681-686.
[76] M.A. Martinez, A. Gutierrez, M. Armand-Ugon, J. Blanco, M. Parera, J. Gomez, B. Clotet, J.A. Este, Suppression of chemokine receptor expression by RNA interference allows for inhibition of HIV-1 replication, AIDS (London, England), 16 (2002) 2385-2390.
[77] D.S. An, R.E. Donahue, M. Kamata, B. Poon, M. Metzger, S.H. Mao, A. Bonifacino, A.E. Krouse, J.L. Darlix, D. Baltimore, F.X. Qin, I.S. Chen, Stable reduction of CCR5 by RNAi through hematopoietic stem cell transplant in non-human primates, Proc Natl Acad Sci U S A, 104 (2007) 13110-13115.
[78] A. Wald, K. Link, Risk of human immunodeficiency virus infection in herpes simplex virus type 2-seropositive persons: a meta-analysis, The Journal of infectious diseases, 185 (2002) 45-52.
[79] L. Corey, A. Wald, C.L. Celum, T.C. Quinn, The effects of herpes simplex virus-2 on HIV-1 acquisition and transmission: a review of two overlapping epidemics, Journal of acquired immune deficiency syndromes (1999), 35 (2004) 435-445.
[80] Z. Ren, S. Li, Q.L. Wang, Y.F. Xiang, Y.X. Cui, Y.F. Wang, R.B. Qi, D.X. Lu, S.M. Zhang, P.Z. Zhang, Effect of siRNAs on HSV-1 plaque formation and relative expression levels of RR mRNA, Virologica Sinica, 26 (2011) 40-46.
[81] D. Palliser, D. Chowdhury, Q.Y. Wang, S.J. Lee, R.T. Bronson, D.M. Knipe, J. Lieberman, An siRNA-based microbicide protects mice from lethal herpes simplex virus 2 infection, Nature, 439 (2006) 89-94.
[82] P. Pisani, F. Bray, D.M. Parkin, Estimates of the world-wide prevalence of cancer for 25 sites in the adult population, International journal of cancer. Journal international du cancer, 97 (2002) 72-81.
[83] H. zur Hausen, Papillomavirus infections--a major cause of human cancers, Biochimica et biophysica acta, 1288 (1996) F55-78.
[84] T. Fujii, M. Saito, E. Iwasaki, T. Ochiya, Y. Takei, S. Hayashi, A. Ono, N. Hirao, M. Nakamura, K. Kubushiro, K. Tsukazaki, D. Aoki, Intratumor injection of small interfering RNA-targeting human papillomavirus 18 E6 and E7 successfully inhibits the growth of cervical cancer, International journal of oncology, 29 (2006) 541-548.
[85] X.Y. Niu, Z.L. Peng, W.Q. Duan, H. Wang, P. Wang, Inhibition of HPV 16 E6 oncogene expression by RNA interference in vitro and in vivo, International journal of gynecological cancer : official journal of the International Gynecological Cancer Society, 16 (2006) 743-751.
[86] A.H. Hall, K.A. Alexander, RNA interference of human papillomavirus type 18 E6 and E7 induces senescence in HeLa cells, J Virol, 77 (2003) 6066-6069.
[87] H. Yin, R.L. Kanasty, A.A. Eltoukhy, A.J. Vegas, J.R. Dorkin, D.G. Anderson, Non-viral vectors for gene-based therapy, Nat Rev Genet, 15 (2014) 541-555.
[88] R. Kanasty, J.R. Dorkin, A. Vegas, D. Anderson, Delivery materials for siRNA therapeutics, Nat Mater, 12 (2013) 967-977.

[89] H. Shen, T. Sun, M. Ferrari, Nanovector delivery of siRNA for cancer therapy, Cancer Gene Ther, 19 (2012) 367-373.
[90] S. Veldhoen, S.D. Laufer, T. Restle, Recent developments in peptide-based nucleic acid delivery, International journal of molecular sciences, 9 (2008) 1276-1320.
[91] D.W. Bartlett, M.E. Davis, Insights into the kinetics of siRNA-mediated gene silencing from live-cell and live-animal bioluminescent imaging, Nucleic Acids Res, 34 (2006) 322-333.
[92] R.P. Hickerson, A.V. Vlassov, Q. Wang, D. Leake, H. Ilves, E. Gonzalez-Gonzalez, C.H. Contag, B.H. Johnston, R.L. Kaspar, Stability study of unmodified siRNA and relevance to clinical use, Oligonucleotides, 18 (2008) 345-354.
[93] J. Burchard, A.L. Jackson, V. Malkov, R.H.V. Needham, Y. Tan, S.R. Bartz, H. Dai, A.B. Sachs, P.S. Linsley, MicroRNA-like off-target transcript regulation by siRNAs is species specific, RNA, 15 (2009) 308-315.
[94] D. Guzman-Villanueva, I.M. El-Sherbiny, D. Herrera-Ruiz, A.V. Vlassov, H.D. Smyth, Formulation approaches to short interfering RNA and MicroRNA: challenges and implications, Journal of pharmaceutical sciences, 101 (2012) 4046-4066.
[95] S. Sivori, M. Falco, M.D. Chiesa, S. Carlomagno, M. Vitale, L. Moretta, A. Moretta, CpG and double-stranded RNA trigger human NK cells by Toll-like receptors: Induction of cytokine release and cytotoxicity against tumors and dendritic cells, Proceedings of the National Academy of Sciences of the United States of America, 101 (2004) 10116-10121.
[96] D. Haussecker, Current issues of RNAi therapeutics delivery and development, Journal of controlled release : official journal of the Controlled Release Society, 195 (2014) 49-54.
[97] K. Karikó, P. Bhuyan, J. Capodici, D. Weissman, Small Interfering RNAs Mediate Sequence-Independent Gene Suppression and Induce Immune Activation by Signaling through Toll-Like Receptor 3, The Journal of Immunology, 172 (2004) 6545-6549.
[98] J.T. Marques, B.R.G. Williams, Activation of the mammalian immune system by siRNAs, Nat Biotech, 23 (2005) 1399-1405.
[99] F. Heil, H. Hemmi, H. Hochrein, F. Ampenberger, C. Kirschning, S. Akira, G. Lipford, H. Wagner, S. Bauer, Species-Specific Recognition of Single-Stranded RNA via Toll-like Receptor 7 and 8, Science, 303 (2004) 1526-1529.
[100] V. Hornung, M. Guenthner-Biller, C. Bourquin, A. Ablasser, M. Schlee, S. Uematsu, A. Noronha, M. Manoharan, S. Akira, A. de Fougerolles, S. Endres, G. Hartmann, Sequence-specific potent induction of IFN-[alpha] by short interfering RNA in plasmacytoid dendritic cells through TLR7, Nat Med, 11 (2005) 263-270.
[101] B. Zhang, S. Mallapragada, The mechanism of selective transfection mediated by pentablock copolymers; Part II: Nuclear entry and endosomal escape, Acta Biomaterialia, 7 (2011) 1580-1587.
[102] M. Robbins, A. Judge, L. Liang, K. McClintock, E. Yaworski, I. MacLachlan, 2[prime]-O-methyl-modified RNAs Act as TLR7 Antagonists, Mol Ther, 15 (2007) 1663-1669.
[103] A.L. Jackson, J. Burchard, D. Leake, A. Reynolds, J. Schelter, J. Guo, J.M. Johnson, L. Lim, J. Karpilow, K. Nichols, W. Marshall, A. Khvorova, P.S. Linsley, Position-specific chemical modification of siRNAs reduces “off-target” transcript silencing, RNA, 12 (2006) 1197-1205.
[104] A.L. Jackson, J. Burchard, J. Schelter, B.N. Chau, M. Cleary, L. Lim, P.S. Linsley, Widespread siRNA “off-target” transcript silencing mediated by seed region sequence complementarity, RNA, 12 (2006) 1179-1187.
[105] M. Stessl, M. Marchetti-Deschmann, J. Winkler, B. Lachmann, G. Allmaier, C.R. Noe, A proteomic study reveals unspecific apoptosis induction and reduction of glycolytic enzymes by the phosphorothioate antisense oligonucleotide oblimersen in human melanoma cells, Journal of Proteomics, 72 (2009) 1019-1030.

[106] K. Ui-Tei, Y. Naito, S. Zenno, K. Nishi, K. Yamato, F. Takahashi, A. Juni, K. Saigo, Functional dissection of siRNA sequence by systematic DNA substitution: modified siRNA with a DNA seed arm is a powerful tool for mammalian gene silencing with significantly reduced off-target effect, Nucleic Acids Research, 36 (2008) 2136-2151.
[107] A. de Fougerolles, H.P. Vornlocher, J. Maraganore, J. Lieberman, Interfering with disease: a progress report on siRNA-based therapeutics, Nat Rev Drug Discov, 6 (2007) 443-453.
[108] S. Chabot, J. Teissié, M. Golzio, Targeted electro-delivery of oligonucleotides for RNA interference: siRNA and antimiR, Advanced Drug Delivery Reviews, 81 (2015) 161-168.
[109] M. Golzio, L. Mazzolini, A. Ledoux, A. Paganin, M. Izard, L. Hellaudais, A. Bieth, M.J. Pillaire, C. Cazaux, J.S. Hoffmann, B. Couderc, J. Teissie, In vivo gene silencing in solid tumors by targeted electrically mediated siRNA delivery, Gene Ther, 14 (2007) 752-759.
[110] Y.-K. Oh, T.G. Park, siRNA delivery systems for cancer treatment, Advanced Drug Delivery Reviews, 61 (2009) 850-862.
[111] H. Xia, Q. Mao, S.L. Eliason, S.Q. Harper, I.H. Martins, H.T. Orr, H.L. Paulson, L. Yang, R.M. Kotin, B.L. Davidson, RNAi suppresses polyglutamine-induced neurodegeneration in a model of spinocerebellar ataxia, Nat Med, 10 (2004) 816-820.
[112] M.D. White, M. Farmer, I. Mirabile, S. Brandner, J. Collinge, G.R. Mallucci, Single treatment with RNAi against prion protein rescues early neuronal dysfunction and prolongs survival in mice with prion disease, Proc Natl Acad Sci U S A, 105 (2008) 10238-10243.
[113] E. Check, Gene therapy put on hold as third child develops cancer, Nature, 433 (2005) 561-561.
[114] P. Guo, O. Coban, N.M. Snead, J. Trebley, S. Hoeprich, S. Guo, Y. Shu, Engineering RNA for Targeted siRNA Delivery and Medical Application, Advanced Drug Delivery Reviews, 62 (2010) 650-666.
[115] J. Zhou, K.-T. Shum, J. Burnett, J. Rossi, Nanoparticle-Based Delivery of RNAi Therapeutics: Progress and Challenges, Pharmaceuticals, 6 (2013) 85-107.
[116] H. Lv, S. Zhang, B. Wang, S. Cui, J. Yan, Toxicity of cationic lipids and cationic polymers in gene delivery, Journal of controlled release : official journal of the Controlled Release Society, 114 (2006) 100-109.
[117] T.M. Allen, P.R. Cullis, Liposomal drug delivery systems: From concept to clinical applications, Advanced Drug Delivery Reviews, 65 (2013) 36-48.
[118] S. Zhang, D. Zhi, L. Huang, Lipid-based vectors for siRNA delivery, Journal of Drug Targeting, 20 (2012) 724-735.
[119] C.N. Landen, Jr., A. Chavez-Reyes, C. Bucana, R. Schmandt, M.T. Deavers, G. Lopez-Berestein, A.K. Sood, Therapeutic EphA2 gene targeting in vivo using neutral liposomal small interfering RNA delivery, Cancer Res, 65 (2005) 6910-6918.
[120] J. Halder, A.A. Kamat, C.N. Landen, Jr., L.Y. Han, S.K. Lutgendorf, Y.G. Lin, W.M. Merritt, N.B. Jennings, A. Chavez-Reyes, R.L. Coleman, D.M. Gershenson, R. Schmandt, S.W. Cole, G. Lopez-Berestein, A.K. Sood, Focal adhesion kinase targeting using in vivo short interfering RNA delivery in neutral liposomes for ovarian carcinoma therapy, Clinical cancer research : an official journal of the American Association for Cancer Research, 12 (2006) 4916-4924.
[121] L. Shao, I. Tekedereli, J. Wang, E. Yuca, S. Tsang, A. Sood, G. Lopez-Berestein, B. Ozpolat, M. Ittmann, Highly specific targeting of the TMPRSS2/ERG fusion gene using liposomal nanovectors, Clinical cancer research : an official journal of the American Association for Cancer Research, 18 (2012) 6648-6657.
[122] T.S. Zimmermann, A.C.H. Lee, A. Akinc, B. Bramlage, D. Bumcrot, M.N. Fedoruk, J. Harborth, J.A. Heyes, L.B. Jeffs, M. John, A.D. Judge, K. Lam, K. McClintock, L.V. Nechev, L.R. Palmer, T. Racie, I. Röhl, S. Seiffert, S. Shanmugam, V. Sood, J. Soutschek, I. Toudjarska, A.J.

Wheat, E. Yaworski, W. Zedalis, V. Koteliansky, M. Manoharan, H.-P. Vornlocher, I. MacLachlan, RNAi-mediated gene silencing in non-human primates, Nature, 441 (2006) 111-114.
[123] R. Kersten, S. van Gaalen, M. Arts, K. Roes, A. de Gast, T. Corbin, F. Oner, The SNAP trial: a double blind multi-center randomized controlled trial of a silicon nitride versus a PEEK cage in transforaminal lumbar interbody fusion in patients with symptomatic degenerative lumbar disc disorders: study protocol, BMC Musculoskeletal Disorders, 15 (2014) 57.
[124] Y. Bao, Y. Jin, P. Chivukula, J. Zhang, Y. Liu, J. Liu, J.P. Clamme, R.I. Mahato, D. Ng, W. Ying, Y. Wang, L. Yu, Effect of PEGylation on biodistribution and gene silencing of siRNA/lipid nanoparticle complexes, Pharmaceutical research, 30 (2013) 342-351.
[125] Y.C. Kuo, H.F. Ko, Targeting delivery of saquinavir to the brain using 83-14 monoclonal antibody-grafted solid lipid nanoparticles, Biomaterials, 34 (2013) 4818-4830.
[126] S. David, B. Pitard, J.P. Benoit, C. Passirani, Non-viral nanosystems for systemic siRNA delivery, Pharmacological research : the official journal of the Italian Pharmacological Society, 62 (2010) 100-114.
[127] J. Xu, S. Ganesh, M. Amiji, Non-condensing polymeric nanoparticles for targeted gene and siRNA delivery, International Journal of Pharmaceutics, 427 (2012) 21-34.
[128] A.C. Grayson, A.M. Doody, D. Putnam, Biophysical and structural characterization of polyethylenimine-mediated siRNA delivery in vitro, Pharmaceutical research, 23 (2006) 1868-1876.
[129] B. Urban-Klein, S. Werth, S. Abuharbeid, F. Czubayko, A. Aigner, RNAi-mediated gene-targeting through systemic application of polyethylenimine (PEI)-complexed siRNA in vivo, Gene Ther, 12 (2005) 461-466.
[130] F.Y. Xie, M.C. Woodle, P.Y. Lu, Harnessing in vivo siRNA delivery for drug discovery and therapeutic development, Drug Discovery Today, 11 (2006) 67-73.
[131] G. Navarro, R.R. Sawant, S. Essex, C. Tros de Ilarduya, V.P. Torchilin, Phospholipid–polyethylenimine conjugate-based micelle-like nanoparticles for siRNA delivery, Drug delivery and translational research, 1 (2011) 25-33.
[132] T.M. Sun, J.Z. Du, L.F. Yan, H.Q. Mao, J. Wang, Self-assembled biodegradable micellar nanoparticles of amphiphilic and cationic block copolymer for siRNA delivery, Biomaterials, 29 (2008) 4348-4355.
[133] C.Q. Mao, J.Z. Du, T.M. Sun, Y.D. Yao, P.Z. Zhang, E.W. Song, J. Wang, A biodegradable amphiphilic and cationic triblock copolymer for the delivery of siRNA targeting the acid ceramidase gene for cancer therapy, Biomaterials, 32 (2011) 3124-3133.
[134] X.Q. Liu, M.H. Xiong, X.T. Shu, R.Z. Tang, J. Wang, Therapeutic delivery of siRNA silencing HIF-1 alpha with micellar nanoparticles inhibits hypoxic tumor growth, Mol Pharm, 9 (2012) 2863-2874.
[135] C.Q. Mao, M.H. Xiong, Y. Liu, S. Shen, X.J. Du, X.Z. Yang, S. Dou, P.Z. Zhang, J. Wang, Synthetic lethal therapy for KRAS mutant non-small-cell lung carcinoma with nanoparticle-mediated CDK4 siRNA delivery, Mol Ther, 22 (2014) 964-973.
[136] M.L. Patil, M. Zhang, T. Minko, Multifunctional triblock Nanocarrier (PAMAM-PEG-PLL) for the efficient intracellular siRNA delivery and gene silencing, ACS Nano, 5 (2011) 1877-1887.
[137] F. Wang, Y. Wang, X. Zhang, W. Zhang, S. Guo, F. Jin, Recent progress of cell-penetrating peptides as new carriers for intracellular cargo delivery, Journal of Controlled Release, 174 (2014) 126-136.
[138] F. Milletti, Cell-penetrating peptides: classes, origin, and current landscape, Drug Discovery Today, 17 (2012) 850-860.

[139] F. Duchardt, M. Fotin-Mleczek, H. Schwarz, R. Fischer, R. Brock, A comprehensive model for the cellular uptake of cationic cell-penetrating peptides, Traffic (Copenhagen, Denmark), 8 (2007) 848-866.
[140] S. Futaki, T. Suzuki, W. Ohashi, T. Yagami, S. Tanaka, K. Ueda, Y. Sugiura, Arginine-rich peptides. An abundant source of membrane-permeable peptides having potential as carriers for intracellular protein delivery, The Journal of biological chemistry, 276 (2001) 5836-5840.
[141] A. Prochiantz, Getting hydrophilic compounds into cells: lessons from homeopeptides, Current opinion in neurobiology, 6 (1996) 629-634.
[142] A.D. Ragin, R.A. Morgan, J. Chmielewski, Cellular import mediated by nuclear localization signal Peptide sequences, Chem Biol, 9 (2002) 943-948.
[143] K. Oglecka, P. Lundberg, M. Magzoub, L.E. Goran Eriksson, U. Langel, A. Graslund, Relevance of the N-terminal NLS-like sequence of the prion protein for membrane perturbation effects, Biochimica et biophysica acta, 1778 (2008) 206-213.
[144] P. Jarver, K. Langel, S. El-Andaloussi, U. Langel, Applications of cell-penetrating peptides in regulation of gene expression, Biochemical Society transactions, 35 (2007) 770-774.
[145] E. Snyder, S. Dowdy, Cell Penetrating Peptides in Drug Delivery, Pharmaceutical research, 21 (2004) 389-393.
[146] F. Simeoni, M.C. Morris, F. Heitz, G. Divita, Insight into the mechanism of the peptide-based gene delivery system MPG: implications for delivery of siRNA into mammalian cells, Nucleic Acids Res, 31 (2003) 2717-2724.
[147] S. Veldhoen, S.D. Laufer, A. Trampe, T. Restle, Cellular delivery of small interfering RNA by a non-covalently attached cell-penetrating peptide: quantitative analysis of uptake and biological effect, Nucleic Acids Research, 34 (2006) 6561-6573.
[148] K.V. Morris, S.W.L. Chan, S.E. Jacobsen, D.J. Looney, Small Interfering RNA-Induced Transcriptional Gene Silencing in Human Cells, Science, 305 (2004) 1289-1292.
[149] F. Simeoni, M.C. Morris, F. Heitz, G. Divita, Peptide-based strategy for siRNA delivery into mammalian cells, Methods in molecular biology (Clifton, N.J.), 309 (2005) 251-260.
[150] S. Balayssac, F. Burlina, O. Convert, G. Bolbach, G. Chassaing, O. Lequin, Comparison of Penetratin and Other Homeodomain-Derived Cell-Penetrating Peptides: Interaction in a Membrane-Mimicking Environment and Cellular Uptake Efficiency†, Biochemistry, 45 (2006) 1408-1420.
[151] G. Drin, M. Mazel, P. Clair, D. Mathieu, M. Kaczorek, J. Temsamani, Physico-chemical requirements for cellular uptake of pAntp peptide. Role of lipid-binding affinity, European journal of biochemistry / FEBS, 268 (2001) 1304-1314.
[152] J. Hoyer, I. Neundorf, Knockdown of a G protein-coupled receptor through efficient peptide-mediated siRNA delivery, Journal of Controlled Release, 161 (2012) 826-834.
[153] K. Fosgerau, T. Hoffmann, Peptide therapeutics: current status and future directions, Drug Discovery Today.
[154] H. He, J. Ye, Y. Wang, Q. Liu, H.S. Chung, Y.M. Kwon, M.C. Shin, K. Lee, V.C. Yang, Cell-penetrating peptides meditated encapsulation of protein therapeutics into intact red blood cells and its application, Journal of Controlled Release, 176 (2014) 123-132.
[155] I. Nakase, G. Tanaka, S. Futaki, Cell-penetrating peptides (CPPs) as a vector for the delivery of siRNAs into cells, Molecular BioSystems, 9 (2013) 855-861.
[156] E. Koren, V.P. Torchilin, Cell-penetrating peptides: breaking through to the other side, Trends in Molecular Medicine, 18 (2012) 385-393.
[157] Y. Matsumura, H. Maeda, A new concept for macromolecular therapeutics in cancer chemotherapy: mechanism of tumoritropic accumulation of proteins and the antitumor agent smancs, Cancer Res, 46 (1986) 6387-6392.

[158] K. Kajimoto, Y. Sato, T. Nakamura, Y. Yamada, H. Harashima, Multifunctional envelope-type nano device for controlled intracellular trafficking and selective targeting in vivo, Journal of Controlled Release, 190 (2014) 593-606.
[159] P. Resnier, T. Montier, V. Mathieu, J.-P. Benoit, C. Passirani, A review of the current status of siRNA nanomedicines in the treatment of cancer, Biomaterials, 34 (2013) 6429-6443.
[160] K.F. Pirollo, G. Zon, A. Rait, Q. Zhou, W. Yu, R. Hogrefe, E.H. Chang, Tumor-targeting nanoimmunoliposome complex for short interfering RNA delivery, Human gene therapy, 17 (2006) 117-124.
[161] S. Dou, Y.-D. Yao, X.-Z. Yang, T.-M. Sun, C.-Q. Mao, E.-W. Song, J. Wang, Anti-Her2 single-chain antibody mediated DNMTs-siRNA delivery for targeted breast cancer therapy, Journal of Controlled Release, 161 (2012) 875-883.
[162] K. Gavrilov, W.M. Saltzman, Therapeutic siRNA: principles, challenges, and strategies, The Yale journal of biology and medicine, 85 (2012) 187-200.
[163] J. Soutschek, A. Akinc, B. Bramlage, K. Charisse, R. Constien, M. Donoghue, S. Elbashir, A. Geick, P. Hadwiger, J. Harborth, M. John, V. Kesavan, G. Lavine, R.K. Pandey, T. Racie, K.G. Rajeev, I. Rohl, I. Toudjarska, G. Wang, S. Wuschko, D. Bumcrot, V. Koteliansky, S. Limmer, M. Manoharan, H.P. Vornlocher, Therapeutic silencing of an endogenous gene by systemic administration of modified siRNAs, Nature, 432 (2004) 173-178.
[164] H.D. Han, L.S. Mangala, J.W. Lee, M.M. Shahzad, H.S. Kim, D. Shen, E.J. Nam, E.M. Mora, R.L. Stone, C. Lu, S.J. Lee, J.W. Roh, A.M. Nick, G. Lopez-Berestein, A.K. Sood, Targeted gene silencing using RGD-labeled chitosan nanoparticles, Clinical cancer research : an official journal of the American Association for Cancer Research, 16 (2010) 3910-3922.
[165] L.Y.T. Chou, K. Ming, W.C.W. Chan, Strategies for the intracellular delivery of nanoparticles, Chemical Society Reviews, 40 (2011) 233-245.
[166] S. Xiang, H. Tong, Q. Shi, J.C. Fernandes, T. Jin, K. Dai, X. Zhang, Uptake mechanisms of non-viral gene delivery, Journal of Controlled Release, 158 (2012) 371-378.
[167] K. Sarkar, M.J. Kruhlak, S.L. Erlandsen, S. Shaw, Selective inhibition by rottlerin of macropinocytosis in monocyte-derived dendritic cells, Immunology, 116 (2005) 513-524.
[168] J.P. Richard, K. Melikov, H. Brooks, P. Prevot, B. Lebleu, L.V. Chernomordik, Cellular Uptake of Unconjugated TAT Peptide Involves Clathrin-dependent Endocytosis and Heparan Sulfate Receptors, Journal of Biological Chemistry, 280 (2005) 15300-15306.
[169] A. Aderem, D.M. Underhill, Mechanisms of phagocytosis in macrophages, Annual review of immunology, 17 (1999) 593-623.
[170] S.D. Conner, S.L. Schmid, Regulated portals of entry into the cell, Nature, 422 (2003) 37-44.
[171] U. Wattendorf, G. Coullerez, J. Vörös, M. Textor, H.P. Merkle, Mannose-Based Molecular Patterns on Stealth Microspheres for Receptor-Specific Targeting of Human Antigen-Presenting Cells, Langmuir, 24 (2008) 11790-11802.
[172] G. Chaudhuri, Scavenger receptor-mediated delivery of antisense mini-exon phosphorothioate oligonucleotide to Leishmania-infected macrophages. Selective and efficient elimination of the parasite, Biochemical pharmacology, 53 (1997) 385-391.
[173] Y. Ikeda, K. Taira, Ligand-targeted delivery of therapeutic siRNA, Pharmaceutical research, 23 (2006) 1631-1640.
[174] S.A. Mousavi, L. Malerød, T. Berg, R. Kjeken, Clathrin-dependent endocytosis, Biochemical Journal, 377 (2004) 1-16.
[175] C. Pangarkar, A.-T. Dinh, S. Mitragotri, Endocytic pathway rapidly delivers internalized molecules to lysosomes: An analysis of vesicle trafficking, clustering and mass transfer, Journal of Controlled Release, 162 (2012) 76-83.

[176] B. Nichols, Caveosomes and endocytosis of lipid rafts, Journal of Cell Science, 116 (2003) 4707-4714.
[177] S. Fagerholm, U. Örtegren, M. Karlsson, I. Ruishalme, P. Strålfors, Rapid Insulin-Dependent Endocytosis of the Insulin Receptor by Caveolae in Primary Adipocytes, PLoS ONE, 4 (2009) e5985.
[178] Y. Ning, T. Buranda, L.G. Hudson, Activated epidermal growth factor receptor induces integrin alpha2 internalization via caveolae/raft-dependent endocytic pathway, The Journal of biological chemistry, 282 (2007) 6380-6387.
[179] S.W. Jones, R. Christison, K. Bundell, C.J. Voyce, S.M.V. Brockbank, P. Newham, M.A. Lindsay, Characterisation of cell-penetrating peptide-mediated peptide delivery, British journal of pharmacology, 145 (2005) 1093-1102.
[180] A. Ferrari, V. Pellegrini, C. Arcangeli, A. Fittipaldi, M. Giacca, F. Beltram, Caveolae-Mediated Internalization of Extracellular HIV-1 Tat Fusion Proteins Visualized in Real Time, Mol Ther, 8 (2003) 284-294.
[181] S. Pujals, E. Giralt, Proline-rich, amphipathic cell-penetrating peptides, Advanced Drug Delivery Reviews, 60 (2008) 473-484.
[182] I.A. Khalil, K. Kogure, H. Akita, H. Harashima, Uptake pathways and subsequent intracellular trafficking in nonviral gene delivery, Pharmacological reviews, 58 (2006) 32-45.
[183] A. Rydström, S. Deshayes, K. Konate, L. Crombez, K. Padari, H. Boukhaddaoui, G. Aldrian, M. Pooga, G. Divita, Direct Translocation as Major Cellular Uptake for CADY Self-Assembling Peptide-Based Nanoparticles, PLoS ONE, 6 (2011) e25924.
[184] B.R. Liu, Y.-w. Huang, J.G. Winiarz, H.-J. Chiang, H.-J. Lee, Intracellular delivery of quantum dots mediated by a histidine- and arginine-rich HR9 cell-penetrating peptide through the direct membrane translocation mechanism, Biomaterials, 32 (2011) 3520-3537.
[185] B. Gupta, T.S. Levchenko, V.P. Torchilin, Intracellular delivery of large molecules and small particles by cell-penetrating proteins and peptides, Advanced Drug Delivery Reviews, 57 (2005) 637-651.
[186] S.B. Fonseca, M.P. Pereira, S.O. Kelley, Recent advances in the use of cell-penetrating peptides for medical and biological applications, Advanced Drug Delivery Reviews, 61 (2009) 953-964.
[187] I. Nakase, H. Hirose, G. Tanaka, A. Tadokoro, S. Kobayashi, T. Takeuchi, S. Futaki, Cell-surface Accumulation of Flock House Virus-derived Peptide Leads to Efficient Internalization via Macropinocytosis, Mol Ther, 17 (2009) 1868-1876.
[188] K.r. Padari, K. Koppel, A. Lorents, M. Hällbrink, M. Mano, M.C. Pedroso de Lima, M. Pooga, S413-PV Cell-Penetrating Peptide Forms Nanoparticle-Like Structures to Gain Entry Into Cells, Bioconjugate chemistry, 21 (2010) 774-783.
[189] P. Bozavikov, D. Rajshankar, W. Lee, C.A. McCulloch, Particle size influences fibronectin internalization and degradation by fibroblasts, Experimental cell research, 328 (2014) 172-185.
[190] H. Shen, M.P. Goldberg, Creatine pretreatment protects cortical axons from energy depletion in vitro, Neurobiology of disease, 47 (2012) 184-193.
[191] H. Wang, C.-Y. Zhong, J.-F. Wu, Y.-B. Huang, C.-B. Liu, Enhancement of TAT cell membrane penetration efficiency by dimethyl sulphoxide, Journal of Controlled Release, 143 (2010) 64-70.
[192] Y.-C. Tseng, S. Mozumdar, L. Huang, Lipid-based systemic delivery of siRNA, Advanced Drug Delivery Reviews, 61 (2009) 721-731.
[193] Y. Shu, F. Pi, A. Sharma, M. Rajabi, F. Haque, D. Shu, M. Leggas, B.M. Evers, P. Guo, Stable RNA nanoparticles as potential new generation drugs for cancer therapy, Advanced Drug Delivery Reviews, 66 (2014) 74-89.

[194] N.S. Gandhi, R.K. Tekade, M.B. Chougule, Nanocarrier mediated delivery of siRNA/miRNA in combination with chemotherapeutic agents for cancer therapy: Current progress and advances, Journal of Controlled Release, 194 (2014) 238-256.
[195] K. Berg, A. Weyergang, L. Prasmickaite, A. Bonsted, A. Hogset, M.T. Strand, E. Wagner, P.K. Selbo, Photochemical internalization (PCI): a technology for drug delivery, Methods in molecular biology (Clifton, N.J.), 635 (2010) 133-145.
[196] M.M. Fretz, A. Hogset, G.A. Koning, W. Jiskoot, G. Storm, Cytosolic delivery of liposomally targeted proteins induced by photochemical internalization, Pharmaceutical research, 24 (2007) 2040-2047.
[197] H. Cabral, M. Nakanishi, M. Kumagai, W.D. Jang, N. Nishiyama, K. Kataoka, A photo-activated targeting chemotherapy using glutathione sensitive camptothecin-loaded polymeric micelles, Pharmaceutical research, 26 (2009) 82-92.
[198] T. Endoh, M. Sisido, T. Ohtsuki, Cellular siRNA delivery mediated by a cell-permeant RNA-binding protein and photoinduced RNA interference, Bioconjugate chemistry, 19 (2008) 1017-1024.
[199] D. De Paula, M.V.L.B. Bentley, R.I. Mahato, Hydrophobization and bioconjugation for enhanced siRNA delivery and targeting, RNA, 13 (2007) 431-456.
[200] M. Jafari, P. Chen, Peptide mediated siRNA delivery, Current topics in medicinal chemistry, 9 (2009) 1088-1097.
[201] P. Xu, E.A. Van Kirk, W.J. Murdoch, Y. Zhan, D.D. Isaak, M. Radosz, Y. Shen, Anticancer Efficacies of Cisplatin-Releasing pH-Responsive Nanoparticles, Biomacromolecules, 7 (2006) 829-835.
[202] D.W. Pack, A.S. Hoffman, S. Pun, P.S. Stayton, Design and development of polymers for gene delivery, Nat Rev Drug Discov, 4 (2005) 581-593.
[203] J.H. Jeong, T.G. Park, Poly(l-lysine)-g-poly(d,l-lactic-co-glycolic acid) micelles for low cytotoxic biodegradable gene delivery carriers, Journal of Controlled Release, 82 (2002) 159-166.
[204] L. Wasungu, D. Hoekstra, Cationic lipids, lipoplexes and intracellular delivery of genes, Journal of controlled release : official journal of the Controlled Release Society, 116 (2006) 255-264.
[205] N.M. Rao, V. Gopal, Cell biological and biophysical aspects of lipid-mediated gene delivery, Bioscience reports, 26 (2006) 301-324.
[206] A.T. Balaban, M.A. Ilies, Recent developments in cationic lipid-mediated gene delivery and gene therapy, Expert Opinion on Therapeutic Patents, 11 (2001) 1729-1752.
[207] S. Deshayes, M. Decaffmeyer, R. Brasseur, A. Thomas, Structural polymorphism of two CPP: an important parameter of activity, Biochimica et biophysica acta, 1778 (2008) 1197-1205.
[208] L. Crombez, A. Charnet, M.C. Morris, G. Aldrian-Herrada, F. Heitz, G. Divita, A non-covalent peptide-based strategy for siRNA delivery, Biochemical Society transactions, 35 (2007) 44-46.
[209] R.S. Tomar, H. Matta, P.M. Chaudhary, Use of adeno-associated viral vector for delivery of small interfering RNA, Oncogene, 22 (2003) 5712-5715.
[210] G.-H. Guibinga, S. Song, J. Loring, T. Friedmann, Characterization of the gene delivery properties of baculoviral-based virosomal vectors, Journal of Virological Methods, 148 (2008) 277-282.
[211] 贾法里穆萨, 卡鲁纳拉特纳内德拉, 多肽序列设计及其在多肽介导的 siRNA 传递中的应用 Polypeptide sequence design and application of siRNA-mediated transfer of the polypeptide, in, Google Patents, 2015.
[212] S. Li, W.C. Tseng, D.B. Stolz, S.P. Wu, S.C. Watkins, L. Huang, Dynamic changes in the characteristics of cationic lipidic vectors after exposure to mouse serum: implications for intravenous lipofection, Gene therapy, 6 (1999) 585-594.

[213] F. Verbaan, I. van Dam, Y. Takakura, M. Hashida, W. Hennink, G. Storm, C. Oussoren, Intravenous fate of poly(2-(dimethylamino)ethyl methacrylate)-based polyplexes, European journal of pharmaceutical sciences : official journal of the European Federation for Pharmaceutical Sciences, 20 (2003) 419-427.
[214] N.N. Sanders, E. Van Rompaey, S.C. De Smedt, J. Demeester, Structural alterations of gene complexes by cystic fibrosis sputum, American journal of respiratory and critical care medicine, 164 (2001) 486-493.
[215] S.H. Lee, S.H. Kim, T.G. Park, Intracellular siRNA delivery system using polyelectrolyte complex micelles prepared from VEGF siRNA-PEG conjugate and cationic fusogenic peptide, Biochemical and biophysical research communications, 357 (2007) 511-516.
[216] S.M. Ryan, G. Mantovani, X. Wang, D.M. Haddleton, D.J. Brayden, Advances in PEGylation of important biotech molecules: delivery aspects, Expert opinion on drug delivery, 5 (2008) 371-383.
[217] N. Bertrand, J.C. Leroux, The journey of a drug-carrier in the body: an anatomo-physiological perspective, Journal of controlled release : official journal of the Controlled Release Society, 161 (2012) 152-163.
[218] R. Bansal, E. Post, J.H. Proost, A. de Jager-Krikken, K. Poelstra, J. Prakash, PEGylation improves pharmacokinetic profile, liver uptake and efficacy of Interferon gamma in liver fibrosis, Journal of controlled release : official journal of the Controlled Release Society, 154 (2011) 233-240.
[219] C. Monfardini, F.M. Veronese, Stabilization of substances in circulation, Bioconjugate chemistry, 9 (1998) 418-450.
[220] G.E. Francis, C. Delgado, D. Fisher, F. Malik, A.K. Agrawal, Polyethylene glycol modification: relevance of improved methodology to tumour targeting, J Drug Target, 3 (1996) 321-340.
[221] M. Ferrari, Frontiers in Cancer Nanomedicine: Directing Mass Transport through Biological Barriers, Trends in biotechnology, 28 (2010) 181-188.
[222] E. Ruoslahti, Vascular zip codes in angiogenesis and metastasis, Biochemical Society transactions, 32 (2004) 397-402.
[223] W. Xu, M. Jafari, F. Yuan, R. Pan, B. Chen, Y. Ding, T. Sheinin, D. Chu, S. Lu, Y. Yuan, P. Chen, In vitro and in vivo therapeutic siRNA delivery induced by a tryptophan-rich endosomolytic peptide, Journal of Materials Chemistry B, 2 (2014) 6010-6019.
[224] W. Xu, R. Pan, D. Zhao, D. Chu, Y. Wu, R. Wang, B. Chen, Y. Ding, P. Sadatmousavi, Y. Yuan, P. Chen, Design and Evaluation of Endosomolytic Biocompatible Peptides as Carriers for siRNA Delivery, Molecular Pharmaceutics, 12 (2015) 56-65.
[225] M. Jafari, W. Xu, R. Pan, C.M. Sweeting, D.N. Karunaratne, P. Chen, Serum stability and physicochemical characterization of a novel amphipathic peptide C6M1 for siRNA delivery, PLoS One, 9 (2014) e97797.
[226] Y. Wen, S. Pan, X. Luo, X. Zhang, W. Zhang, M. Feng, A biodegradable low molecular weight polyethylenimine derivative as low toxicity and efficient gene vector, Bioconjugate chemistry, 20 (2009) 322-332.
[227] K. Konopka, N. Overlid, A.C. Nagaraj, N. Duzgunes, Serum decreases the size of Metafectene- and Genejammer-DNA complexes but does not affect significantly their transfection activity in SCCVII murine squamous cell carcinoma cells, Cellular & molecular biology letters, 11 (2006) 171-190.
[228] T. Merdan, K. Kunath, H. Petersen, U. Bakowsky, K.H. Voigt, J. Kopecek, T. Kissel, PEGylation of poly(ethylene imine) affects stability of complexes with plasmid DNA under in vivo conditions in a dose-dependent manner after intravenous injection into mice, Bioconjugate chemistry, 16 (2005) 785-792.

[229] Y. Liu, T.M. Reineke, Poly(glycoamidoamine)s for gene delivery: stability of polyplexes and efficacy with cardiomyoblast cells, Bioconjugate chemistry, 17 (2006) 101-108.
[230] M. Lee, J. Rentz, S.O. Han, D.A. Bull, S.W. Kim, Water-soluble lipopolymer as an efficient carrier for gene delivery to myocardium, Gene Ther, 10 (2003) 585-593.
[231] M. Ruponen, S. Yla-Herttuala, A. Urtti, Interactions of polymeric and liposomal gene delivery systems with extracellular glycosaminoglycans: physicochemical and transfection studies, Biochimica et biophysica acta, 1415 (1999) 331-341.
[232] G. Creusat, A.S. Rinaldi, E. Weiss, R. Elbaghdadi, J.S. Remy, R. Mulherkar, G. Zuber, Proton sponge trick for pH-sensitive disassembly of polyethylenimine-based siRNA delivery systems, Bioconjugate chemistry, 21 (2010) 994-1002.
[233] D.-W. Ryu, H.A. Kim, J.H. Ryu, D.Y. Lee, M. Lee, Amphiphilic peptides with arginine and valine residues as siRNA carriers, Journal of Cellular Biochemistry, 113 (2012) 619-628.
[234] A. Harada, H. Togawa, K. Kataoka, Physicochemical properties and nuclease resistance of antisense-oligodeoxynucleotides entrapped in the core of polyion complex micelles composed of poly(ethylene glycol)-poly(L-lysine) block copolymers, European journal of pharmaceutical sciences : official journal of the European Federation for Pharmaceutical Sciences, 13 (2001) 35-42.
[235] Y.H. Choi, F. Liu, J.S. Kim, Y.K. Choi, J.S. Park, S.W. Kim, Polyethylene glycol-grafted poly-L-lysine as polymeric gene carrier, Journal of controlled release : official journal of the Controlled Release Society, 54 (1998) 39-48.
[236] D. Fischer, T. Bieber, Y. Li, H.P. Elsasser, T. Kissel, A novel non-viral vector for DNA delivery based on low molecular weight, branched polyethylenimine: effect of molecular weight on transfection efficiency and cytotoxicity, Pharmaceutical research, 16 (1999) 1273-1279.
[237] K. Buyens, B. Lucas, K. Raemdonck, K. Braeckmans, J. Vercammen, J. Hendrix, Y. Engelborghs, S.C. De Smedt, N.N. Sanders, A fast and sensitive method for measuring the integrity of siRNA-carrier complexes in full human serum, Journal of controlled release : official journal of the Controlled Release Society, 126 (2008) 67-76.
[238] O. Zelphati, L.S. Uyechi, L.G. Barron, F.C. Szoka, Jr., Effect of serum components on the physico-chemical properties of cationic lipid/oligonucleotide complexes and on their interactions with cells, Biochimica et biophysica acta, 1390 (1998) 119-133.
[239] H. Shen, T. Sun, M. Ferrari, Nanovector delivery of siRNA for cancer therapy, Cancer Gene Ther, 19 (2012) 367-373.
[240] J. Zhou, J. Rossi, Aptamer-Targeted RNAi for HIV-1 Therapy, in: R.P. van Rij (Ed.) Antiviral RNAi, Humana Press, 2011, pp. 355-371.
[241] J. Zhou, C.P. Neff, P. Swiderski, H. Li, D.D. Smith, T. Aboellail, L. Remling-Mulder, R. Akkina, J.J. Rossi, Functional In Vivo Delivery of Multiplexed Anti-HIV-1 siRNAs via a Chemically Synthesized Aptamer With a Sticky Bridge, Mol Ther, 21 (2013) 192-200.
[242] T.M. Hinton, A. Challagulla, C.R. Stewart, C. Guerrero-Sanchez, F.A. Grusche, S. Shi, A.G. Bean, P. Monaghan, P.A. Gunatillake, S.H. Thang, M.L. Tizard, Inhibition of influenza virus in vivo by siRNA delivered using ABA triblock copolymer synthesized by reversible addition-fragmentation chain-transfer polymerization, Nanomedicine, 9 (2013) 1141-1154.
[243] J. Valencia-Serna, H. Gul-Uludağ, P. Mahdipoor, X. Jiang, H. Uludağ, Investigating siRNA delivery to chronic myeloid leukemia K562 cells with lipophilic polymers for therapeutic BCR-ABL down-regulation, Journal of Controlled Release, 172 (2013) 495-503.
[244] L. Flintoft, Gene-based therapies: Getting RNAi therapies to the brain, Nat Rev Genet, 12 (2011) 296-296.
[245] C.I. Wooddell, D.B. Rozema, M. Hossbach, M. John, H.L. Hamilton, Q. Chu, J.O. Hegge, J.J. Klein, D.H. Wakefield, C.E. Oropeza, J. Deckert, I. Roehl, K. Jahn-Hofmann, P. Hadwiger, H.-P.

Vornlocher, A. McLachlan, D.L. Lewis, Hepatocyte-targeted RNAi Therapeutics for the Treatment of Chronic Hepatitis B Virus Infection, Mol Ther, 21 (2013) 973-985.
[246] A. Fire, S. Xu, M.K. Montgomery, S.A. Kostas, S.E. Driver, C.C. Mello, Potent and specific genetic interference by double-stranded RNA in Caenorhabditis elegans, Nature, 391 (1998) 806-811.
[247] B.N. Taylor, R.R. Mehta, T. Yamada, F. Lekmine, K. Christov, A.M. Chakrabarty, A. Green, L. Bratescu, A. Shilkaitis, C.W. Beattie, T.K. Das Gupta, Noncationic Peptides Obtained From Azurin Preferentially Enter Cancer Cells, Cancer Research, 69 (2009) 537-546.
[248] S.-E. Han, H. Kang, G.Y. Shim, S.J. Kim, H.-G. Choi, J. Kim, S.K. Hahn, Y.-K. Oh, Cationic derivatives of biocompatible hyaluronic acids for delivery of siRNA and antisense oligonucleotides, Journal of Drug Targeting, 17 (2009) 123-132.
[249] M. Nothisen, M. Kotera, E. Voirin, J.-S. Remy, J.-P. Behr, Cationic siRNAs Provide Carrier-Free Gene Silencing in Animal Cells, Journal of the American Chemical Society, 131 (2009) 17730-17731.
[250] S. Futaki, T. Suzuki, W. Ohashi, T. Yagami, S. Tanaka, K. Ueda, Y. Sugiura, Arginine-rich Peptides: AN ABUNDANT SOURCE OF MEMBRANE-PERMEABLE PEPTIDES HAVING POTENTIAL AS CARRIERS FOR INTRACELLULAR PROTEIN DELIVERY, Journal of Biological Chemistry, 276 (2001) 5836-5840.
[251] J. Hoon Jeong, L.V. Christensen, J.W. Yockman, Z. Zhong, J.F.J. Engbersen, W. Jong Kim, J. Feijen, S. Wan Kim, Reducible poly(amido ethylenimine) directed to enhance RNA interference, Biomaterials, 28 (2007) 1912-1917.
[252] D. Kalderon, B.L. Roberts, W.D. Richardson, A.E. Smith, A short amino acid sequence able to specify nuclear location, Cell, 39 (1984) 499-509.
[253] F. Simeoni, M.C. Morris, F. Heitz, G. Divita, Insight into the mechanism of the peptide‐based gene delivery system MPG: implications for delivery of siRNA into mammalian cells, Nucleic Acids Research, 31 (2003) 2717-2724.
[254] K. Tanaka, T. Kanazawa, T. Ogawa, Y. Takashima, T. Fukuda, H. Okada, Disulfide crosslinked stearoyl carrier peptides containing arginine and histidine enhance siRNA uptake and gene silencing, International Journal of Pharmaceutics, 398 (2010) 219-224.
[255] I.A. Khalil, S. Futaki, M. Niwa, Y. Baba, N. Kaji, H. Kamiya, H. Harashima, Mechanism of improved gene transfer by the N-terminal stearylation of octaarginine: enhanced cellular association by hydrophobic core formation, Gene Ther, 11 (2004) 636-644.
[256] T. Lehto, R. Abes, N. Oskolkov, J. Suhorutšenko, D.-M. Copolovici, I. Mäger, J.R. Viola, O.E. Simonson, K. Ezzat, P. Guterstam, E. Eriste, C.I.E. Smith, B. Lebleu, E.L.A. Samir, Ü. Langel, Delivery of nucleic acids with a stearylated (RxR)4 peptide using a non-covalent co-incubation strategy, Journal of Controlled Release, 141 (2010) 42-51.
[257] A. Kichler, A.J. Mason, A. Marquette, B. Bechinger, Histidine-Rich Cationic Amphipathic Peptides for Plasmid DNA and siRNA Delivery, in: M. Ogris, D. Oupicky (Eds.) Nanotechnology for Nucleic Acid Delivery, Humana Press, 2013, pp. 85-103.
[258] M. Al Soraj, L. He, K. Peynshaert, J. Cousaert, D. Vercauteren, K. Braeckmans, S.C. De Smedt, A.T. Jones, siRNA and pharmacological inhibition of endocytic pathways to characterize the differential role of macropinocytosis and the actin cytoskeleton on cellular uptake of dextran and cationic cell penetrating peptides octaarginine (R8) and HIV-Tat, Journal of Controlled Release, 161 (2012) 132-141.
[259] S.D. Li, L. Huang, Gene therapy progress and prospects: non-viral gene therapy by systemic delivery, Gene Ther, 13 (0000) 1313-1319.
[260] J. Kong, S. Yu, Fourier Transform Infrared Spectroscopic Analysis of Protein Secondary Structures, Acta Biochimica et Biophysica Sinica, 39 (2007) 549-559.

[261] J.P. Richard, K. Melikov, E. Vives, C. Ramos, B. Verbeure, M.J. Gait, L.V. Chernomordik, B. Lebleu, Cell-penetrating Peptides: A REEVALUATION OF THE MECHANISM OF CELLULAR UPTAKE, Journal of Biological Chemistry, 278 (2003) 585-590.
[262] J.B. Lee, J. Hong, D.K. Bonner, Z. Poon, P.T. Hammond, Self-assembled RNA interference microsponges for efficient siRNA delivery, Nat Mater, 11 (2012) 316-322.
[263] M. Jayaraman, S.M. Ansell, B.L. Mui, Y.K. Tam, J. Chen, X. Du, D. Butler, L. Eltepu, S. Matsuda, J.K. Narayanannair, K.G. Rajeev, I.M. Hafez, A. Akinc, M.A. Maier, M.A. Tracy, P.R. Cullis, T.D. Madden, M. Manoharan, M.J. Hope, Maximizing the Potency of siRNA Lipid Nanoparticles for Hepatic Gene Silencing In Vivo, Angewandte Chemie International Edition, 51 (2012) 8529-8533.
[264] M. Shen, F. Gong, P. Pang, K. Zhu, X. Meng, C. Wu, J. Wang, H. Shan, X. Shuai, An MRI-visible non-viral vector for targeted Bcl-2 siRNA delivery to neuroblastoma, International Journal of Nanomedicine, 7 (2012) 3319-3332.
[265] R.T. Marquez, L. Xu, Bcl-2:Beclin 1 complex: multiple, mechanisms regulating autophagy/apoptosis toggle switch, American Journal of Cancer Research, 2 (2012) 214-221.
[266] G. Sithanandam, L.W. Fornwald, J.R. Fields, N.L. Morris, L.M. Anderson, Anti-tumor efficacy of naked siRNAs for ERBB3 or AKT2 against lung adenocarcinoma cell xenografts, International Journal of Cancer, 130 (2012) 251-258.
[267] A. Morin, C. Gallou-Kabani, J.R. Mathieu, F. Cabon, Systemic delivery and quantification of unformulated interfering RNAs in vivo, Current topics in medicinal chemistry, 9 (2009) 1117-1129.
[268] R. Pan, W. Xu, F. Yuan, D. Chu, Y. Ding, B. Chen, M. Jafari, Y. Yuan, P. Chen, A novel peptide for efficient siRNA delivery in vitro and therapeutics in vivo, Acta Biomater, 21 (2015) 74-84.
[269] D. Chu, W. Xu, R. Pan, Y. Ding, W. Sui, P. Chen, Rational modification of oligoarginine for highly efficient siRNA delivery: structure–activity relationship and mechanism of intracellular trafficking of siRNA, Nanomedicine: Nanotechnology, Biology and Medicine, 11 435-446.
[270] R. Pan, W. Xu, F. Yuan, D. Chu, Y. Ding, B. Chen, M. Jafari, Y. Yuan, P. Chen, A novel peptide for efficient siRNA delivery in vitro and therapeutics in vivo, Acta Biomater, (2015).
[271] J. Wang, Z. Lu, M.G. Wientjes, J.L. Au, Delivery of siRNA therapeutics: barriers and carriers, The AAPS journal, 12 (2010) 492-503.
[272] L. Li, J. Hou, X. Liu, Y. Guo, Y. Wu, L. Zhang, Z. Yang, Nucleolin-targeting liposomes guided by aptamer AS1411 for the delivery of siRNA for the treatment of malignant melanomas, Biomaterials, 35 (2014) 3840-3850.
[273] M. Damen, J. Aarbiou, S.F.M. van Dongen, R.M. Buijs-Offerman, P.P. Spijkers, M. van den Heuvel, K. Kvashnina, R.J.M. Nolte, B.J. Scholte, M.C. Feiters, Delivery of DNA and siRNA by novel gemini-like amphiphilic peptides, Journal of Controlled Release, 145 (2010) 33-39.
[274] P. Midoux, C. Pichon, J.J. Yaouanc, P.A. Jaffres, Chemical vectors for gene delivery: a current review on polymers, peptides and lipids containing histidine or imidazole as nucleic acids carriers, British journal of pharmacology, 157 (2009) 166-178.
[275] J.G. Hashimoto, A.S. Beadles-Bohling, K.M. Wiren, Comparison of RiboGreen and 18S rRNA quantitation for normalizing real-time RT-PCR expression analysis, BioTechniques, 36 (2004) 54-56, 58-60.
[276] S.D. Li, L. Huang, Gene therapy progress and prospects: non-viral gene therapy by systemic delivery, Gene Ther, 13 (2006) 1313-1319.
[277] J. Mueller, I. Kretzschmar, R. Volkmer, P. Boisguerin, Comparison of cellular uptake using 22 CPPs in 4 different cell lines, Bioconjugate chemistry, 19 (2008) 2363-2374.

[278] J. Rejman, V. Oberle, I.S. Zuhorn, D. Hoekstra, Size-dependent internalization of particles via the pathways of clathrin- and caveolae-mediated endocytosis, The Biochemical journal, 377 (2004) 159-169.
[279] D. Reischl, A. Zimmer, Drug delivery of siRNA therapeutics: potentials and limits of nanosystems, Nanomedicine: Nanotechnology, Biology and Medicine, 5 (2009) 8-20.
[280] D. Cun, D.K. Jensen, M.J. Maltesen, M. Bunker, P. Whiteside, D. Scurr, C. Foged, H.M. Nielsen, High loading efficiency and sustained release of siRNA encapsulated in PLGA nanoparticles: Quality by design optimization and characterization, European Journal of Pharmaceutics and Biopharmaceutics, 77 (2011) 26-35.
[281] C. Olbrich, N. Scholer, K. Tabatt, O. Kayser, R.H. Muller, Cytotoxicity studies of Dynasan 114 solid lipid nanoparticles (SLN) on RAW 264.7 macrophages-impact of phagocytosis on viability and cytokine production, The Journal of pharmacy and pharmacology, 56 (2004) 883-891.
[282] D.M. Copolovici, K. Langel, E. Eriste, Ü. Langel, Cell-Penetrating Peptides: Design, Synthesis, and Applications, ACS Nano, 8 (2014) 1972-1994.
[283] H. Raagel, P. Saalik, M. Pooga, Peptide-mediated protein delivery-which pathways are penetrable?, Biochimica et biophysica acta, 1798 (2010) 2240-2248.
[284] A.T. Jones, E.J. Sayers, Cell entry of cell penetrating peptides: tales of tails wagging dogs, Journal of Controlled Release, 161 (2012) 582-591.
[285] S. Fawell, J. Seery, Y. Daikh, C. Moore, L.L. Chen, B. Pepinsky, J. Barsoum, Tat-mediated delivery of heterologous proteins into cells, Proc Natl Acad Sci U S A, 91 (1994) 664-668.
[286] R. Fischer, M. Fotin-Mleczek, H. Hufnagel, R. Brock, Break on through to the other side-biophysics and cell biology shed light on cell-penetrating peptides, Chembiochem : a European journal of chemical biology, 6 (2005) 2126-2142.
[287] R. Brock, The Uptake of Arginine-Rich Cell-Penetrating Peptides: Putting the Puzzle Together, Bioconjugate chemistry, 25 (2014) 863-868.
[288] M.C. Morris, S. Deshayes, F. Heitz, G. Divita, Cell-penetrating peptides: from molecular mechanisms to therapeutics, Biology of the cell / under the auspices of the European Cell Biology Organization, 100 (2008) 201-217.
[289] J.M. Gump, S.F. Dowdy, TAT transduction: the molecular mechanism and therapeutic prospects, Trends Mol Med, 13 (2007) 443-448.
[290] R.J. Linhardt, T. Toida, Role of glycosaminoglycans in cellular communication, Accounts of chemical research, 37 (2004) 431-438.
[291] G.M. Poon, J. Gariepy, Cell-surface proteoglycans as molecular portals for cationic peptide and polymer entry into cells, Biochemical Society transactions, 35 (2007) 788-793.
[292] A. Walrant, C. Bechara, I.D. Alves, S. Sagan, Molecular partners for interaction and cell internalization of cell-penetrating peptides: how identical are they?, Nanomedicine (London, England), 7 (2012) 133-143.
[293] M. Rodrigues, D. Andreu, N.C. Santos, Uptake and cellular distribution of nucleolar targeting peptides (NrTPs) in different cell types, Biopolymers, 104 (2015) 101-109.
[294] H.L. Amand, H.A. Rydberg, L.H. Fornander, P. Lincoln, B. Norden, E.K. Esbjorner, Cell surface binding and uptake of arginine- and lysine-rich penetratin peptides in absence and presence of proteoglycans, Biochimica et biophysica acta, 1818 (2012) 2669-2678.
[295] A. Kim, T.H. Shin, S.M. Shin, C.D. Pham, D.K. Choi, M.H. Kwon, Y.S. Kim, Cellular internalization mechanism and intracellular trafficking of filamentous M13 phages displaying a cell-penetrating transbody and TAT peptide, PLoS One, 7 (2012) e51813.

[296] I.D. Alves, C.Y. Jiao, S. Aubry, B. Aussedat, F. Burlina, G. Chassaing, S. Sagan, Cell biology meets biophysics to unveil the different mechanisms of penetratin internalization in cells, Biochimica et biophysica acta, 1798 (2010) 2231-2239.
[297] C. Bechara, S. Sagan, Cell-penetrating peptides: 20 years later, where do we stand?, FEBS letters, 587 (2013) 1693-1702.
[298] G.M. Poon, J. Gariépy, Cell-surface proteoglycans as molecular portals for cationic peptide and polymer entry into cells, Biochemical Society transactions, 35 (2007) 788-793.
[299] M.-L. Jobin, I.D. Alves, On the importance of electrostatic interactions between cell penetrating peptides and membranes: A pathway toward tumor cell selectivity?, Biochimie, 107, Part A (2014) 154-159.
[300] A.E. Ziegler, J. Seelig, Contributions of glycosaminoglycan binding and clustering to the biological uptake of the nonamphipathic cell-penetrating peptide WR 9, Biochemistry, 50 (2011) 4650-4664.
[301] I. Nakase, A. Tadokoro, N. Kawabata, T. Takeuchi, H. Katoh, K. Hiramoto, M. Negishi, M. Nomizu, Y. Sugiura, S. Futaki, Interaction of arginine-rich peptides with membrane-associated proteoglycans is crucial for induction of actin organization and macropinocytosis, Biochemistry, 46 (2007) 492-501.
[302] A. Walrant, I. Correia, C.Y. Jiao, O. Lequin, E.H. Bent, N. Goasdoué, C. Lacombe, G. Chassaing, S. Sagan, I.D. Alves, Different membrane behaviour and cellular uptake of three basic arginine-rich peptides, Biochimica et Biophysica Acta - Biomembranes, 1808 (2011) 382-393.
[303] K. Matsuda, H. Maruyama, F. Guo, J. Kleeff, J. Itakura, Y. Matsumoto, A.D. Lander, M. Korc, Glypican-1 is overexpressed in human breast cancer and modulates the mitogenic effects of multiple heparin-binding growth factors in breast cancer cells, Cancer Res, 61 (2001) 5562-5569.
[304] D. Nikitovic, M. Mytilinaiou, A. Berdiaki, N.K. Karamanos, G.N. Tzanakakis, Heparan sulfate proteoglycans and heparin regulate melanoma cell functions, Biochimica et Biophysica Acta (BBA) - General Subjects, 1840 (2014) 2471-2481.
[305] F.H. Blackhall, C.L.R. Merry, E.J. Davies, G.C. Jayson, Heparan sulfate proteoglycans and cancer, British Journal of Cancer, 85 (2001) 1094-1098.
[306] E.H. Knelson, J.C. Nee, G.C. Blobe, Heparan sulfate signaling in cancer, Trends in Biochemical Sciences, 39 (2014) 277-288.
[307] N. Afratis, C. Gialeli, D. Nikitovic, T. Tsegenidis, E. Karousou, A.D. Theocharis, M.S. Pavão, G.N. Tzanakakis, N.K. Karamanos, Glycosaminoglycans: key players in cancer cell biology and treatment, FEBS Journal, 279 (2012) 1177-1197.
[308] L.J. Jones, S.T. Yue, C.Y. Cheung, V.L. Singer, RNA quantitation by fluorescence-based solution assay: RiboGreen reagent characterization, Analytical biochemistry, 265 (1998) 368-374.
[309] G.J. Doherty, H.T. McMahon, Mechanisms of endocytosis, Annual review of biochemistry, 78 (2009) 857-902.
[310] R.J. Linhardt, T. Toida, Role of Glycosaminoglycans in Cellular Communication, Accounts of chemical research, 37 (2004) 431-438.
[311] M. Tyagi, M. Rusnati, M. Presta, M. Giacca, Internalization of HIV-1 tat requires cell surface heparan sulfate proteoglycans, The Journal of biological chemistry, 276 (2001) 3254-3261.
[312] P. Liu, Y. Sun, Q. Wang, Y. Sun, H. Li, Y. Duan, Intracellular trafficking and cellular uptake mechanism of mPEG-PLGA-PLL and mPEG-PLGA-PLL-Gal nanoparticles for targeted delivery to hepatomas, Biomaterials, 35 (2014) 760-770.
[313] I. Fiorentino, R. Gualtieri, V. Barbato, V. Mollo, S. Braun, A. Angrisani, M. Turano, M. Furia, P.A. Netti, D. Guarnieri, S. Fusco, R. Talevi, Energy independent uptake and release of polystyrene nanoparticles in primary mammalian cell cultures, Experimental cell research, 330 (2015) 240-247.

[314] Y. Li, G. Wen, D. Wang, X. Zhang, Y. Lu, J. Wang, L. Zhong, H. Cai, X. Zhang, Y. Wang, A Complementary Strategy for Enhancement of Nanoparticle Intracellular Uptake, Pharmaceutical research, 31 (2014) 2054-2064.
[315] R. Roy, V. Parashar, L.K.S. Chauhan, R. Shanker, M. Das, A. Tripathi, P.D. Dwivedi, Mechanism of uptake of ZnO nanoparticles and inflammatory responses in macrophages require PI3K mediated MAPKs signaling, Toxicology in Vitro, 28 (2014) 457-467.
[316] S.K. Mamidyala, S. Dutta, B.A. Chrunyk, C. Préville, H. Wang, J.M. Withka, A. McColl, T.A. Subashi, S.J. Hawrylik, M.C. Griffor, S. Kim, J.A. Pfefferkorn, D.A. Price, E. Menhaji-Klotz, V. Mascitti, M.G. Finn, Glycomimetic Ligands for the Human Asialoglycoprotein Receptor, Journal of the American Chemical Society, 134 (2012) 1978-1981.
[317] S. Pavlides, J. Gutierrez-Pajares, J. Iturrieta, M. Lisanti, P. Frank, Endothelial caveolin-1 plays a major role in the development of atherosclerosis, Cell Tissue Res, 356 (2014) 147-157.
[318] E. Trushina, C.A. Canaria, D.-Y. Lee, C.T. McMurray, Loss of caveolin-1 expression in knock-in mouse model of Huntington's disease suppresses pathophysiology in vivo, Human Molecular Genetics, 23 (2014) 129-144.
[319] D. Vercauteren, R.E. Vandenbroucke, A.T. Jones, J. Rejman, J. Demeester, S.C. De Smedt, N.N. Sanders, K. Braeckmans, The Use of Inhibitors to Study Endocytic Pathways of Gene Carriers: Optimization and Pitfalls, Mol Ther, 18 (2010) 561-569.
[320] M. Dondarski, B. Cohen, Human follicle stimulating hormone receptor signaling is membrane cholesterol and internalization dependent (609.16), The FASEB Journal, 28 (2014).
[321] A. Walrant, L. Matheron, S. Cribier, S. Chaignepain, M.-L. Jobin, S. Sagan, I.D. Alves, Direct translocation of cell-penetrating peptides in liposomes: A combined mass spectrometry quantification and fluorescence detection study, Analytical biochemistry, 438 (2013) 1-10.
[322] D.M. Monti, D. Guarnieri, G. Napolitano, R. Piccoli, P. Netti, S. Fusco, A. Arciello, Biocompatibility, uptake and endocytosis pathways of polystyrene nanoparticles in primary human renal epithelial cells, Journal of Biotechnology, 193 (2015) 3-10.
[323] J. Dausend, A. Musyanovych, M. Dass, P. Walther, H. Schrezenmeier, K. Landfester, V. Mailänder, Uptake Mechanism of Oppositely Charged Fluorescent Nanoparticles in HeLa Cells, Macromolecular Bioscience, 8 (2008) 1135-1143.
[324] V. Polyakov, V. Sharma, J.L. Dahlheimer, C.M. Pica, G.D. Luker, D. Piwnica-Worms, Novel Tat-Peptide Chelates for Direct Transduction of Technetium-99m and Rhenium into Human Cells for Imaging and Radiotherapy, Bioconjugate chemistry, 11 (2000) 762-771.
[325] I. Mäger, K. Langel, T. Lehto, E. Eiríksdóttir, Ü. Langel, The role of endocytosis on the uptake kinetics of luciferin-conjugated cell-penetrating peptides, Biochimica et Biophysica Acta (BBA) - Biomembranes, 1818 (2012) 502-511.
[326] T. Suzuki, S. Futaki, M. Niwa, S. Tanaka, K. Ueda, Y. Sugiura, Possible Existence of Common Internalization Mechanisms among Arginine-rich Peptides, Journal of Biological Chemistry, 277 (2002) 2437-2443.
[327] M. Hällbrink, A. Florén, A. Elmquist, M. Pooga, T. Bartfai, Ü. Langel, Cargo delivery kinetics of cell-penetrating peptides, Biochimica et Biophysica Acta (BBA) - Biomembranes, 1515 (2001) 101-109.
[328] E. Eiríksdóttir, I. Mäger, T. Lehto, S. El Andaloussi, Ü. Langel, Cellular Internalization Kinetics of (Luciferin-)Cell-Penetrating Peptide Conjugates, Bioconjugate chemistry, 21 (2010) 1662-1672.
[329] G. Drin, M. Mazel, P. Clair, D. Mathieu, M. Kaczorek, J. Temsamani, Physico-chemical requirements for cellular uptake of pAntp peptide, European Journal of Biochemistry, 268 (2001) 1304-1314.

[330] I. Mager, E. Eiriksdottir, K. Langel, S. El Andaloussi, U. Langel, Assessing the uptake kinetics and internalization mechanisms of cell-penetrating peptides using a quenched fluorescence assay, Biochimica et biophysica acta, 1798 (2010) 338-343.
[331] C.L. Watkins, D. Schmaljohann, S. Futaki, A.T. Jones, Low concentration thresholds of plasma membranes for rapid energy-independent translocation of a cell-penetrating peptide, The Biochemical journal, 420 (2009) 179-189.
[332] M.C. Morris, J. Depollier, J. Mery, F. Heitz, G. Divita, A peptide carrier for the delivery of biologically active proteins into mammalian cells, Nature biotechnology, 19 (2001) 1173-1176.